PERFORMANCE ANALYSIS OF CHILLED WATER SYSTEMS AND THE EFFECT OF INCORPORATION OF EJECTOR COOLING SYSTEM

BY

SYED AMMAR A. TIRMIZI SUJAULHAQ S.

A Thesis Presented to the
DEANSHIP OF GRADUATE STUDIES

KING FAHD UNIVERSITY OF PETROLEUM & MINERALS

DHAHRAN, SAUDI ARABIA

In Partial Fulfillment of the
Requirements for the Degree of

MASTER OF SCIENCE

In

MECHANICAL ENGINEERING

MARCH 2010

KING FAHD UNIVERSITY OF PETROLEUM AND MINERALS

DHAHRAN 31261, SAUDI ARABIA

DEANSHIP OF GRADUATE STUDIES

This thesis, written by Syed Ammar A. Tirmizi Sujaulhaq Shafiulh., under the direction of his thesis advisor and approved by his thesis committee, has been presented to and accepted by the Dean of Graduate Studies, in partial fulfillment of the requirements for the degree of **MASTER OF SCIENCE IN MECHANICAL ENGINEERING**.

Thesis Committee

11/5/2010

Dr. P. Gandhidasan (Advisor)

May 11, 2010

Dr. Syed M. Zubair (Member)

11 May 2010

Dr. Haitham Bahaidarah (Member)

Dr. Amro M Al - Qutub
Department Chairman

Dr. Salam A. Zummo
Dean of Graduate Studies

23/5/10

Date

ACKNOWLEDGEMENTS

I would like to express my gratitude to my advisor Dr. P. Gandhidasan, for his guidance, support, encouragement, and patience throughout my graduate study. Sincere thanks go to both the members of my advisory committee, Dr. S. M. Zubair and Dr.Haitham Bahaidarah for their constructive guidance and technical support.

I would further like to express my deep gratitude to Mr. Syed Younus Ahmed for going out of his way to help me in all possible means. Thanks are also due to the Department secretaries, Mr. Jameel and Mr. Lateef for their help and assistance.

Special thanks are due to my senior colleagues at the university, Misbahuddin, Murtuza, Omer, Zahid, Shujath, Sarfaraz, Abdul Rahman, Mumtaz, Mazhar, Hassan, Nizam, and Asrar who were always there to provide thoughtful solutions to the various problems encountered in my research. I would also like to thank all my friends, Hussain, Nadeem, Aves, Ehsan, Abdul Ghani, Shahid, Omeir, Islam, Abdullah, Aashik, Aqeel, and Imtiaz for wonderful company and good memories that will last a life time. Furthermore, I would like to express my heartfelt feelings for Abdurrahman. Including him in the category of friends would not do justice to the relationship that we share.

Finally, thanks are due to my dearest (late) mother and father, my wife, by sisters and brother as well as all my family members for their emotional and moral support throughout my academic career and also for their love, forbearance, encouragement and prayers.

TABLE OF CONTENTS

LIST OF TABLES

LIST OF FIGURES

THESIS ABSTRACT (ENGLISH)

NAME: SYED AMMAR A. TIRMIZI SUJAULHAQ S.

TITLE: PERFORMANCE ANALYSIS OF CHILLED WATER SYSTEMS AND THE EFFECT OF INCORPORATION OF EJECTOR COOLING SYSTEM

MAJOR: MECHANICAL ENGINEERING

DATE: MARCH 2010

Air conditioning is one of the major consumers of energy in the Kingdom of Saudi Arabia and attempts have to be made to bring down the power consumption required for space cooling without undermining the performance of the air conditioning systems. With the development of sophisticated control technology, employing microprocessors, the manufacture of chillers capable of handling variable flow of water with extreme precision has been made possible. Significant reduction in energy consumption can be achieved by employing variable pumping of water through the chillers depending upon the load. In this thesis, the effect of replacing an existent central chilled water with a constant primary-variable secondary as well as the variable primary pumping schemes is analyzed and the results are presented in terms of annual energy consumption .It is found that the annual energy consumption is reduced by almost 12% by adopting the variable primary scheme and by 8% by utilizing the constant primary-variable secondary pumping scheme. An exergy balance performed on the chilled water system reveals that the pumping schemes have a negligible effect on the total exergy destruction, whereas the compressor followed by the air handlers are the two major sources of irreversibilities. Owing to the hot humid conditions prevailing in the Kingdom during the summer months, the potential of condensate extraction from the cooling coils of the air handler during these months is explored for several locations. Finally, the effect of replacing the cooling tower of the chilled water system with an ejector cooling system is analyzed. Results indicate that this combined system is quite advantageous at conditions of high ambient relative humidity when the cooling capacity of the cooling tower is greatly diminished but the performance of the ejector cooling system remains unaffected.

MASTER OF SCIENCE DEGREE

KING FAHD UNIVERSITY OF PETROLEUM and MINERALS

Dhahran, Saudi Arabia

خلاصة الرسالة

الاسم : سيد عماراحمد ترميذي شجيع الحق شفيع الحق

العنوان: دراسه تحليليه لنظام تبريد المياه وتأثير استخدام نظام قذف التبريد

التخصص: هندسه ميكانيكه

التاريخ : مارس 2010 م

مكيفات الهواء هي واحدة من أكبر مستهلكي الطاقة في المملكة العربية السعودية وهناك محاولات مبذولة لخفض استهلاك الطاقة اللازمة لتبريد الفضاء دون تقويض أداء أنظمة تكييف الهواء. مع تطور تقنية التحكم المتطورة ، التي تستخدم معالجات الميكروبروسيسر ، أحرزت صناعة المبردات قدره على التعامل مع تدفق متغير للمياه وبدقة متناهية. ويمكن تحقيق خفض كبير في استهلاك الطاقة من خلال توظيف متغير ضخ المياه من خلال المبردات تبعا للحمولة. في هذه الرسالة ، تم دراسه تاثير تغيرمبرده المياه المركزيه بثابت الابتدائية ومتغير الثانوية وكذلك مخططات الضخ للمتغير الأساسي وتم تحليلها وعرض النتائج من حيث استهلاك الطاقة السنوية. وجد أن الاستهلاك السنوي للطاقة خفضت بنسبة 12 ٪ تقريبا من خلال اعتماد نظام متغير الابتدائية وبنسبة 8 ٪ من خلال الاستفادة من الابتدائي الثانوية نظام متغير ثابت الضخ. كما تم ايضا" دراسه الزياده في الطاقه على مبردات المياه والتي اظهرت ان مخططات الضخ ليس لها تأثير على حسابات الطاقه الزائده في حين أن الضاغط تليه معالجات الهواء هما المصدران الرئيسيان لعدم العكوسيه. ونظرا للظروف السائدة الرطبة الساخنة في المملكة العربيه السعوديه خلال أشهر الصيف ، تم استكشاف إمكانات استخراج التكثيف من ملفات تبريد المعالج خلال هذين الشهرين لعدة مواقع. وأخيرا ، تم تحليل تأثير استبدال برج التبريد لنظام المياه المبردة مع نظام التبريد القاذف للهواء . وتشير النتائج إلى أن هذا النظام الجامع هو مفيد جدا في ظروف ارتفاع نسبة الرطوبة النسبية المحيطة حيث يتم تقليص قدرة تبريد برج التبريد إلى حد كبير ولكن أداء نظام التبريد القاذف لم يتأثر.

درجه الماجستير في العلوم

جامعه الملك فهد للبترول والمعادن

الظهران-المملكه العربيه السعوديه

NONENCLATURE

A	area (ft^2 or m^2)
$A_1,A_2,..A_{10}$	constants
C	specific heat capacitance (BTU/hr-R)
C_p	specific heat (BTU/lbm-hr)
C_{pm}	mean specific heat of air water mixture (BTU/lbm-hr)
C_s	saturation specific heat (BTU/lbm-hr)
D	diameter (ft or m)
EWT	entering water temperature (^oF)
f	fin
f_f	friction factor for fins
f_i	friction factor for inner surface of tubes
f_{tube}	friction factor for outer surface of tubes
g	gravitational constant (ft/s^2)
G_a	mass velocity based on minimum area ($lbm/hr\text{-}ft^2$)
GPM	gallons per minute
h	heat transfer coefficient (BTU/ $hr\text{-}ft^2\text{-}R$)
h_a, i	enthalpy (BTU/lbm)
h_{fg}	latent heat of vaporization (BTU/lbm)
hp	horse power
I	irreversibility (kW)
K	bend coefficient
k	thermal conductivity (BTU/ hr-ft-R)
L	length (ft or m)
LWT	leaving water temperature (^oF)
M	Mach number
M^*	critical Mach number
MW	mega watts

$\dot{m}$	mass flow rate (lbm/hr)
NPSH	net positive suction head (ft)
n_{row}	number of rows
n_t	number of tubes
NTU	number of transfer units
P	pressure (psia)
Pr	Prandtl number
$\dot{Q}$	heat transfer rate (BTU/hr)
Re	Reynolds number
Ref.	refrigerant
rpm	revolutions per minute
S, s	entropy (BTU/lbm-R)
T, Temp.	temperature (^oC, K)
T_0	dead state temperature (^oC, K)
TR	ton of refrigeration
UA	overall heat conductance(BTU/ hr-R)
v,V	velocity (ft/sec)
$\dot{W}$	rate of work done (BTU/hr)
X	exergy

Greek Symbols

Δ	change/difference
ε	effectiveness
ε_{pipe}	average roughness of pipe
ω	specific humidity/humidity ratio
ψ	flow exergy
η	efficiency, surface effectiveness
$\eta_{1,a}$	nozzle efficiency

$\eta_{b,3}$	diffuser efficiency
ρ	density

Subscripts

1,2……6	ejector cooling cycle locations
a	air
act	actual
ah	air handler
amb	ambient
ave	average
b	Based on longitudinal spacing
chw	chilled water system
comp	compressor
cond, c	condensate, condenser
CV	control volume
D	based on diameter
dest	destroyed
e	exit
eff	effective
ejec	ejector
evap	evaporator
f	fin
fan	fan
g	generator
i	inlet state conditions, inside
in	inlet
L	based on the tube spacing in flow direction
m	mean
max	maximum

min	minimum
o	outlet/outside
p	pump
ref	refrigerant
rev	reversible
s	saturation
t	tubes
tot	total
tow	cooling tower
vsd	variable speed drive
w	water

CHAPTER 1

INTRODUCTION

1.1 Background

Saudi Arabia has a population of more than 27 million, growing at an annual rate of 3.8%., which is the highest rate in the world. It is the largest producer of crude oil and also one of the biggest consumers of energy in the world. Saudi consumption of primary energy, conventional oil and natural gas, has grown from 88.1 million tons/year of oil equivalent[1] in 1993 to about 149.2 million tons/year of oil equivalent in 2006 [1]. With the increase in population and the massive expansion of the industrial sector, the demand for energy is further likely to skyrocket in the coming few decades. Thus along with employing methods to increase the energy production, the need to utilize energy conservation techniques is also something to be pondered about.

Surveys have showed that almost 75% of the total electrical energy generated in Saudi Arabia is utilized for space cooling [2]. This cooling is accomplished by either small

[1]One metric ton of oil equivalent (toe) is defined as 41.868 gigajoules, equal to the amount of energy contained in 1 metric ton of crude oil.

window type units for small residential applications or large central units for large residential, commercial and industrial applications. The cooling capacity of the central units may vary from a few (more than two) tons of refrigeration (TR) to several thousand tons of refrigeration. The main source of energy consumption in the central air conditioning plants are the compressors, the pumps and the air handler fans. Thus by employing techniques to minimize the power usage of these components, the overall efficiency of the central air conditioning plants can be significantly increased translating into considerable savings in energy and thereby costs.

Furthermore, the combination of the simple ejector cooling system with the conventional chilled water system, by utilizing the waste heat from the latter can add to the energy savings.

1.2 Overview of Central Air Conditioning Systems

The central air conditioning plants are divided into two main components: the chillers and the air handling units (AHU). Chillers can be of either absorption or vapor compression type. The chillers are further classified as air cooled or water cooled, based on whether air or water is used to cool the refrigerant in the condenser. In the Kingdom of Saudi Arabia, vapor compression chillers are most widely used for nearly all applications. As the name suggests the vapor compression chillers follow the refrigeration cycle to produce chilled water. This water is then pumped to the air handler. The air handler utilizes the supplied water to generate cool air and also supplies the cool air to the conditioned space via ducts. Based on the load the central air conditioning plant may consist of several chillers and air handlers.

1.3 Distribution of Chilled Water

Supplying chilled water to the AHU is perhaps one of the most important aspects of the air conditioning system especially in large commercial and industrial applications. The chilled water, in turn, provides a means to transfer the heat from the conditioned spaces to the refrigeration system. There are mainly three schemes in which the chilled water can be distributed from the chiller (evaporator) to the load (air handling units):

1. Constant primary flow
2. Constant primary-variable secondary flow
3. Variable primary flow

1.3.1 Constant Primary Flow

In the constant primary flow systems, a single (constant speed) pump operates continuously to maintain a constant flow rate of water throughout the entire system. This system is shown in Fig. 1.1. Although; only one air handler is shown n the figure the system may comprise of several air handlers. A Three way valve is employed to regulate the flow of chilled water in the air handler by allowing some of the water to bypass the cooling coil during part load conditions. Thus the net quantity of water returned to the chiller always remains constant irrespective of the load. This system although widely used during the 1960's and early 1970's, had the following two major drawbacks:

a) Low operating temperature differential (ΔT) issues.

b) Constant pumping requirement.

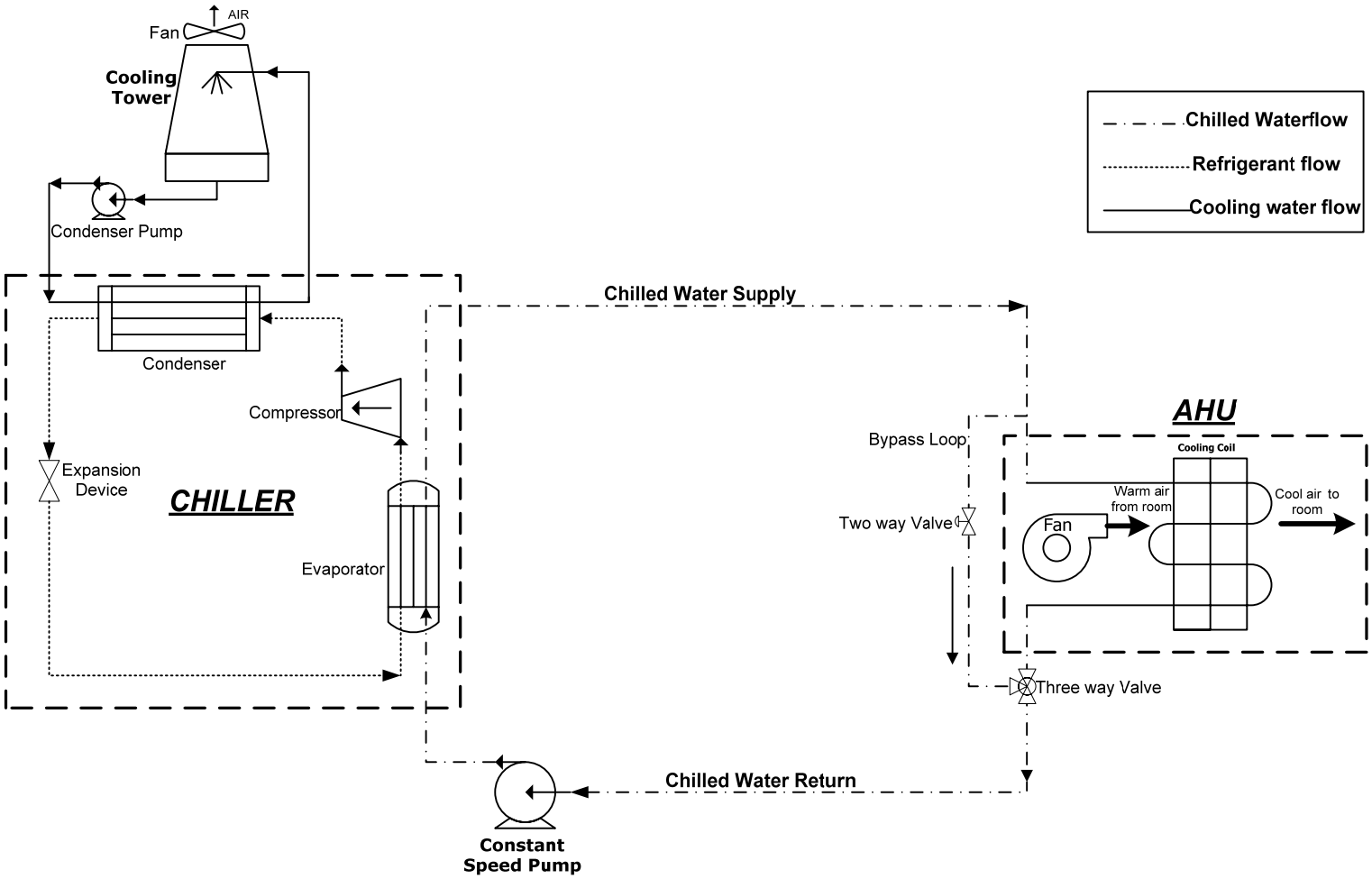

Figure 1.1 Schematic of constant primary flow systems.

These two disadvantages are discussed in the following sections.

1.3.1. (a) Low Operating Temperature Differential (ΔT) Issues

The flow through the chiller is set up for the peak design condition (i.e.100% load) and the chillers are designed to deliver the chilled water at a specific temperature based on this condition. But this condition occurs only for either 1 or 2.5% of the time based on the design strategy [3] If the plant runs on full load only for 2.5% of the total operational time, for the remaining 97.5% of the time, the plant is operating at part load conditions.

Consequently, some of the chilled water which is supplied to the air handler will always be bypassed through the three way valves without being used in the cooling coils. This water when continuously mixed with the water leaving the cooling coil reduces the temperature of the return water supplied to the chiller. This in turn reduces the operating temperature differential (ΔT) across the chiller as the supply water temperature has already been fixed. This phenomenon is commonly known as the low delta T (ΔT) syndrome.

The reduced temperature differential reduces the maximum capacity of the chillers to which it can be operated. In order to compensate this loss, additional chillers have to be 'brought online' to match the load conditions. This will ultimately result in the inefficient operation of chillers thereby increasing the plant energy consumption.

1.3.1. (b) Constant Pumping Requirement

Since a constant speed pump is used for water circulation, the pumping requirement and hence the pumping power of the system remains constant irrespective of the load on the

plant and the ambient conditions. Thus the power used by the plant for the summer is the same as that used in winter.

1.3.2 Constant Primary, Variable Secondary Flow

In the late 1970's, the increased cost of energy as well as the development of the variable speed drives compelled the designers to think of alternatives to the constant primary flow scheme. This paved the way for the primary-secondary system of the chilled water distribution.

The characteristic feature of the primary secondary scheme is shown in Fig. 1.2. In this scheme the production of chilled water (primary loop) is 'decoupled' from the distribution in the air handlers (secondary loop) and in most cases a bypass is provided between the two loops in order to facilitate constant flow through the chiller evaporator. A constant speed pump circulates the water in the primary circuit whereas a variable speed pump is employed for varying the water circulation in the secondary loop depending upon the requirement of the load. This system has a major advantage of maintaining constant water flow rate through the chiller as well as providing the desired chilled water to the air handler corresponding to the load.

Although the provision of the secondary variable pump emphatically brings down the pumping requirement which translates directly into savings in terms of cost, the system has several undesirable features. First of all the issue of low temperature differential

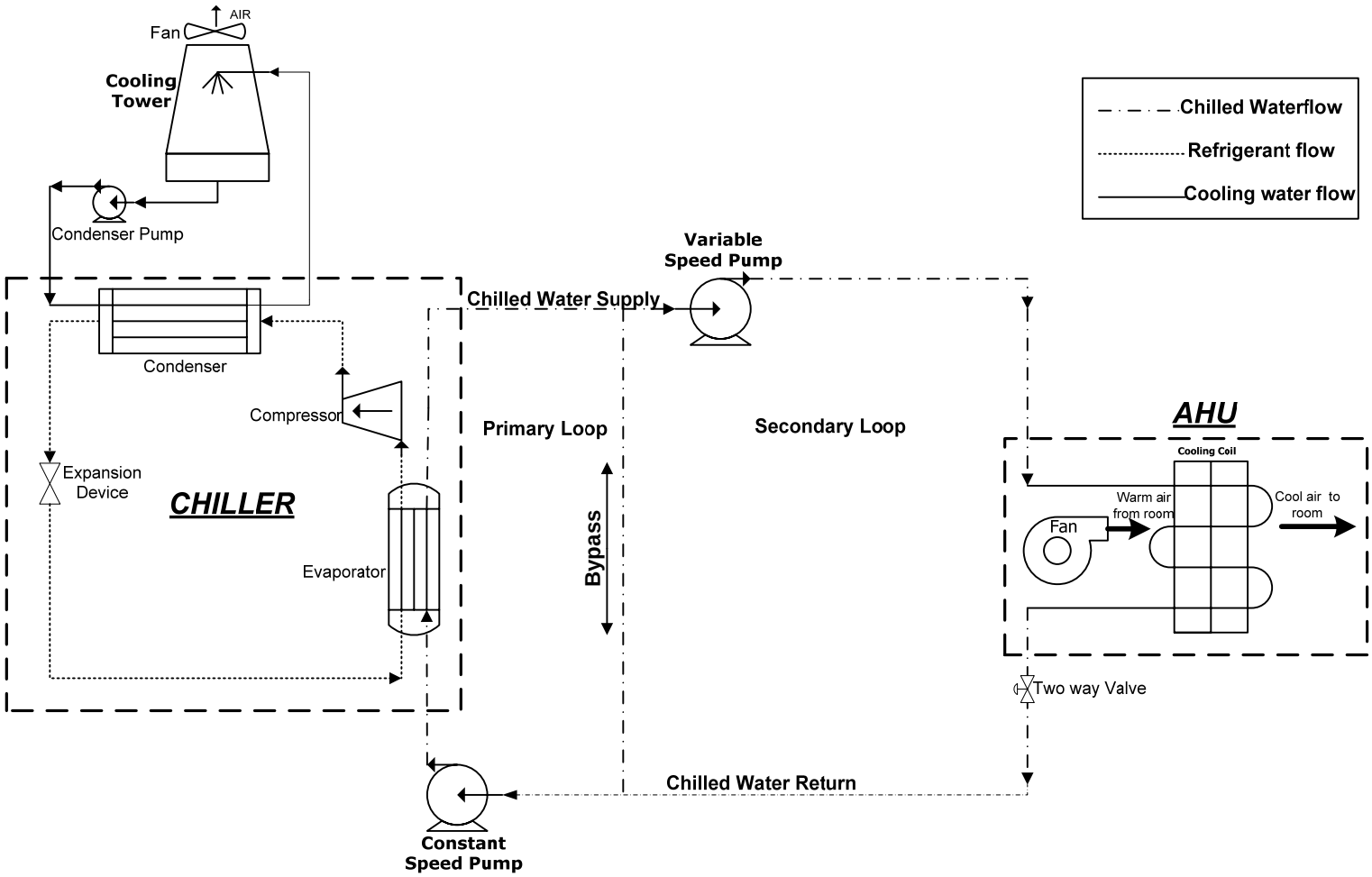

Figure 1.2 Schematic of primary-secondary flow systems

(ΔT) across the chiller (primary loop), which arises during the part load or overdesign condition, is not resolved. Moreover the initial cost of acquiring the secondary variable speed pump and the associated cost of the necessary piping related to the bypass loop (labor, material, maintenance, etc.) tend to somewhat neutralize (though not completely) the savings achieved by the reduced pumping power.

1.3.3 Variable Primary Flow

The development of highly sophisticated microprocessors and electronic control strategies provided the motivation for a third pumping scheme. In this arrangement, as shown in Fig. 1.3, a single variable speed pump circulates the chilled water through the entire system.

The chilled water flow rate is varied corresponding to the load (air handlers) and the regulation of the entire system is accomplished by a two way valve. The obvious reduction in pumping power translates into savings in both energy and cost when computed on an annual basis. Furthermore, the detrimental mixing between supply and the return chilled, which is one of the major causes of low ΔT across the chiller, is almost avoided, except in a few cases. The absence of the bypass loop and its associated costs, further add to the savings.

In spite of these advantages, the designers as well as the customers are reluctant to employ this scheme of distribution. This is mainly due to the complexity involved in maintaining variable flow through the evaporator of the chiller and also due to possibility of laminar flow in the chiller at low chilled water flow rates (at small loads).

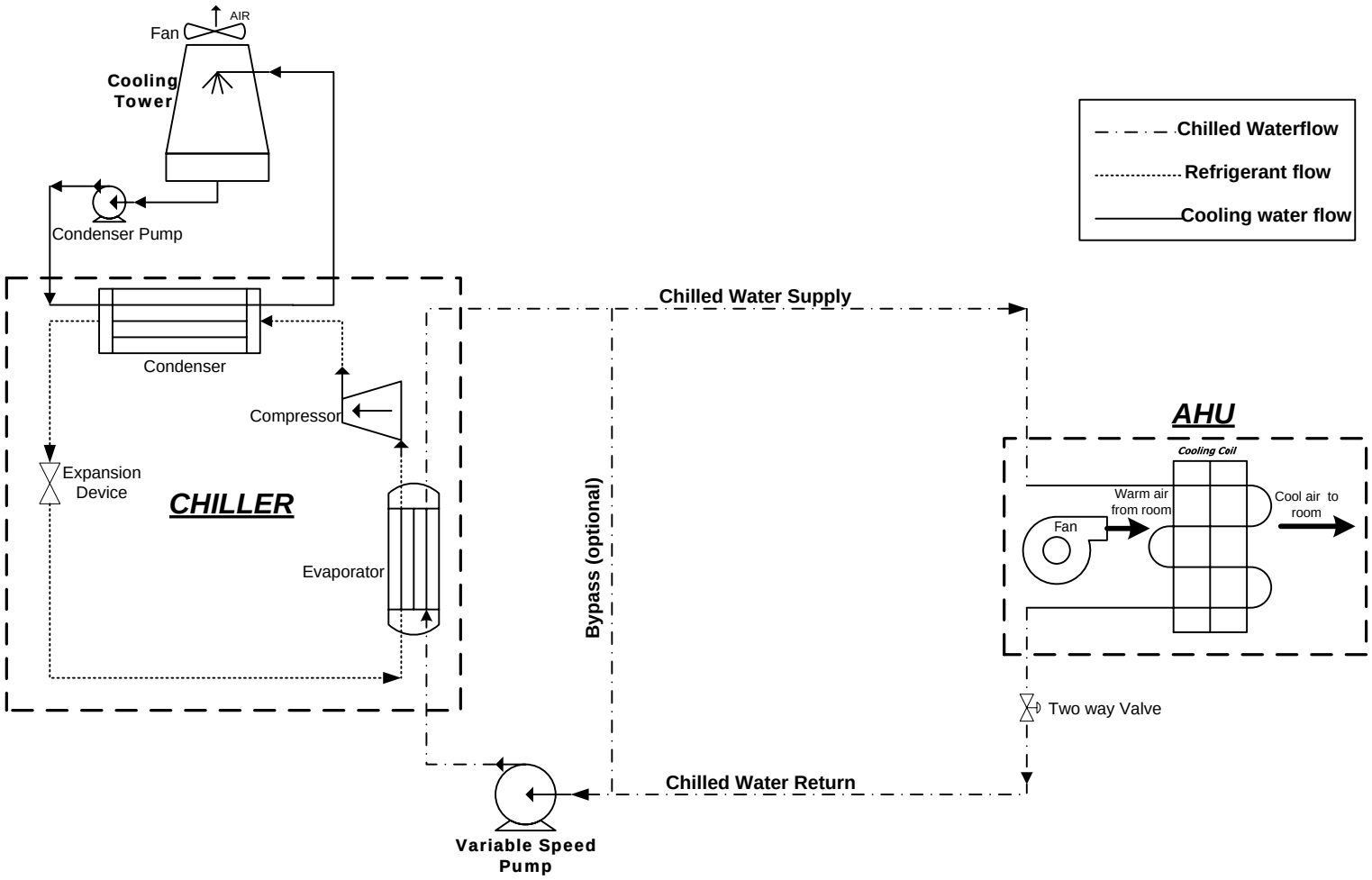

Figure 1.3 Schematic of variable primary flow systems.

In this thesis, a central air conditioning plant with all its major components such as the chiller, the pumps, the air handler and the cooling tower are modeled. The effects of the three aforementioned pumping schemes on the individual components as well as on the entire system are also analyzed.

1.4 Exergy Analysis

The exergy of a system is the maximum work possible during a process that brings the system into equilibrium with a heat reservoir [4]. When the surroundings are the reservoir, exergy is the potential of a system to cause a change as it achieves equilibrium with its environment. Typically, the environment is specified by stating its temperature and pressure. Exergy is not simply a thermodynamic property, but rather is a co-property of a system and the reference environment [5]. Thus exergy can be summarized as the amount of energy that can be extracted as useful work. After the system and surroundings reach equilibrium (dead state), the exergy becomes zero.

An important concept that has to be highlighted at this point is the principle of decrease of exergy or the exergy destruction. Combining the first and second law of thermodynamics with the definition of exergy, it can be shown that for an isolated system which undergoes a process, the exergy always decreases or in the limiting case of a reversible process, remains constant. This decrease in exergy is equivalent to the exergy destroyed.

The main rationale behind performing an exergy analysis/balance of the various components comprising a system is to identify the sources and magnitudes of irreversibilities that are occurring during the various processes. Once identified, suitable

remedial measures can be taken to improve the work potential or reduce the exergy destruction (lost work). Due to these reasons, the principle of exergy balance is applied to a central chilled water system in this thesis.

1.5 Ejector Cooling

In water cooled chillers, the cooling of the working refrigerant is accomplished by the water flowing through the condenser. This water which takes the heat from the refrigerant is in turn cooled by cooling towers. An interesting possibility is the replacement of the cooling tower with an ejector cooling system in which the evaporator of the ejector cooling system acts as an intercooler for the purpose of cooling the condenser water of the chilled water system. This scenario is investigated in this thesis.

An ejector refrigeration system is similar to a vapor-compression system except for the method of compressing the refrigerant. Instead of a mechanical compressor, an ejector is used to compress the refrigerant vapor from the evaporator to the condenser. As the ejector does not contain any moving parts, no external power is required for its operation and thus considerable amount of energy can be saved as compared to the vapor - compression system.

An ejector is a pump-like device that uses the ‘venturi effect’ of a converging diverging nozzle, as shown in Fig. 1.4, to convert the pressure energy of a motive fluid to velocity energy which creates a low pressure zone that draws in and entrains a suction fluid and then recompresses the mixed fluids by converting velocity energy back into pressure energy.

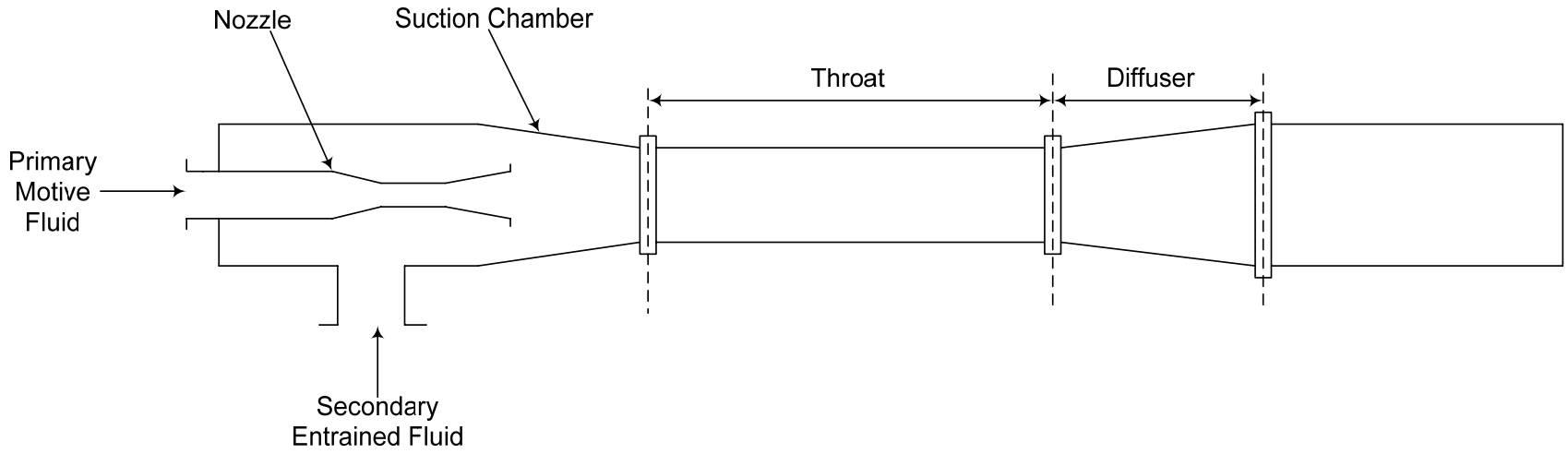

Figure 1.4 Schematic view of an ejector

1.5.1 Working Principle of the Ejector Cooling System

The operation of an ejector cooling system is represented schematically in Fig. 1.5. The saturated motive vapor of working fluid (refrigerant or water) enters the ejector's nozzle from the generator at a high temperature and pressure. This motive fluid undergoes expansion and leaves the nozzle with a very high velocity and a low pressure. This ejector action of this jet draws working fluid vapor (suction fluid) from the evaporator and maintains the vacuum necessary for operation. When the mixing of the two streams is complete, the diverging section slows the mixture down, thereby increasing its pressure. This is the reverse of the process occurring in the nozzle. This feature enables the ejector to discharge at a pressure that is greater than that at the suction branch. Thus, the ejector is capable of compressing or boosting the pressure of the fluid entrained.

The key design parameters of the ejector are the compression ratio and the entrainment ratio. The compression ratio of the ejector is defined as ratio of the ejector's outlet pressure (P_2), to the inlet pressure of the suction fluid (P_1). The entrainment ratio of the ejector is defined as the amount of motive fluid required to entrain and compress a given amount of suction fluid.

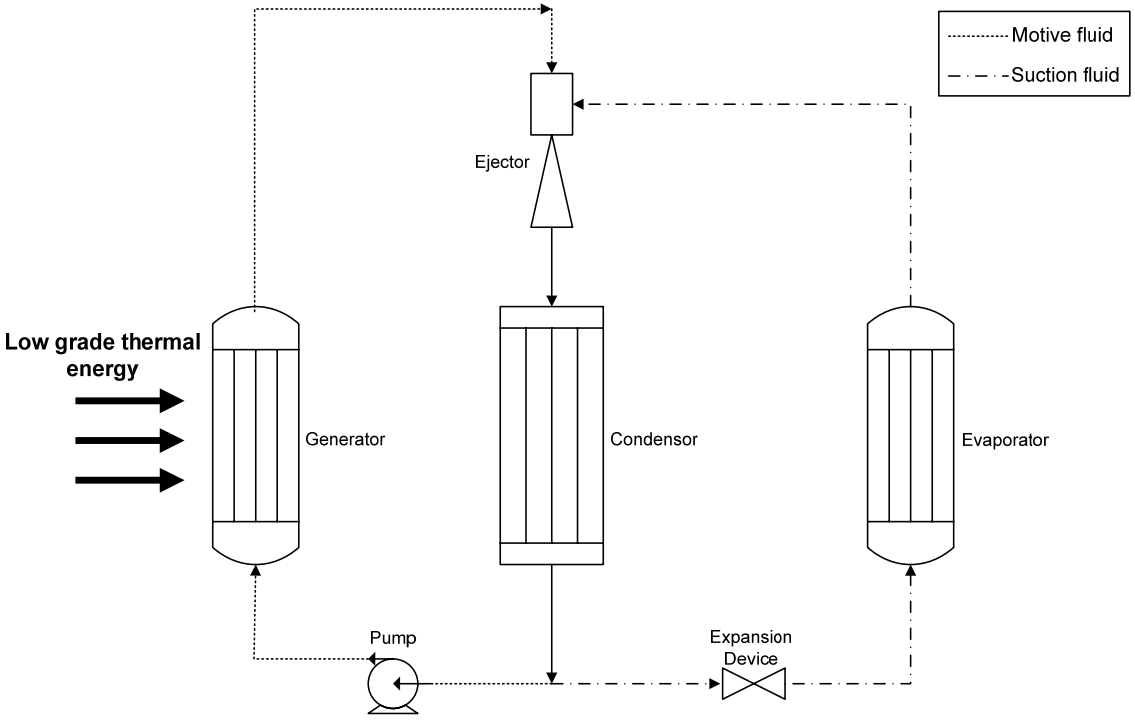

Figure 1.5 Working principle of ejector cooling system

Although the ejector refrigeration system has a small coefficient of performance in comparison with that of a vapor-compression systems, economical system can be obtained when waste heat, solar energy and exhaust heat are used to operate the system [6]. This low grade thermal energy is utilized in the generator to heat the working fluid. Other advantages of ejector cooling systems include simplicity and reliability as well as low initial and operating costs.

1.6 Water Extraction from Cooling Coils

Water is perhaps one of the most essential natural resource on this planet. Besides forming more than seventy percent of the human body[2], it is an indispensable asset for almost all fields of manufacturing, ranging from basic industries, such as agriculture, to highly sophisticated ones like microprocessors and semiconductors. In Saudi Arabia, the majority of the water used for domestic as well industrial purposes, is obtained through the desalination of the seawater. For agricultural purposes, the use of groundwater is more dominant. In 1981, the extensive involvement of the government in the agricultural sector and its provision of heavy subsidies, led to an agricultural revolution with the aim of achieving food self-sufficiency, particularly in wheat and dairy products[3]. As a result, the added value in agriculture increased by more than 70% in the period 1985-1991.

Due to this development in the agricultural sector, which is by far the largest water user, the depletion of groundwater has taken place at very fast rates. It is estimated that if this

---

[2] http://chemistry.about.com/cs/howthingswork/f/blbodyelements.htm

[3] http://www.eoearth.org/article/Water_profile_of_Saudi_Arabia

rate of ground water extraction is continued, the entire ground water reserves in Saudi Arabia will be exhausted in a period of 20 to 35 years.

Although, Saudi Arabia is already by far the largest producer of desalinated water, this water cannot be used for agricultural processes due to high cost involved in desalination. Thus other alternatives such as the reuse of treated wastewater or further refinement of the desalination process have to be considered in order to provide a substitute for the groundwater usage.

One such alternative could be the use of the water that is extracted from the cooling coils of large chilled water units. The cold air that is provided to the conditioned space is a mixture of the return air (from the conditioned space) and the fresh air (ambient unconditioned air). This percentage of fresh air may vary from zero (for common residential window units) to 100 percent (for hospitals and medical facilities), depending upon the application. In the coastal regions of Saudi Arabia, like the eastern province and the Makkah province, the average value of relative humidity is quite high reaching a maximum (100%) in the summer months. The flow of this ambient air over the cooling coils (in the evaporator or the air handler-based on the configuration of the air conditioning system) can lead to a significantly high rate of condensation, provided that the surface temperature of the coil is lower than the dew point temperature of the incoming air.

This condensate, if not removed from the unit, will tend to collect around the AHU and may lead to the formation of a small pond [7]. If the AHU is installed on roof top, the

collected water can have an adverse effect on the life and permeability of the roof. Thus the safe disposal of this condensate is very essential.

Studies have shown that although the water collected through this process may not be suitable for drinking, it can be an excellent for the purpose of irrigation[4]. Furthermore, in large air conditioning plants, the chemical composition of this extracted water makes it a frontrunner for use as makeup water for the cooling towers.

In the present study, due to the hot and humid conditions prevailing in the region of Dhahran in the summer months, the potential for water extraction from the cooling coils of the air handler are investigated.

1.7 Motivation and Objectives of the Present Study

The air conditioning in the Academic Complex (Jebel) of KFUPM[5] is accomplished by several central chilled water plants. These plants employ chillers of varying capacity ranging from 400 TR to about 1000 TR. But the pumping scheme, through which the chilled water is delivered to the air handler, in all these plants is the constant speed primary flow. By changing this primitive pumping scheme with the more advanced ones (primary-secondary and variable primary pumping schemes), significant amount of energy can be saved. Thus, the main objective of the present study is to assess the overall energy consumption of the three aforementioned pumping schemes for a particular academic building in the KFUPM campus. This is accomplished by developing a

---

[4] http://www.allianceforwaterefficiency.org/Condensate_Water_Introduction.aspx

[5] King Fahd University of Petroleum and Minerals

numerical model depicting the entire chilled water cooling system for the building concerned.

Once the working model of the chiller is finalized and operational, an exergy analysis for the individual components and that for the entire plant as a whole (taking into account the different pumping schemes) will be carried out in order to identify the various inefficiencies and also to study the effect of the different pumping schemes on these inefficiencies.

As an innovation, the effect of incorporating an ejector cooling system into the existing central plant, in place of the cooling tower required to cool the condenser water of the chilled water system, is investigated as the location of Dhahran and its average solar insolation permit the use of solar energy as an auxiliary energy source for the generator of the ejector cooling system.

Finally, an investigation of the rate of condensation in the air handler, during the summer months, is carried out by solving the governing equations. The possible utilization of the collected condensate, both within the existing chiller plant and the added ejector cooling system, is explored.

CHAPTER 2

LITERATURE REVIEW

Due to the widespread use of central chilled water systems over the span of several decades, considerable experimental as well as numerical studies have been conducted regarding the various aspects of these systems. Furthermore, several studies, observations and recommendations of on site field engineers who are directly involved with the chilled water systems have also been published. A brief account of the major work concerning the primary objectives of this thesis is presented in the following sections.

2.1 Pumping Schemes

Since the introduction of variable speed drives, variable speed pumping has been employed extensively in the air conditioning industry. But the method in which it is adapted for the chilled water distribution (Primary-Secondary or Variable Primary) remains highly debated till date.

In one of the earliest works concerning the variable flow pumping schemes, Kirsner [8] argued that a constant flow rate through the chiller evaporators was no longer necessary due to the development of microprocessor based controls and concluded that the low ΔT syndrome which is predominant in most chilled water systems could only be resolved by adopting variable flow oversized pumps.

Schwedler and Bradley [9] provided a detailed discussion on variable primary flow in chilled water systems and highlighted the fact that the power consumption for a given chiller virtually remains the same, irrespective of whether the system's primary flow is variable or constant. It was also pointed out that the major cost savings encountered by the use of variable primary flow was from the elimination secondary pump and the cost of its associated piping. For the case of a medical office building in Atlanta, Georgia, it was shown that the pump operating cost was reduced by almost 38% if the system was changed from constant primary-constant secondary to constant primary-variable secondary flow, and by a whopping 50% if the variable primary flow arrangement was adapted.

Liu [10] proposed a new scheme for a variable flow chilled water system. The distinctive feature of this scheme was the provision of an additional building bypass to maintain the minimum water flow rate through the chillers along with a chiller bypass which limits the flow of chilled water to the designed flow. Although significant improvement in terms of energy consumption over the more commonly used variable flow arrangement was not achieved, the decoupling capability of the primary-secondary system was retained to provide the necessary excess water when required.

Taylor [11] argues that in spite of its various advantages, the variable primary flow systems cannot be applied to all situations. The complexity of the bypass control and its possible failure as well as the problems related with chiller staging adversely affect the utilizability of the variable flow primary only arrangement. Emphasizes was laid on the fact that only in plants having several chillers with high base loads and where the manpower (engineers, operators, etc.) having adequate knowledge about the complicated

bypass control exist, should the variable primary flow be employed. In the absence of these conditions, the more commonly used primary-secondary arrangement is more suited.

Bahnfleth and Peyer [12] analyzed the different chilled water distribution schemes by conducting several parametric studies on numerically modeled central air conditioning plant equipment. The major parameters considered included the cooling load profile and climatic conditions, the number of chillers in the plant and the chiller temperature difference. Three different load types were selected to obtain a variation in the size and load profile shape. The cost factor was also incorporated into the study by considering the initial as well as the operating costs for the different pumping schemes. It was concluded that the variable primary flow arrangement surpassed the primary-secondary system in both the initial as well as the operating cost even when the primary-secondary system was not inflicted by low ΔT syndrome. However this edge of the variable flow scheme is decreased when multiple chillers are considered. The insensitivity of the power consumption of the chiller to the different distribution schemes was another highlighted statement.

Baker et al. [13] presented a detailed report which dealt with the air conditioning of two new office buildings, which were part of an expansion of an already existing large medical complex in Winchester, Virginia. A central chilled water plant that minimizes operating costs and at the same time maximizes efficiency and flexibility was the obvious choice for this purpose. The article traced the evolution of the design of this chilled water plant, from the initial challenges posed mainly by the integration of the plant with the existing system to the initial startup. Several alternatives concerning the flow of chilled

water, the power consumption by the various components and the temperatures of the fluids were analyzed. The most captivating feature of the design was that all the dynamic components of the plant were required to operate at variable speed. This meant that the chillers, cooling tower fans, and pumps had to be provided with finest efficiency variable frequency drives. Various tests for all the components with variable water flow rate were performed and the results were reported. For the chillers it was established that unless the lift between the condenser and the evaporator is reduced, the reduced speed of the chilled water pump was not economical. Similarly, a tradeoff between condenser water flow rate and the chilled water pumping power was also reported. In conclusion it was highlighted that constant monitoring and control by skilled operators and technicians was necessary for the smooth and optimum operation of the complex and dynamic plant

2.2 Exergy Analysis

The exergy analysis serves as a tool to locate and analyze the various inefficiencies occurring in a system. Several studies and analyses involving the principles of exergy analysis applied to the air conditioning systems have been conducted. But most of these studies deal with absorption and ejector cooling systems or cogeneration systems. Only a few studies concerned with the exergy analysis of vapor compression systems have been published to date. The main aim of these works was to identify the major components responsible for the inefficiencies occurring in the system in order to explore methods to reduce them.

Dincer and Cengel [5] provided a detailed discussion on the concepts of energy, entropy and exergy and the interactions between the three were presented. With the help of illustrative examples, the differences between the concept of energy and exergy were

highlighted. Furthermore, it was argued that several designers and engineers prefer the exergy analysis of a system in addition to or in place of the energy analysis, as it provides better insight and is more effective in efficiency improvement efforts than the energy analysis.

Yumrutas et al. [14] carried out an exergy analysis for the vapor compression refrigeration system (cooling capacity of 1kW) .The effect of evaporating and condensing temperatures on the various losses and the performance parameters of the system was investigated. It was observed that the evaporating and condensing temperatures have substantial effects on the exergy losses in the evaporator and condenser, in addition to the second law efficiency and COP of the cycle. The observation that a low temperature differential between the evaporator and the refrigerated space as well as between the condenser and outside air leads to an increase in second law efficiency as well as the COP with a simultaneous decrease in total exergy loss was also pointed out.

Harrell [15] conducted a detailed study of the chilled water distribution system being used in the Southern Illinois University Carbondale campus, which consists of a primary-secondary-tertiary water distribution system cooled by two centrifugal chillers, each powered by a dedicated steam turbine. All the necessary information regarding the operation of the in situ air conditioning system was collected. Statistical curve fitting models that characterized the chiller loads along with the operation of the chilled water distribution systems were developed. Following this, a comprehensive system model was created incorporating the steady-state, control volume, rate balances for mass, energy, exergy, and cost flows. The exergy analysis of the system showed that the steam turbine is the major source of exergy destruction. Moreover the water distribution losses at low

loads and the refrigeration cycle losses (contributed mainly by the compressor and evaporator) at high loads also added to the exergy cost. Conversion of the water distribution system to an all variable drive system and the replacement of the turbine with electric motors (to drive the chillers), was recommended to improve the efficiency of the chilled water system.

Taufiq et al. [16] developed a model for an evaporative cooling system and optimized it for the conditions of Malaysia. The direct evaporative cooling method was chosen for the study. An elaborate exergy analysis based on the open system and taking the atmospheric state as the dead state was carried. It was concluded that the exergy efficiency of the system increased with an increase in the relative humidity and that the mixing of the return and fresh air was the main cause of exergy destruction in direct evaporative cooling process.

In more recent works, Dai et al. [17] performed an exergy analysis as well as a parametric study on a novel combined power generation and ejector refrigeration system, based on the integration of the Rankine cycle with the ejector cooling cycle. The working fluid was taken as R123 for several advantages. The exergy analysis revealed that the major exergy loss occurs in the boiler closely followed by the ejector. The effect of various parameters such as, the evaporator and condenser temperatures and the turbine inlet and back pressure on the turbine power, refrigeration output and exergy efficiency was investigated. Finally, a parametric optimization with the exergy efficiency as the objective function was carried out for the combined cycle by means of genetic algorithms and the results were reported.

Khaliq et al. [18] conducted an exergy analysis of a cogeneration cycle for combined power production and refrigeration. The system considered was a combination of the Rankine cycle and the vapor absorption cycle, utilizing the waste heat from the industries as the heat source. Water along with lithium bromide was used as the refrigerant in the cycle. A new term defined as the power to cold ratio along with the first and second law efficiencies were used to analyze the performance of the system. The heat recovery steam generator was identified as the main source irreversibility and the effect of the composition and temperature of the flue gases on the performance of the system was investigated.

Yu et al. [19] performed an exergy analysis of a Joule-Thomson cryogenic refrigeration cycle with the addition of an ejector. The system was based on a conventional Joule-Thomson cycle with the exception that the expansion in the cycle was accomplished by an ejector in addition to the expansion valve. It was shown that the addition of the ejector reduced the total energy destruction as compared to the basic Joules-Thomson cycle. It was concluded that the compressor is the main source of exergy destruction and that the ejector pressure ratio is one of the most important factors affecting the distribution of exergy as well as the exergetic efficiency of the cycle.

2.3 Ejector Cooling

Over the past two decades numerous investigations, both experimental as well as numerical, have been carried out in the field of ejector cooling systems. The majority of these studies consider the use of solar energy as a means for providing the heat necessary for the generator, due to its abundant availability.

Abdulateef et al. [20] conducted an exhaustive literature review on solar driven ejector refrigeration systems starting from the invention of the ejector in 1901 and its subsequent utilization in the first ejector cooling system in 1910 to the most recent trends and developments. The selection criteria for the working fluid and their corresponding effects on the performance of the ejector cooling system were discussed in detail. The most common feasible designs (providing maximum energy with minimum cost) prevailing for the solar driven ejector cooling system were described along with their respective merits and drawbacks. The overwhelming dependence of solar ejector cooling systems on environmental factors such as cooling water temperatures, solar radiation, wind speed etc. and the need for extensive research in order to improve the performance of the solar ejector cooling system was also stressed upon.

Guo and Shen [21] investigated the performance of a solar ejector cooling system applied to a commercial building in Shanghai based on a lumped analysis combined with the dynamic model. The dynamic model was chosen to take advantage of its capability to provide a detailed model of the choking, shock and mixing phenomena occurring in the ejector. Particular ejector geometry was chosen and R134a was taken as the working fluid. The results of the mathematical simulations demonstrated that the solar-driven ejector refrigeration system could be designed to meet the cooling requirements of air conditioning for office buildings. An average COP of about 0.43 was achieved and it was emphasized that as much as 75% reduction in energy consumption can be obtained by using the solar assisted ejector cooling system in place of the conventional compressor powered system during the day time for commercial office buildings.

Wang et al. [22] carried out an experimental study of a ejector cooling system equipped with a multi functional generator. Along with providing the necessary heat for the process, the generator also doubled up as a thermal heat pump thereby eliminating the use of an electric pump. The construction of the ejector was optimized for using R141b as the working fluid and was later modified to suit the properties of a relatively new refrigerant R365mfc in order to maintain a high coefficient of performance (COP). The use of R365mfc, which had previously never been used for the ejector cooling system, was justified by highlighting the fact that it had an ODP[6] of almost zero as compared to that of R141b which has an ODP of 0.11 (both ODPs relative to R11). The experimental results demonstrated reliable performance operating at full cycle. Eventually, it was concluded that R365mfc could replace R141b without compromising the system performance provided the ejector design was optimized.

An experimental analysis of a solar powered steam ejector chiller was performed by Pollerberg [23]. The experimental setup consisted of a small test rig having a cooling capacity of 1kW, located at the University of Bochum, Germany. The performance of the system with two types of solar collectors namely, a parabolic trough collector and a vacuum tube collector, was studied for one year and the effect of the operating temperatures and pressures on the efficiency of the solar collectors and the COP of the system were reported. Following this, dynamic simulations were also performed to determine the annual mean efficiency of the solar collector, the annual mean COP of the

---

[6] Ozone depletion potential: The potential for a single molecule of the refrigerant to destroy the Ozone Layer. (http://www.comfort.uk.com/refrigerants.htm)

solar jet ejector cooling system and the annual mean total efficiency of the system for several international locations. In conclusion, based on the simulation results, the economic aspects of the system were analyzed for the two types of solar collectors possessing different areas. The economic analysis showed that the parabolic trough collectors are more profitable for large area collector fields and that the ratio of direct insolation to global insolation for a particular location had a significant impact on the economy of the system.

Rusly et al. [24] performed a computational fluid dynamics (CFD) analysis on an ejector cooling system combined with the vapor compression system. In this combined system, the evaporator of the ejector cooling system was used as an intercooler to cool the refrigerant being used in the vapor compression system. It was argued that the CFD analysis offered more complete flow field information and the results thus obtained were more in agreement with the experimental data than the one dimensional model. The effect of ejector geometry on the performance of the system was the main focus of the study. For a range of area ratios, it was shown that the performance of the ejector system was improved with an increase in the area ratio as long as the ejector operated in the critical (double-choking) mode. Moreover, for selected refrigerants and a range of operating conditions, the location of the maximum entrainment ratio was also determined.

Vidal and Colle [25] also performed a numerical study of a combined vapor compression ejector cooling cycle. The method of combination of these two systems was the same as that of Rusly et al. [24]. Refrigerant R134a was used as the working fluid in the mechanical vapor compression system whereas R141b was chosen for the solar energy driven ejector cycle. The performance of the system was simulated for the climatic

conditions of Florianópolis, Brazil, with specific values of cooling load, ejector dimensions and solar collector configuration. Variation of COP of the individual as well as the combined systems with changes in the evaporator, generator, condenser and intercooler temperatures were presented. Furthermore, an optimization process was carried out through which optimum values of specific collector area and inter cooler temperature were determined, with all the other variables remaining constant. Finally, the cost factor, taking into account the various costs such as the energy costs, the capital cost of collectors, inflation costs etc., was incorporated into the analysis in order to determine a breakeven point for the collector area. Beyond this point, the double stage solar ejector refrigeration system is comparable to an equivalent mechanical compression cooling system.

2.4 Water Extraction from Cooling Coils

Although the concept of water extraction from cooling coils has not been investigated in great detail, few studies are present. In the early nineties, Khalil [26] investigated the possibilities of dehumidification of atmospheric air as a potential source of fresh water. He presented the argument that for climatic conditions with high temperature and relative humidity (such as those prevailing in the coastal areas of UAE), the cooling system could be optimized to obtain substantial amount of fresh water. To achieve this, the operating and the ambient conditions that provide the maximum condensate rate were analyzed. It was indicated that for the region of Abu Dhabi, when the value of relative humidity was between 60 to 100% as much as 4 litres of water per person per day could be collected from a typical domestic air conditioning application.

In recent works, Habeebullah [27] investigated the idea of water production along with its limitations, from atmospheric air when passed through evaporator coils, in areas where hot and humid conditions are prevalent such as the city of Jeddah in the Kingdom of Saudi Arabia. It was observed that the maximum rate of water collection was achieved when the air velocity was at or near the design value. Increase of air velocity beyond the design value, resulted in a decreased water yield, due to the reduced capacity of the evaporator to handle the excessive flow rate, whereas supplying air below the design value led to frosting in the evaporator coils. It was concluded that for the considered geometry, ambient conditions and refrigerant an average water yield of 16.97 kg/m^2h for the month of August and 14.44 kg/m^2h for the month of February could be achieved.

CHAPTER 3

MODELING OF COMPONENTS

In order to depict and simulate the performance of the chilled water system being considered, a detailed numerical model was developed using the fundamental concepts and basic equations of heat and mass transfer. The main components of the central chilled water systems that were modeled included the air handler, the chiller - consisting of an evaporator, a condenser, a compressor and an expansion device, the pumps - both constant speed and variable speed, and the cooling tower. Each of these components was first modeled individually, and then combined together to describe the performance of the entire chilled water system. The software package Engineering Equation Solver (EES) [28] was employed for the purpose of compilation of the various equations used. The main reason for utilizing EES this is due to the fact that it possesses several interesting features, a few of which are listed below:

i) Large built in database of thermodynamic properties for various fluids as well as materials

ii) Simple set of perceptive commands which are easy to learn[7]

iii) Capability to perform a variety of parametric studies

iv) Utilization of enhanced convergence techniques for the solution of large number of transcendental equations.

Consecutively, a model of an ejector cooling system was also developed and incorporated with the central chilled water system. Once again EES was utilized for this purpose.

3.1 System Description

The academic and administrative buildings in the KFUPM campus are designated by numbers, starting from 1 to 59, depending on the location and the chronological order of construction. All these buildings are serviced by central chilled water air conditioning systems. In the present study the building 59 is selected for analysis. This building is serviced by three chillers each of 500 TR capacities. Each chiller is provided with a dedicated chilled water distribution pump. A cooling tower with a corresponding condenser water pump is provided for each chiller in order to cool the refrigerant.

In the present study only a single set of chiller-pump-cooling tower unit is considered for analysis. The chilled water is distributed to several air handlers which vary slightly in dimension and capacity. For the purpose of ease of calculation and analysis, all the air handlers are considered of equal dimensions and capacity (25 TR). This consideration has

[7] http://sel.me.wisc.edu/ees/new_ees.html

a negligible effect on the overall performance of the system as the total capacity of the air handlers remains equal to 500 TR which is equal to the full load capacity of the chiller.

3.2 Air Handler Modeling

The air handlers present in building 59 are variable air volume (VAV) systems. Air handlers mainly consist of a fan, a cold deck, a hot deck and bypass as shown in Fig. 3.1. As the effect of the hot deck and bypass on the chilled water system is insignificant, only the fan and cold deck are considered in this analysis. The fan of the air hander is equipped with a variable speed drive to vary the air volume corresponding to the load. In order to maintain a constant room temperature of 75^{o}F (24^{o}C) and a maximum relative humidity of 55%, the cold deck temperature is fixed at 58^{o}F (14.4^{o}C). Any variation in the temperature of the room is accompanied by a corresponding change in the flow rate of air and/or flow rate of water. The change in the flow rate of air is accomplished by changing the speed of the fan which is made possible by a variable speed drive, whereas the change in the flow rate of water is accomplished by two way valves. A ratio of 15% fresh air to 85% return air is maintained in the air handler

The cooling coil of the cold deck is nothing but a plate-fin heat exchanger having staggered arrangement of tubes. Owing to propriety reasons, the constructional details of the air handler cannot be disclosed.

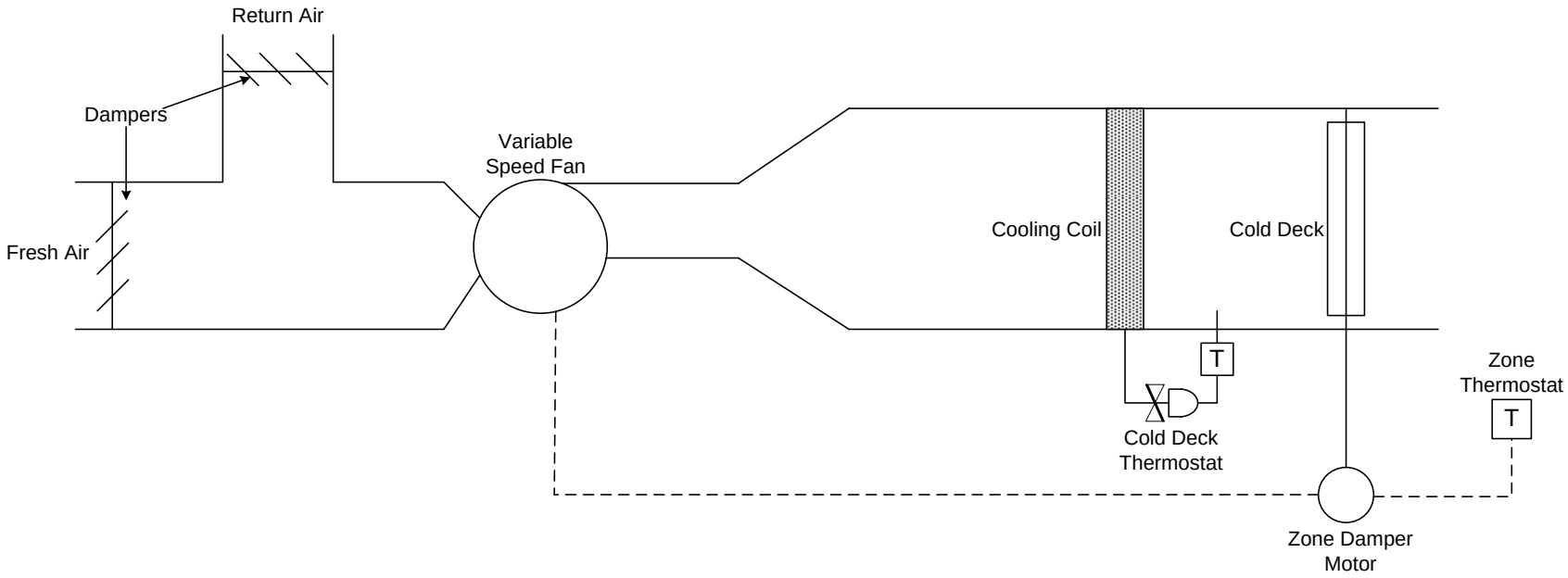

Figure 3.1 Schematic of variable volume air handler

A cross flow arrangement is created as the fan blows the air over the tubes of the cooling coil through which the chilled water is flowing. A typical chilled water cooling coil is shown in Fig. 3.2.[8]

The air handler is modeled using number of transfer units (NTU) - effectiveness relations and the air handler load is assumed to be a function of outdoor dry bulb temperature [29]. This load profile is discussed in detail in the subsequent chapter.

3.2.1 Heat Transfer Calculations

The air handler is modeled using the following three basic heat transfer equations [30]

The heat transfer rate on the air side of the cooling coil is given by:

$$\dot{Q}_{load,ah} = \dot{m}_{a,ah} C_{p,eff} \left(T_{a,ah,in} - T_{a,ah,out}\right) \tag{3.1}$$

and on the water side by:

$$\dot{Q}_{load,ah} = \dot{m}_{w,ah} C_{p,w,ah} \left(T_{w,ah,out} - T_{w,ah,in}\right) \tag{3.2}$$

The heat transfer for the heat exchanger using the effectiveness is given by:

$$\dot{Q}_{load,ah} = \varepsilon_{ah} C_{min,ah} \left(T_{a,ah,in} - T_{w,ah,in}\right) \tag{3.3}$$

[8] www.colmaccoil.com

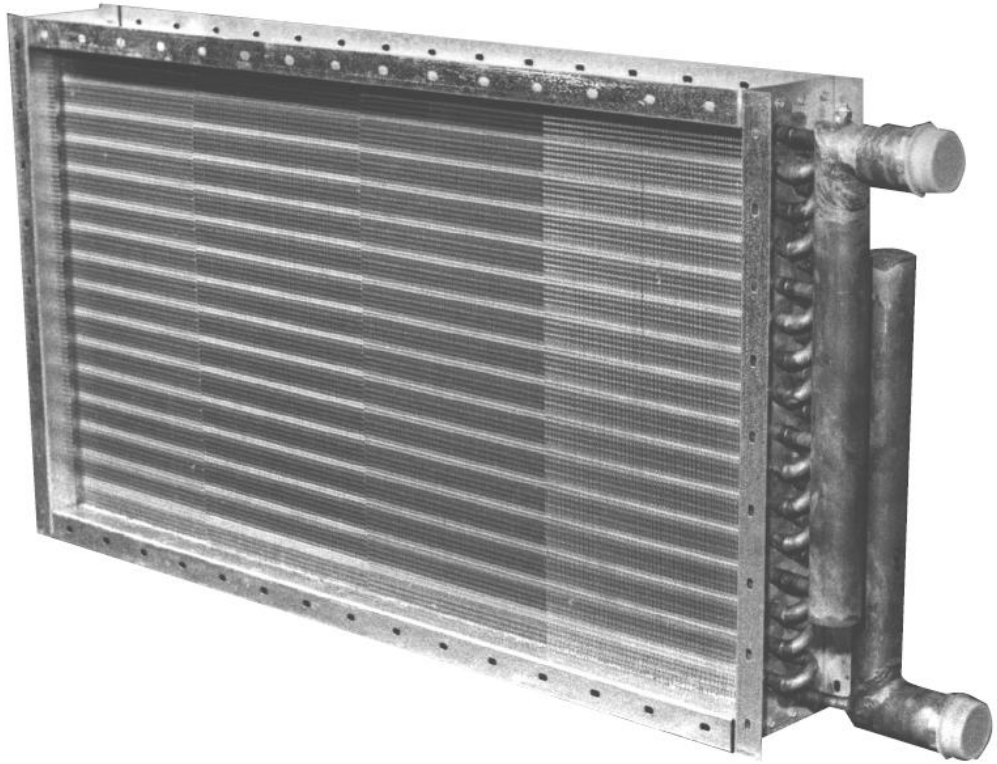

Figure 3.2 Chilled water cooling coil used in air handlers

The effective specific heat of the air-water vapor mixture flowing over the tubes of the coil is given by:

$$Cp_{eff} = \frac{h_{a,ah,in} - h_{a,ah,out}}{T_{a,ah,in} - T_{a,ah,out}} \tag{3.4}$$

The relationship between the effectiveness and NTU for a cross flow heat exchanger with one fluid mixed (water in this case) and the other unmixed (air water vapor mixture) can be obtained from the classical heat transfer textbook [30].

The overall heat transfer conductance of the coil, $UA_{tot,ah}$ is given by:

$$\frac{1}{UA_{tot,ah}} = \frac{1}{h_{i,ah}A_{i,ah}} + \frac{ln\left(D_{o,ah} / D_{i,ah}\right)}{2 \cdot \pi \cdot k_{pipe} L_{ah} n_{row} n_{column}} + \frac{1}{h_{o,ah}A_{o,ah}\eta_{o,ah}} \tag{3.5}$$

The outer surface effectiveness is related to the fin efficiency and the air handler geometry using the following expression:

$$\eta_{o,ah} = 1 - \left(A_{f,ah} / A_{o,ah}\right)\left(1 - \eta_{fin}\right) \tag{3.6}$$

Where

$$A_{o,ah} = A_{t,ah} + A_{f,ah} \tag{3.7}$$

The air side heat transfer coefficient is calculated using the method given in [31]. This method requires the determination of a factor, JP, which is a function of the air hander geometry as well as flow characteristics.

$$JP = Re_{D,o,ah}^{-0.4}\left(A_{o,ah} / A_{t,ah}\right)^{-0.15} \tag{3.8}$$

The factor JP is related to another factor j_4, which determines a four-row coil's heat transfer performance, as shown below:

$$j_4 = 0.2618JP + 0.0014 \tag{3.9}$$

The variable, j_n for a coil with other than four rows is found by,

$$\frac{j_n}{j_4} = \frac{1-\left(1280 n_{row} Re_{L,ah}{}^{-1.2}\right)}{1-\left(1280 \times 4 Re_{L,ah}{}^{-1.2}\right)} \tag{3.10}$$

The j_n factor is then related to the heat transfer coefficient by,

$$h_{o,ah} = \left(Cp_{eff} G_{a,ah} \frac{j_n}{Pr_{a,ah}{}^{2/3}} \right) \tag{3.11}$$

The heat transfer coefficient on the water side is a function of fluid and flow properties. Depending upon whether the flow is turbulent or laminar, the heat transfer coefficient can be determined from the correlations given by Incropera and Dewitt [30] and Bejan [32].

Once the heat transfer coefficients have been determined, the next step is to calculate the pressure drop on the air as well as the water side.

3.2.2 Pressure Drop Calculations

The air side pressure drop is calculated by the model developed Rich [33]. In this method the total pressure drop is assumed to be combination of two individual components: one due to the tubes alone and the other due to the presence of the fins.

The pressure drop due to the fins is given by:

$$\Delta P_{f,ah} = f_{f,ah} \frac{G_{a,ah}^{\ 2}}{\left(2 \cdot \rho_{m,ah}\right)} . \sigma_{ah} \tag{3.12}$$

The friction factor $f_{f,ah}$ is related to the Reynolds number (based on longitudinal spacing) by the equation:

$$f_{f,ah} = 1.7 Re_{b,ah}^{\ -0.5} \tag{3.13}$$

The pressure drop caused by the staggered tubes is given by [34]:

$$\Delta P_{t,ah} = n_{row} f_{tube,ah} \chi_{ah} \left(\rho_{a,ah} \cdot \frac{\left(V_{a,ah,\max}\right)^2}{2} \right) \tag{3.14}$$

The factors $f_{tube,ah}$ and χ_{ah} are determined graphically from Fig. 3.3 [34]

Thus the total pressure drop on the air side is given by the expression

$$\Delta P_{tot,ah} = \Delta P_{f,ah} + \Delta P_{t,ah} \tag{3.15}$$

The pressure drop across the water side of the air handler is once again the sum of two quantities. Firstly the pressure drop due to the straight portion of the tubes and the pressure drop due to the bends and the header.

The friction factor for the water flowing inside the tubes is found by the relation given by Haaland [35] :

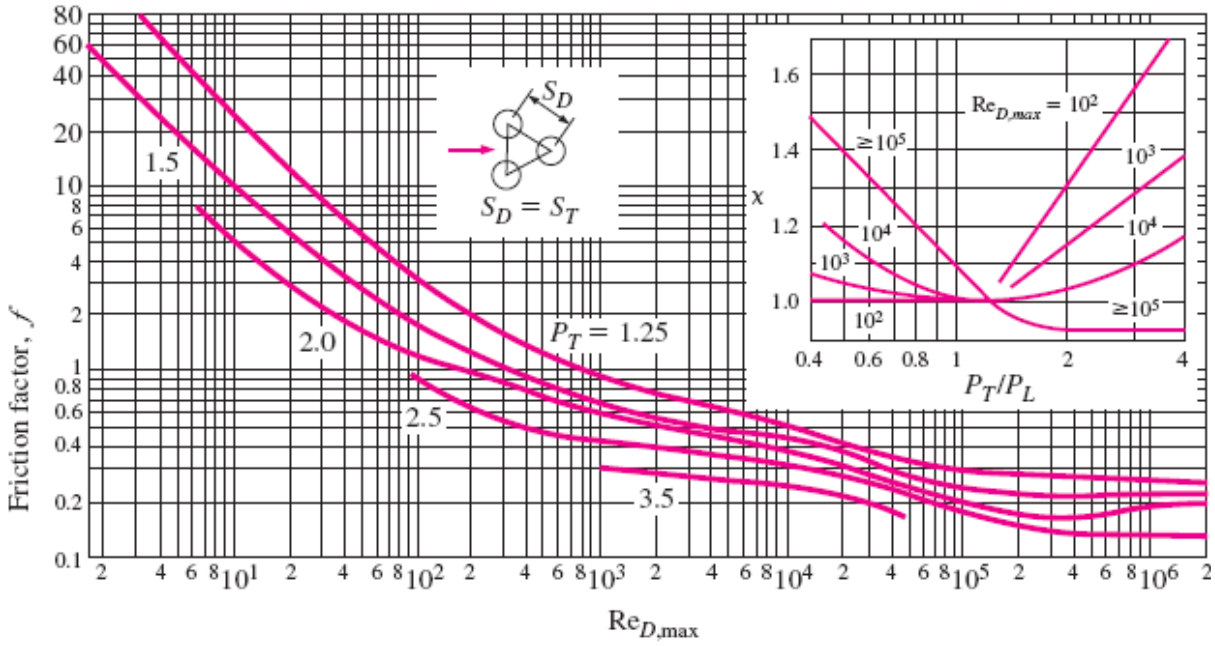

Figure 3.3 Friction factor and correction factor χ for staggered tube arrangement

$$f_{i,ah} = \frac{1}{\left(-1.8 \cdot log_{10} \left(\frac{6.9}{Re_{D,i,ah}} + \left(\frac{\varepsilon_{pipe,ah}}{D_{i,ah} \cdot 3.7} \right)^{1.11} \right) \right)^2} \tag{3.16}$$

where Re_D is the Reynolds number based on the diameter of the tube.

From this friction factor, the pressure drop is calculated as:

$$\Delta P_{tube,ah} = n_{row} \frac{f_{i,ah} L_{ah}}{D_{i,ah}} \left(\rho_{w,ah} \frac{V_{w,ah}^{\ 2}}{2} \right) \cdot \tag{3.17}$$

In order to calculate the pressure drop in bends the assumption used by Klawunder [29] is used. Under this situation each header of the cooling coil in the air handler contains two 90^0 bends or one 180^0 bend. Thus the air handler has a total of five 180^0 bends, two resulting from the inlet and outlet headers and the remaining three as a result of the connections between the four passes of the air handler. The head due to the bends is given by [36] :

$$Head_{bend} = K \frac{V_{w,ah}^{\ 2}}{2 \cdot g} \tag{3.18}$$

where K is a constant commonly known as the bend coefficient and is dependent on the tube diameter as well as bend geometry.

3.2.3 Air Handler Fan Modeling

In order to model the fan, an isentropic efficiency of 0.65 is assumed. This isentropic efficiency is the ratio of the change in enthalpy under isentropic conditions to the change in enthalpy under actual conditions.

With this value of isentropic efficiency, the exit enthalpy can be calculated as:

$$h_{a,fan,out} = \left(\frac{h_{a,fan,out,rev} - h_{a,fan,in}}{\eta_{fan}} \right) + h_{a,fan,in} \tag{3.19}$$

The term $h_{a,fan,out,rev}$ represents the leaving enthalpy of the air if the fan was operated reversibly. In order to calculate this value of the enthalpy, three independent properties of the air water vapor mixture at the exit are required. For this purpose, the exit pressure is taken as the sum of the inlet pressure and the pressure drop occurring outside the tubes of the chilled water coil. Additionally, the values of the humidity ratio and the entropy are taken equal to the inlet condition.

3.3 Modeling of Pumps

In the existing central chilled water system being used for air conditioning the building 59, a constant speed pump is used to circulate the chilled water. Similarly a constant speed pump is also used for the circulation of condenser cooling water. The design parameters of these pumps such as the required NPSH, the impeller diameter, the suction and discharge pressures, the flow rate, the pump off pressure etc. are known. The power consumption as well as rpm of the pump motor is also available. But the operating characteristic curves of these pumps (provided by the manufacturer) are not available. Keeping these factors in mind , the Goulds Pump Selection Software (PSS) [37] is used to select those pumps that match the existing pumps in all aspects. The selection of variable speed pumps is also performed in a similar manner. While selecting the pumps, an attempt was made to choose those pumps that have comparable values of best efficiency points (BEPs).

3.3.1 Constant Speed Pumps

From the operating characteristic curves, the three important parameters of the pump namely the pump head, the pump efficiency and the shaft power, are determined as a function of flow rate.

The variation of the pump head with the flow rate (GPM) is shown in Fig. 3.4. This relationship can be represented by the equation,

$$Head_{pump} = A_1 + B_1 \cdot GPM_{pump} + C_1 \cdot GPM_{pump}^{\ 2} + D_1 \cdot GPM_{pump}^{\ 3} \qquad (3.20)$$

Where

$A_1 = 190.99$

$B_1 = -0.154$

$C_1 = 8.22E\text{-}07$

$D_1 = -2.76E\text{-}08$

The relationship between the pump efficiency and the flow rate as shown in Fig. 3.5 can be represented by the equation

$$\eta_{pump} = A_2 + B_2 \cdot GPM_{pump} + C_2 \cdot GPM_{pump}^{\ 2} + D_3 \cdot GPM_{pump}^{\ 3} \qquad (3.21)$$

Where

$A_2 = 0.0022$

$B_2 = 0.00183$

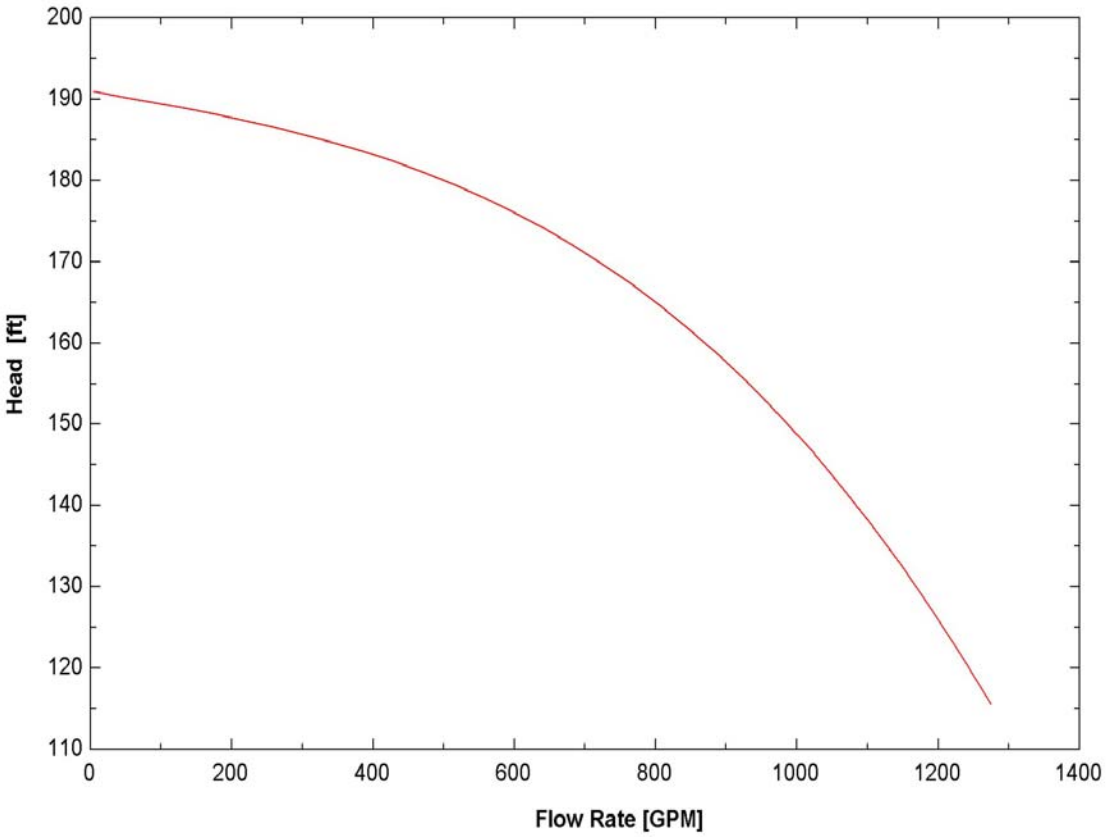

Figure 3.4 Variation of pump head with flow rate

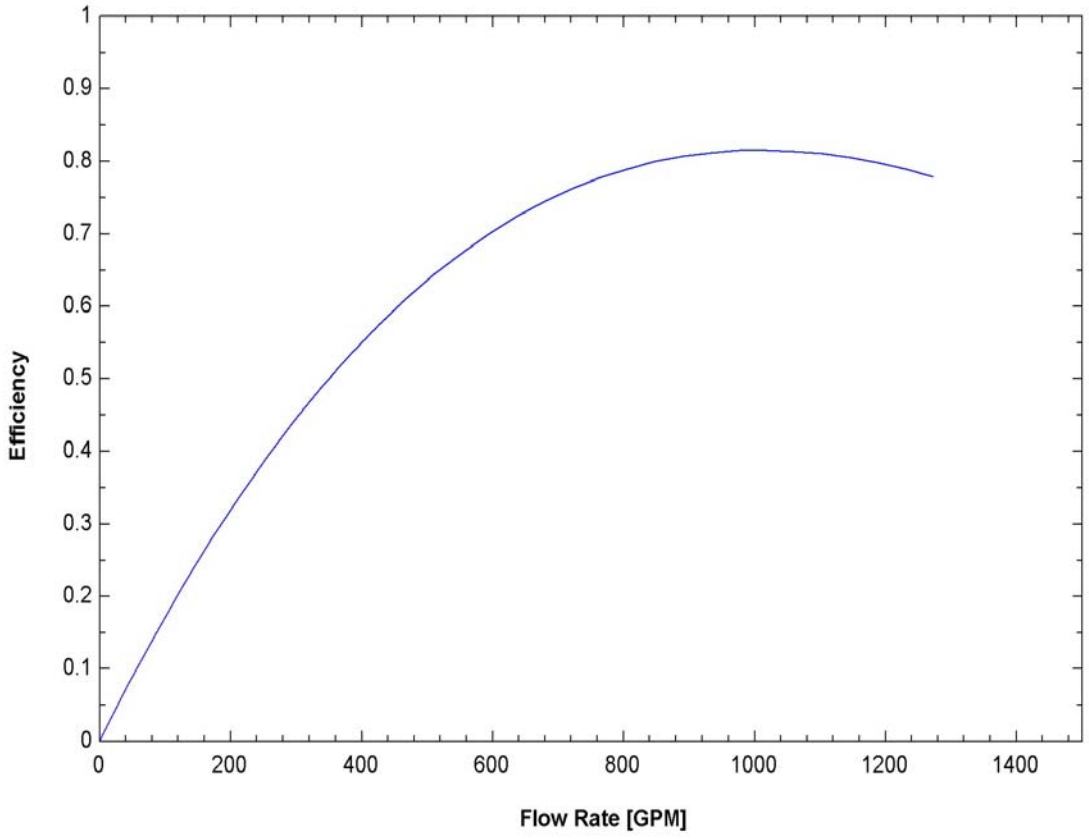

Figure 3.5 Variation of pump efficiency with flow rate

C_2 = -1.228E-06

D_2 = 2.125E-10

Finally, the relationship between the shaft power and the flow rate (Fig. 3.6) can be expressed y the equation

$$\dot{W}_{shaft} = A_3 + B_3 \cdot GPM_{pump} + C_3 \cdot GPM_{pump}^{\ 2} + D_3 \cdot GPM_{pump}^{\ 3} + E_3 \cdot GPM_{pump}^{\ 4} \quad (3.22)$$

Where

A_3 = 25.746

B_3 = 0.0202

C_3 = -8.032E-06

D_3 = 2.0743E-08

E_3 = 1.271E-11

The total power consumed by the pump is determined by:

$$\dot{W}_{pump} = \frac{\dot{W}_{shaft}}{\eta_{motor}} \quad (3.23)$$

Where η_{motor} is the efficiency of the motor and is taken as a constant value of 93%.

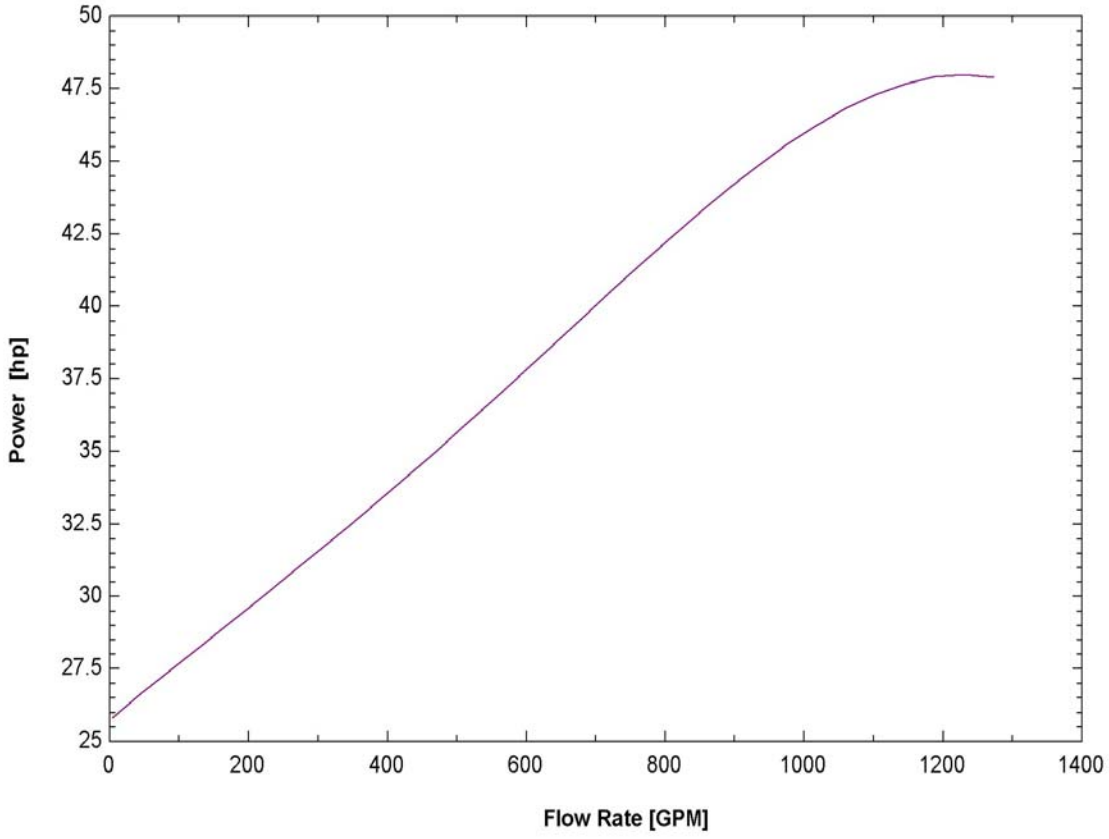

Figure 3.6 Variation of power with flow rate

3.3.2 Variable Speed Pumps

As the variable speed pump does not actually exist in the present chilled water system, a variable speed pump is chosen such that it takes care of one third of the total head in the chilled water circulation loop. In a variable speed pumping system the system head is dictated by the flow rate through the air handler. The pressure differential between the chilled water coil inlet and exit is maintained at a constant value, and the pump speed is altered to maintain this value. The pump head varies due to the contribution of several factors such as piping, tube bends and evaporator head losses.

The operating characteristic curves of the variable pump being used, at the design speed as well as two other speeds are shown in Fig. 3.7 [37]. In order to determine the operating characteristics of the pump, a design speed at which the pump operates most frequently, is chosen. The variation of pump head with the flow rate at this design speed is referred to as the design pump curve and can be represented by the equation:

$$Head_{design} = A_4 + B_4 GPM_{design} + C_4 GPM_{design}^{\ 2} + D_4 GPM_{design}^{\ 3} \qquad (3.24)$$

Where

A_4 = 52.271

B_4 = -0.0083

C_4 = 1.826E-06

D_4 = -3.498E-09

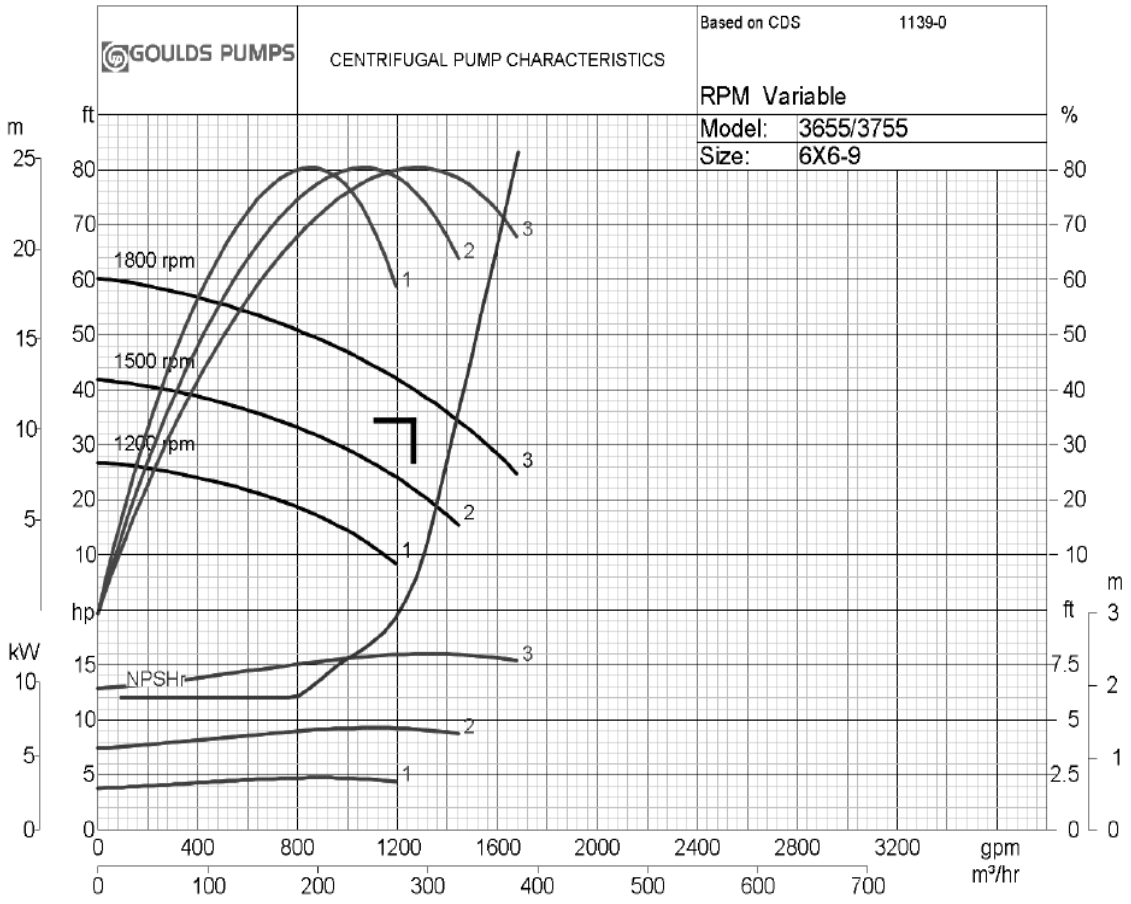

Figure 3.7 Operating characteristics of variable speed pump

The efficiency of the pump as a function of the flow rate, at the design speed can be described by the following equation:

$$\eta_{design} = A_5 + B_5 GPM_{design} + C_5 GPM_{design}^{\ 2} + D_5 GPM_{design}^{\ 3} + E_5 GPM_{design}^{\ 2} \qquad (3.25)$$

Where

A_5 = -0.0055

B_5 = 0.0014

C_5 = -7.934E-07

D_5 = 3.452E-10

E_5 = -1.2780E-13

In situations when the pump is not operating at the design speed, the actual speed and the corresponding head of the pump is determined by the following affinity laws:

$$N_{pump,act} = N_{pump,design}\left(\frac{GPM_{pump}}{GPM_{design}}\right) \qquad (3.26)$$

And

$$Head_{actual} = \left(\frac{N_{pump,act}}{N_{pump,design}}\right)^2 Head_{design} \qquad (3.27)$$

Similarly the efficiency of the pump is also reduced at lower pump speeds. Therefore, the following relation is used to calculate the actual pump efficiency [38]:

$$\eta_{pump} = \eta_{design}\left[0.816 + \left(0.403\frac{N_{pump,act}}{N_{pump,design}}\right) - 0.218\left(\frac{N_{pump,act}}{N_{pump,design}}\right)^2\right] \quad (3.28)$$

The total pumping power of the pump is calculated by the relation:

$$\dot{W}_{pump} = \dot{m}_{w,pump}\frac{h_{pump,out} - h_{pump,in}}{\eta_{motor,vsd}} \quad (3.29)$$

Where $\eta_{motor,vsd}$ is a combination of motor and variable speed drive efficiency given by the expression [29]:

$$\eta_{motor,vsd} = 0.0982 + 1.846339\left(\frac{N_{pump,act}}{N_{pump,design}}\right) - 1.029\left(\frac{N_{pump,act}}{N_{pump,design}}\right)^2 \quad (3.30)$$

The pump described in section 3.3.1 is used as the primary pump in both the single loop constant flow as well as the single loop variable primary flow pumping scheme and as the secondary pump in the primary-secondary flow pumping scheme. The pump delineated in section 3.3.2 is used as the primary pump in the primary-secondary flow pumping scheme.

3.4 Chiller Modeling

The chiller considered in the present study is a 500 TR capacity modern day chiller. Due to propriety reasons, any reference to the manufacturer has been omitted. Furthermore, the geometrical details of the various components of the chiller are also unavailable. The main components of the chiller that are modeled include the compressor, the evaporator and the condenser. All these components are modeled without the use of geometrical details, utilizing only the data provided by the manufacturer. The main purpose of

modeling is to prognosticate the performance of the various components at different loads temperatures and pressures. The data obtained from the manufacturer for different operating conditions are shown is table 3.1.

3.4.1 Compressor Model

The compressor power consumption is modeled as a function of the load on the chiller. The expression obtained is,

$$KW_{comp} = A_6 Q_{ton,evap}{}^2 + B_6 Q_{ton,evap} + C_6 \tag{3.31}$$

Where

$A_6 = 0.0004$

$B_6 = 0.4021$

$C_6 = 80.631$

The comparison between the actual power consumption of the compressor is shown in Fig. 3.8. The value of R^2 obtained for the above correlation comes out to be 0.999. The maximum error obtained is about 2.4% whereas the average error is around 1.2%.

3.4.2 Evaporator Model

The evaporator is a shell and tube heat exchanger. But due to the lack of the geometrical details concerning the evaporator construction, the heat transfer and pressure drop calculations cannot be carried out using the conventional procedures defined for the analysis of such type of heat exchangers.

Table 3.1 Manufacturer's data for 500 TR Chiller

Compressor				Evaporator					Condenser				
Tons	% Load	kW	KW/Ton	LWT	GPM	EWT	Ref. Temp	PD (ft)	EWT	GPM	LWT	Ref.	PD (ft)
500	100	391	0.782	42	1200	51.98	40.08	16	93	1600	102.09	103.48	12.7
450	90	351	0.78	42	1200	50.99	40.08	16	93	1600	101.17	102.5	12.7
400	80	309	0.772	42	1200	49.99	40.08	16	93	1600	100.25	101.4	12.7
350	70	273	0.78	42	1200	48.99	40.08	16	93	1600	99.36	100.4	12.7
300	60	240	0.8	42	1200	47.99	40.08	16	93	1600	98.47	99.33	12.7
250	50	209	0.836	42	1200	46.99	40.08	16	93	1600	97.6	98.32	12.7
200	40	181	0.905	42	1200	45.99	40.08	16	93	1600	96.73	97.32	12.7
150	30	152	1.013	42	1200	44.99	40.08	16	93	1600	95.86	96.31	12.7
100	20	124	1.24	42	1200	44	40.08	16	93	1600	94.99	95.3	12.7
91.7	18.3	120	1.308	42	1200	43.83	40.08	16	93	1600	94.84	95.13	12.7
450	90	350	0.778	42	1080	51.98	40.29	13.3	93	1600	101.17	102.5	12.7
375	75	291	0.776	42	900	51.98	40.42	9.7	93	1600	99.81	100.9	12.8
300	60	240	0.8	42	720	51.98	40.41	6.5	93	1600	98.48	99.34	12.8
256	51.2	213	0.832	42	615	51.97	40.36	5	93	1600	97.7	98.44	12.8

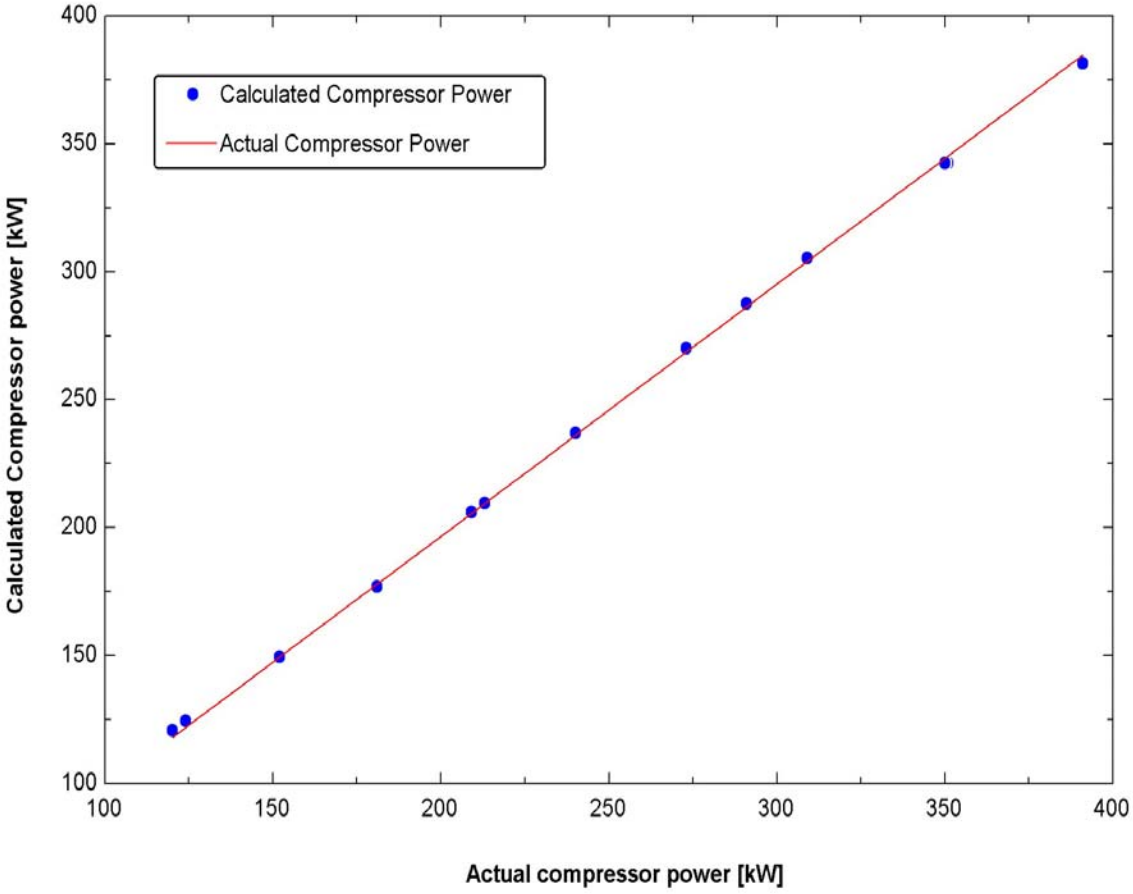

Figure 3.8 Comparison between the actual and modeled compressor power

3.4.2. (a) Heat Transfer Calculation

Using the assumptions made in [39] and [29], and by performing several multiple regression analyses [40], the evaporator UA was modeled as a function of chiller load and flow rate. The relation obtained takes the in the form of the following equation:

$$UA_{evap} = A_7 Q_{ton,evap}{}^2 + B_7 Q_{ton,evap} + C_7 GPM_{evap} + D_7 \quad (3.32)$$

Where

A_7 = -0.224E+01

B_7 = 0.301E+04

C_7 = 0.282E+03

D_7 = -0.186E+06

The value of R^2 for the above correlation is 0.998 where as R^2_{adj} = 0.997. The comparison of the values of UA obtained from this correlation and those obtained from the manufacturer's data is shown in fig 3.9. The maximum error encountered is less than 2% whereas the average error is about 0.01%.

3.4.2. (b) Pressure drop Calculation

From the manufacturer's data it can be clearly seen that the pressure drop is dependent on the flow rate only. This variation can be represented by the equation

$$Head_{evap} = A_8 \left(GPM_{w,evap} \right)^{B_8} \quad (3.33)$$

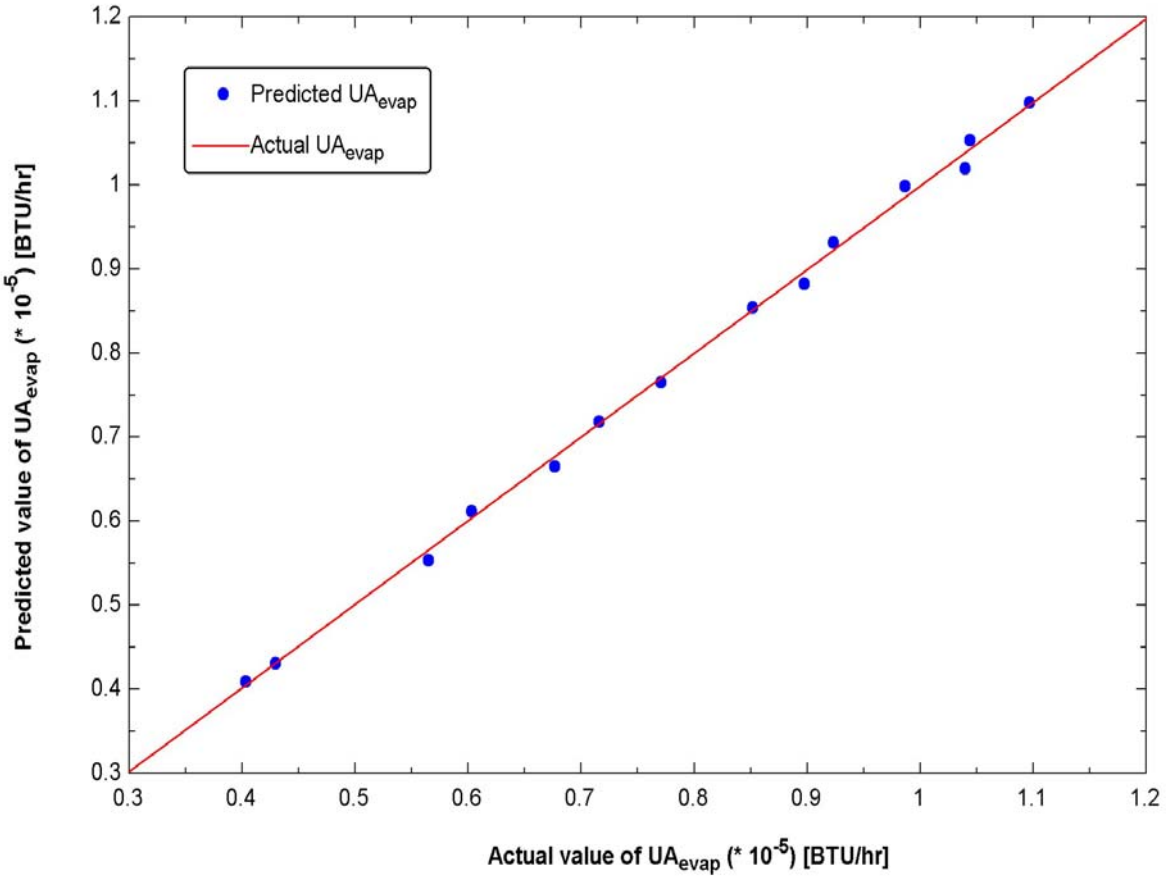

Figure 3.9 Comparison of the evaporator actual UA with the calculated UA

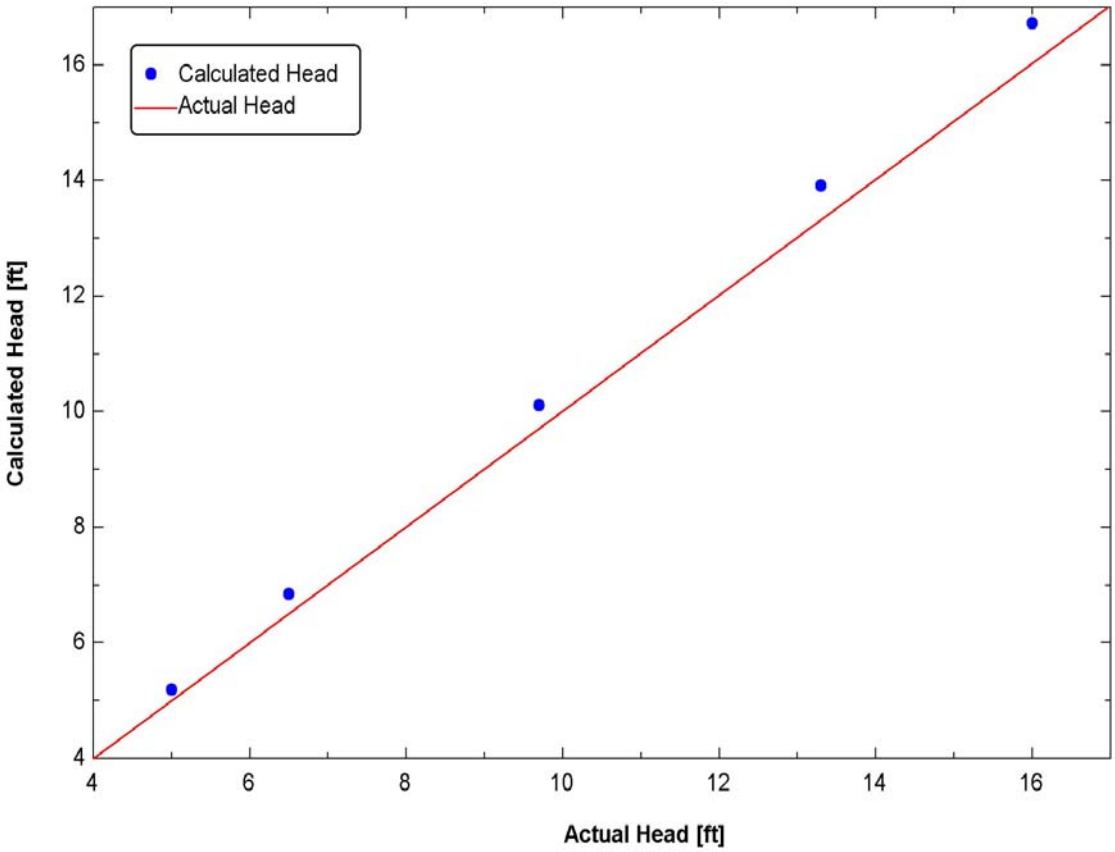

Figure 3.10 Comparison of actual and calculated values of evaporator pressure drop

Where A_8 = 7E-05 and B_8 = 1.7467

The comparison of this developed relationship with the actual data is shown in Fig. The value of R^2 is obtained as 0.99. The maximum, as well as the average error is around 5%.

3.4.3 Condenser Modeling

The modeling of the condenser is accomplished by the following fundamental heat transfer equations used for the analysis heat exchangers [41] :

$$\dot{Q}_{cond} = \dot{m}_{w,cond} \cdot C_{w,cond} \cdot \left(T_{w,cond,out} - T_{w,cond,in} \right) \tag{3.34}$$

$$\dot{Q}_{cond} = \varepsilon_{cond} \cdot \dot{m}_{w,cond} \cdot C_{w,cond} \cdot \left(T_{ref\,,cond} - T_{w,cond,in} \right) \tag{3.35}$$

$$\varepsilon_{cond} = 1 - exp\left(-NTU_{cond} \right) \tag{3.36}$$

$$NTU_{cond} = \frac{UA_{cond}}{\dot{m}_{w,cond} \cdot C_{w,cond}} \tag{3.37}$$

Utilizing the above equations and also considering the relation that,

$$\dot{Q}_{cond} = \dot{Q}_{evap} + \dot{W}_{comp} \tag{3.38}$$

the effectiveness of the condenser can be calculated. This calculated value comes out to be approximately 0.86 for all the different loads and flow conditions. Thus in order to calculate the UA value of the condenser, a constant value of the effectiveness equal to 0.8644 is chosen. The results obtained are shown in Fig. 3.11

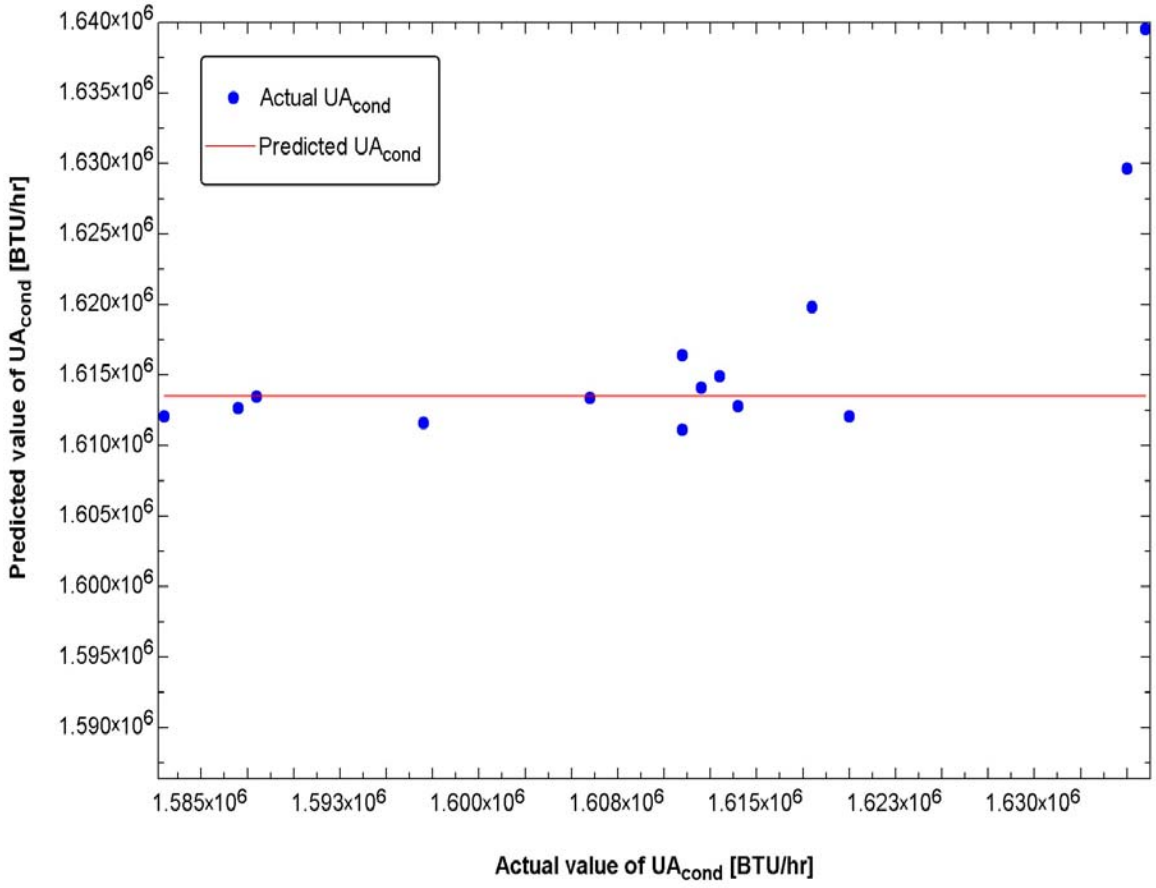

Figure 3.11 Comparison of the evaporator actual UA with the calculated UA

The maximum error encountered while using the above approximation is less than 2%, and the average error is less than 0.5%.

In case of the pressure drop through the condenser, a careful examination of the manufacturer's data reveals that the condenser head remains constant for all the test conditions. Thus a constant pressure head of 12.72 ft., corresponding to the manufacturer's data is taken.

3.5 Cooling Tower Model

The main two components being affected by the ambient conditions are the air handler and the cooling tower. The cooling tower controls the condenser water inlet temperature, which in turn influences the compressor operation. Due to this reason, the inclusion of the cooling tower was necessary in the chilled water system model.

The cooling tower was modeled on similar grounds as given in [29], and was then adapted for the conditions of building 59. The most interesting feature of this model was the introduction of a quantity known as the saturation specific heat (C_s) which is the derivative of the saturation air enthalpy with respect to the air-water interface temperature. This saturation specific heat can be described by the equation,

$$C_s = \left(\frac{dh_s}{dT} \right)_{T=T_s} \tag{3.39}$$

If the saturation specific heat is assumed to be uniform throughout the cooling tower, the above equation can be approximated as:

$$C_s = \frac{h_{s,w,tow,in} - h_{s,w,tow,out}}{T_{w,tow,in} - T_{w,tow,out}} \tag{3.40}$$

The heat transfer occurring in the cooling tower is calculated from the equation below:

$$\dot{Q}_{tow} = \varepsilon_{a,tow} \dot{m}_{a,tow} \left(h_{s,w,tow,in} - h_{a,tow,in} \right) \tag{3.41}$$

Considering a counter flow arrangement, the air side effectiveness is obtained from the relation

$$\varepsilon_{a,tow} = \frac{1 - exp\left(-NTU_{tow} \left(1 - C_{r_{tow}} \right) \right)}{1 - C_{r_{tow}} exp\left(-NTU_{tow} \left(1 - C_{r_{tow}} \right) \right)} \tag{3.42}$$

Where the heat capacity ratio $C_{r,tow}$ is obtained by,

$$C_{r_{tow}} = \frac{\dot{m}_{a,tow} C_s}{\dot{m}_{w,tow} C_{p_{w,tow}}} \tag{3.43}$$

This effectiveness is nothing but the ratio of the actual heat transfer to the maximum possible heat transfer that would occur if the air stream would leave at saturated condition corresponding to the entering water temperature.

The NTU for the tower is determined by the relation:

$$NTU_{tow} = A_9 \left(\dot{m}_{w,tow} / \dot{m}_{a,tow} \right)^{1+B_9} \tag{3.44}$$

Where A_9 and B_9 are constants that are defined for particular cooling tower box geometry, and are obtained by correlations from the manufacturer's data. The tower box size used in the present study is,

Length = 4.84 m (15.879 ft)

Width = 4.84 m (15.879 ft)

Height = 5.56 m (18.241 ft)

The cooling tower fan power consumption is modeled as:

$$\dot{W}_{fan,tow} = exp\left(A_{10} + \left(\frac{ln\left(cfm_{tow}\right) - 10.5}{2} \right) B_{10} \right) \tag{3.45}$$

This relationship is obtained by curve fitting the manufacturer's data which indicates the fan shaft power for a specific air flow rate and a particular box size.

A minimum condenser water inlet set point is maintained by turning the fans on and off as applicable [29]. This set point is taken as 70^0 F. When the cooling tower water exit temperature is above 70^0 F, the fan runs continuously and when the water temperature falls below 70^0 F, the fan is turned off. The ratio of the time that the fans are running is called the fan duty. Thus the total fan power is obtained by multiplying the fan power with fan duty.

3.6 Piping Model

The pipe flow is taken is as an isenthalpic process. The pressure drop in the pipe is taken as:

$$Head_{pipe} = f_{loop} \frac{Length_{loop}}{D_{i,pipe}} \frac{V_w^{\,2}}{2g} \tag{3.46}$$

Where f_{loop} is the friction factor and is determined by [35]:

$$f_{loop} = \frac{1}{\left(-1.8 \cdot log_{10}\left(\frac{6.9}{Re_{D,i,pump}} + \left(\frac{\varepsilon_{pipe}}{3.7 D_{i,pipe}} \right)^{1.11} \right) \right)^2} \tag{3.47}$$

The factor $Length_{loop}$ is the total effective length of the chilled water system loop and includes the length of the piping, the length of the air handler as well as the chilled water coil, and also the length of the pipe from the chiller to the cooling coil. In addition to the head loss due to pipes, the head loss resulting from the bends and valves is also considered in order to determine the total pressure drop of the system. The length of the loop does not have a significant influence over the performance of the system, especially when comparative analyses are to be performed. The inner diameter of the pipe, $D_{i,pipe}$,is taken as 10 in. whereas the average roughness of the pipe, ε_{pipe} ,is taken as 0.0015[9], which is the average value for most commercial pipes.

Having modeled all the major system components as described in the above sections, these components are then combined to depict the performance of the entire chilled water system.

3.7 Exergy analysis

The main objective behind performing the exergy analysis is to identify the major sources of exergy destruction so that possible measures can be taken to minimize these inefficiencies.

---

[9] http://www.cheresources.com/invision/index.php?/topic/4149-pipe-roughness/

The exergy balance equation in the rate form for control volume is given as [42] as:

$$\sum\left(1-\frac{T_o}{T_k}\right)\dot{Q}_k-\left(\dot{W}-P_o\frac{dV_{CV}}{dt}\right)+\sum\dot{m}_i\psi_i-\sum\dot{m}_e\psi_e-\dot{X}_{destoyed}=\frac{dX_{CV}}{dt} \qquad (3.48)$$

Where $\dot{Q}_k$ is the heat transfer through the boundary at temperature T_k at location k.

The above equation (3.48) clearly implies that for the case of steady flow control volume systems, the amount of exergy entering the system must be equal to the exergy leaving the system plus the exergy destroyed. This destroyed exergy is the result of various irreversibilities.

For the exergy analysis of the chilled water system, the different components comprising the system are considered as steady state, control volume systems. Thus by applying equation (3.48) to the various components, combined with the knowledge of the inlet and exit states of the component fluids, the exergy destruction can be calculated as shown in the following discussion. Throughout the analysis the ambient design temperature is taken as the dead state temperature. Additionally, all the temperatures have to be converted to the absolute (Rankine or Kelvin) scale to be used in the analysis.

3.7.1 Heat Exchangers

The heat exchangers in the chilled water system include: the air handler, the evaporator, the condenser and the cooling tower.

For the air handler, the exergy destruction is calculated as:

$$\dot{X}_{dest,ah} = \dot{W}_{lost,ah} = \left(\dot{m}_{w,ah} \left(s_{w,ah,out} - s_{w,ah,in} \right) - \frac{\dot{Q}_{load,ah}}{T_{amb}} \right) T_{amb} \tag{3.49}$$

The above equation (3.49) shows that in order to minimize the irreversibility in the air handler, a balance has to be achieved between the load, the mass flow rate of the water and the inlet and outlet conditions of the air handler.

Furthermore, the exergy destruction or irreversibility for the air handler fan can be expressed as:

$$\dot{X}_{dest,\,fan,ah} = \dot{W}_{lost,\,fan,ah} = \left(N_{ah} \dot{m}_{a,ah} \left(s_{a,\,fan,out} - s_{a,\,fan,in} \right) \right) T_{amb} \tag{3.50}$$

Where N_{ah} is the total number of air handlers.

The exergy destruction in the evaporator is calculated by the equation:

$$\dot{X}_{dest,evap} = \dot{W}_{lost,evap} = \left(\dot{m}_{w,evap} \cdot \left(s_{w,evap,out} - s_{w,evap,in} \right) - \left(\frac{-\dot{Q}_{evap}}{T_{evap}} \right) \right) T_{amb} \tag{3.51}$$

The negative sign in the term $\dot{Q}_{evap}$ indicates that the heat is removed from the water.

The irreversibility in the condenser can be represented by:

$$\dot{X}_{dest,cond} = \dot{W}_{lost,cond} = \left(\dot{m}_{w,cond} \left(s_{w,cond,out} - s_{w,cond,in} \right) - \left(\frac{\dot{Q}_{cond}}{T_{cond}} \right) \right) T_{amb} \tag{3.52}$$

Finally, the exergy loss in the cooling tower is accounted for by the equation:

$$\dot{X}_{dest,tow} = \dot{W}_{lost,tow} = \left(\dot{m}_{w,tow} \left(s_{w,tow,out} - s_{w,tow,in} \right) - \left(-\frac{\dot{Q}_{tow}}{T_{w,tow,ave}} \right) \right) T_{amb} \tag{3.53}$$

3.7.2 Pumps

The exergy destruction for the chilled water pump can be expressed as:

$$\dot{X}_{dest,pump} = \dot{W}_{lost,pump} = \left(\dot{m}_{w,pump} \cdot \left(s_{w,pump,out} - s_{w,pump,in} \right) \right) T_{amb} \tag{3.54}$$

And for the case of the condenser pump as:

$$\dot{X}_{dest,pump,cond} = \dot{W}_{lost,pump,cond} = \left(\dot{m}_{w,cond} \left(s_{w,pump,cond,out} - s_{w,pump,cond,in} \right) \right) T_{amb} \tag{3.55}$$

3.7.3 Compressor

The exergy destruction for the compressor is given by the relation

$$\dot{X}_{dest,comp} = \dot{W}_{lost,comp} = \dot{W}_{comp} - \dot{W}_{carnot} \tag{3.56}$$

Where $\dot{W}_{comp}$ is the actual compressor power and $\dot{W}_{carnot}$ is the power required by a reverse Carnot cycle that compresses the refrigerant from the evaporator pressure to the higher compressor pressure. This Carnot power can be evaluated as:

$$\dot{W}_{carnot} = \dot{Q}_{evap} \left(\frac{T_{ref,cond}}{T_{ref,evap}} - 1 \right) \tag{3.57}$$

3.7.4 Piping

Although the exergy loss in the pipes is not a significant quantity, it is included in order to improve the accuracy of the analysis.

The exergy loss in the primary loop through which the chilled water flows is given by:

$$\dot{X}_{dest,loop,pri} = \dot{W}_{lost,loop,pri} = \left(\dot{m}_{w,pump} \left(s_{w,pump,in} - s_{w,ah,out} + s_{w,ah,in} - s_{w,evap,out} \right) \right) T_{amb} \quad (3.58)$$

In case of the primary-secondary system, the analysis of the secondary loop is carried out in the same manner as the primary loop.

Finally, the exergy destruction in the condenser loop through which the condenser cooling water flows is given by the equation:

$$\dot{X}_{dest,loop,cond} = \dot{W}_{lost,loop,cond} = \left(\dot{m}_{w,cond} \left(s_{w,pump,cond,in} - s_{w,tow,out} + s_{w,tow,in} - s_{w,cond,out} \right) \right) T_{amb} \quad (3.59)$$

In conclusion the total exergy destruction of the entire chilled water system can be summed up as:

$$\dot{X}_{dest,tot} = \dot{X}_{dest,fan,ah} + \dot{X}_{dest,ah} + \dot{X}_{dest,pump} + \dot{X}_{dest,evap} + \dot{X}_{dest,cond} + \dot{X}_{dest,comp} + \dot{X}_{dest,tower} + \dot{X}_{dest,pump,cond} + \dot{X}_{dest,loop,pri} + \dot{X}_{dest,loop,cond} \quad (3.60)$$

3.8 Condensate Extraction in the Air Handler

The air that is flowing through the cooling coil of the air handler comprises the return air from the conditioned space combined with a certain percentage of fresh air from the atmosphere to take care of the ventilation requirement. For residential and commercial buildings like offices this value is taken as 15% [43]. During hot and humid weather, even this 15% of fresh air can bring a considerable amount of moisture to the air handler, which must be removed in order to maintain the comfort conditions. When the surface temperature of the coil tubes is less than the dew point temperature of the air water vapor mixture, condensation will occur in the cooling coil. The mass and energy balance on the cooling coil control volume can be shown as follows:

$$\dot{Q}_{load,ah} = \dot{m}_{a,ah}\left\{C_{pm}(T_{a,ah,in} - T_{a,ah,out}) + i_{fg}(\omega_{a,ah,in} - \omega_{a,ah,out})\right\} + \dot{m}_{w,cond}h_{w,cond} \quad (3.61)$$

Thus, depending upon the load and the ambient conditions, the amount of condensate collected from the air handler cooling coils can be evaluated.

CHAPTER 4

EJECTOR COOLING

The working principle of the ejector cooling system has already been discussed in section 1.5.1. Several numerical methods for modeling the ejector cooling system have been reported in recent literature [6,21,25,44-47]. Almost all these methods follow a one dimensional approach for modeling the ejector. The most important aspect of ejector modeling is the determination of the entrainment ratio which can be defined as the ratio of the mass flow rate of the secondary stream to the mass flow rate of primary/motive stream.

4.1 Entrainment Ratio

In order to determine the entrainment ratio the methodology put forward by Alexis [6] is adopted in the present study. This method is based on the following assumptions:

- The exit of the condenser is at saturated liquid state.
- The fluid at the exit of the evaporator is at saturated state.
- The fluid at the exit of the generator is at the saturated vapor state.
- The expansion through the expansion valve is an isenthalpic throttling process.

- The velocity of the compressed mixture leaving the ejector is insignificant.
- The motive stream and the entrained vapor have the same molecular weight specific heat ratio.
- The mixing process in the ejector takes place at constant pressure.

Furthermore, a constant value for the nozzle as well as the diffuser efficiency is assumed to take care of the losses occurring in these two components. Fig 4.1 is used for the analysis of the ejector cooling system, and the corresponding *T*-*s* diagram is shown in Fig. 4.2. A sequential simulation is carried out in order to determine the entrainment ratio and hence evaluate the system performance. To start with, a particular combination of the three temperatures i.e. T_1, T_2 and T_3 is selected from a predefined range. With these temperatures an initial value of the entrainment ratio is assumed. Using this value of the entrainment ratio and the thermodynamic equation, the value of enthalpy at point 3 (h_3) is obtained. The value of h_3 is also calculated from the pressure, temperature and entropy relationships. If the two values of the enthalpy coincide, the assumed entrainment ratio is accepted, otherwise the entrainment ratio is modified and the iterations are continued until the value of h_3 converges. The overview of the simulation process is shown in Fig. 4.3 and the performance equations are listed in the blocks.

The evaporator heat transfer rate is given as:

$$\dot{Q}_e = \dot{m}_e (h_2 - h_1) \tag{4.1}$$

Whereas the heat transfer in the generator is represented by:

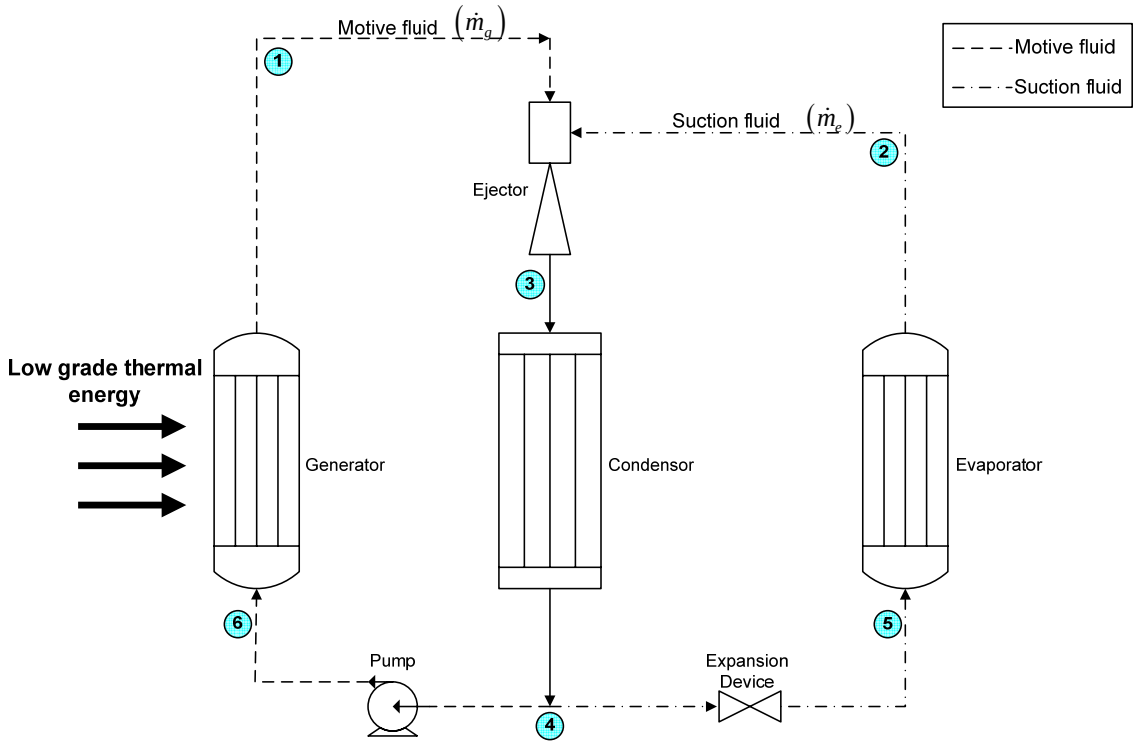

Figure 4.1 State points used in the analysis of the ejector cooling system

$$\dot{Q}_g = \dot{m}_g (h_1 - h_6) \tag{4.2}$$

Finally, the power consumption of the pump is calculated as:

$$\dot{W}_p = \dot{m}_g (h_4 - h_6) \tag{4.3}$$

Thus the COP of the ejector cooling system, determined by its operating conditions, can be obtained from the equation:

$$COP = \frac{\dot{Q}_e}{\dot{Q}_g + \dot{W}_p} = w\left(\frac{h_2 - h_5}{h_1 - h_6}\right) \tag{4.4}$$

Where

$$w = \frac{\dot{m}_e}{\dot{m}_g}$$
$$m_c = \dot{m}_e + \dot{m}_g \tag{4.5}$$

4.2 Area Ratios

Once the entrainment ratio for the ejector at a given set of operating temperatures has been determined, the next step is to determine the area ratios. These area ratios can be defined as the ratio of the nozzle throat area to the diffuser constant area, and the ratio of the area of the nozzle throat to the nozzle outlet. In this study, the area ratios are calculated by the method put forward in [48] and further used in [46]. In addition to figures 4.1 and 4.2, the Fig. 4.4 which depicts the fluctuation of pressure and velocity along the location of the ejector, is also referred for this analysis.

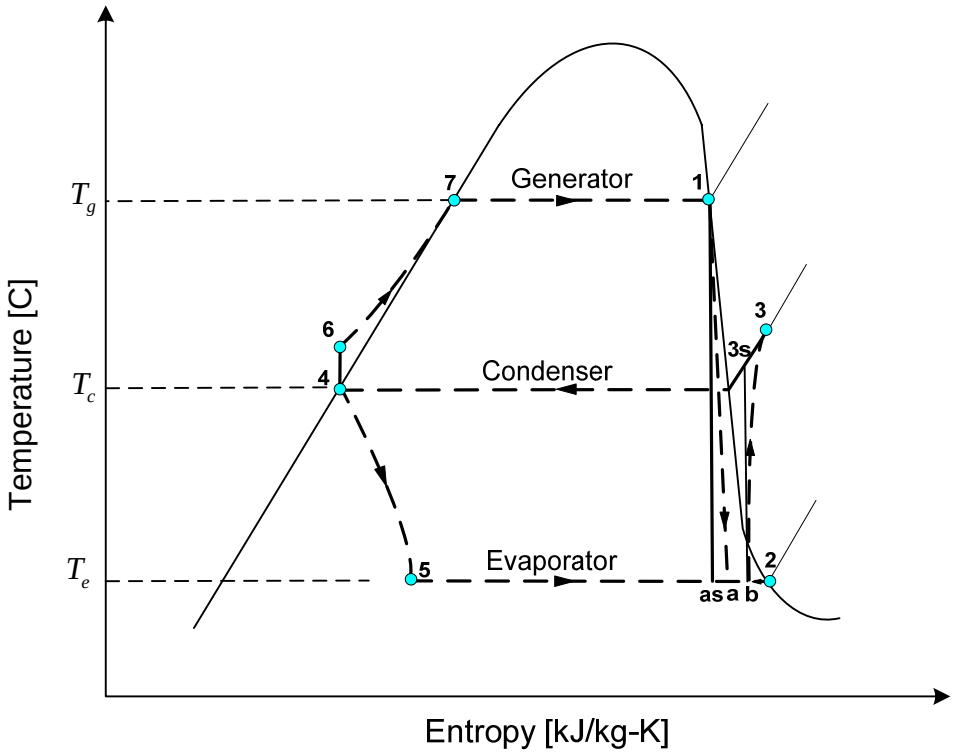

Figure 4.2 T-s diagram of ejector cooling system

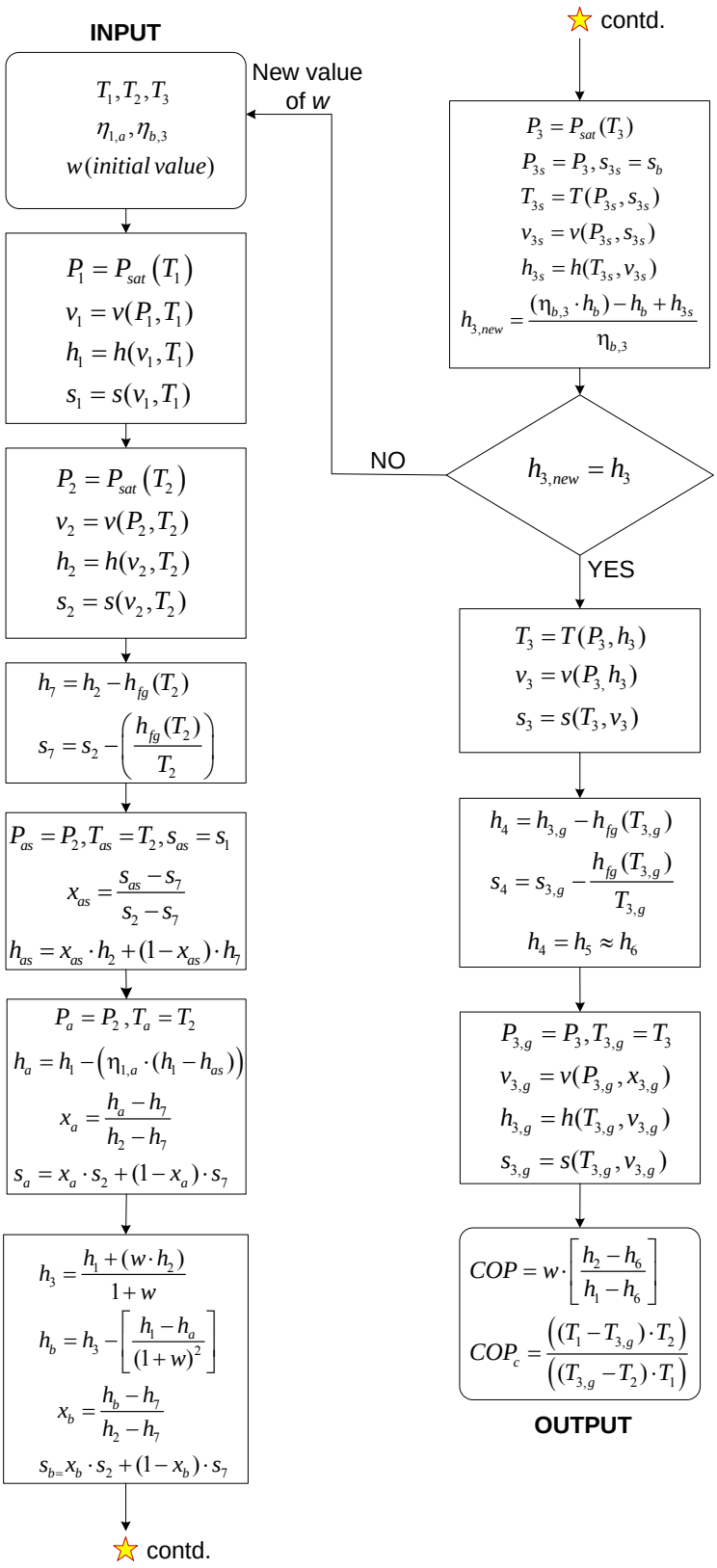

Figure 4.3 Flow chart for the ejector system analysis

The isentropic expansion of the primary fluid in terms of its Mach number at the nozzle exit can be expressed as:

$$M_{g_i} = \sqrt{\frac{2\eta_{1,a}}{\gamma - 1}\left(\left(\frac{P_g}{P_i}\right)^{\frac{\gamma-1}{\gamma}} - 1\right)} \tag{4.6}$$

Where γ is the coefficient of isentropic expansion.

Similarly, the isentropic expansion of the entrained fluid at the nozzle outlet can be expressed as:

$$M_{e_2} = \sqrt{\frac{2}{\gamma - 1}\left(\left(\frac{P_e}{P_i}\right)^{\frac{\gamma-1}{\gamma}} - 1\right)} \tag{4.7}$$

The critical Mach number (M^*), defined as the ratio of the local fluid velocity to the velocity of sound at critical conditions, for the primary fluid at location *'i'* (Fig. 4.4) is given by the expression:

$$M^*_{g_i} = \sqrt{\frac{M_{g_i}^{\,2}(\gamma+1)}{M_{g_i}^{\,2}(\gamma-1)+2}} \tag{4.8}$$

And for the secondary fluid by the expression:

$$M^*_{e_i} = \sqrt{\frac{M_{e_i}^{\,2}(\gamma+1)}{M_{e_i}^{\,2}(\gamma-1)+2}} \tag{4.9}$$

Thus, the critical Mach number of the mixture at location *'l'* in terms of the critical Mach number for the primary and secondary fluids at point *'i'* can be represented as:

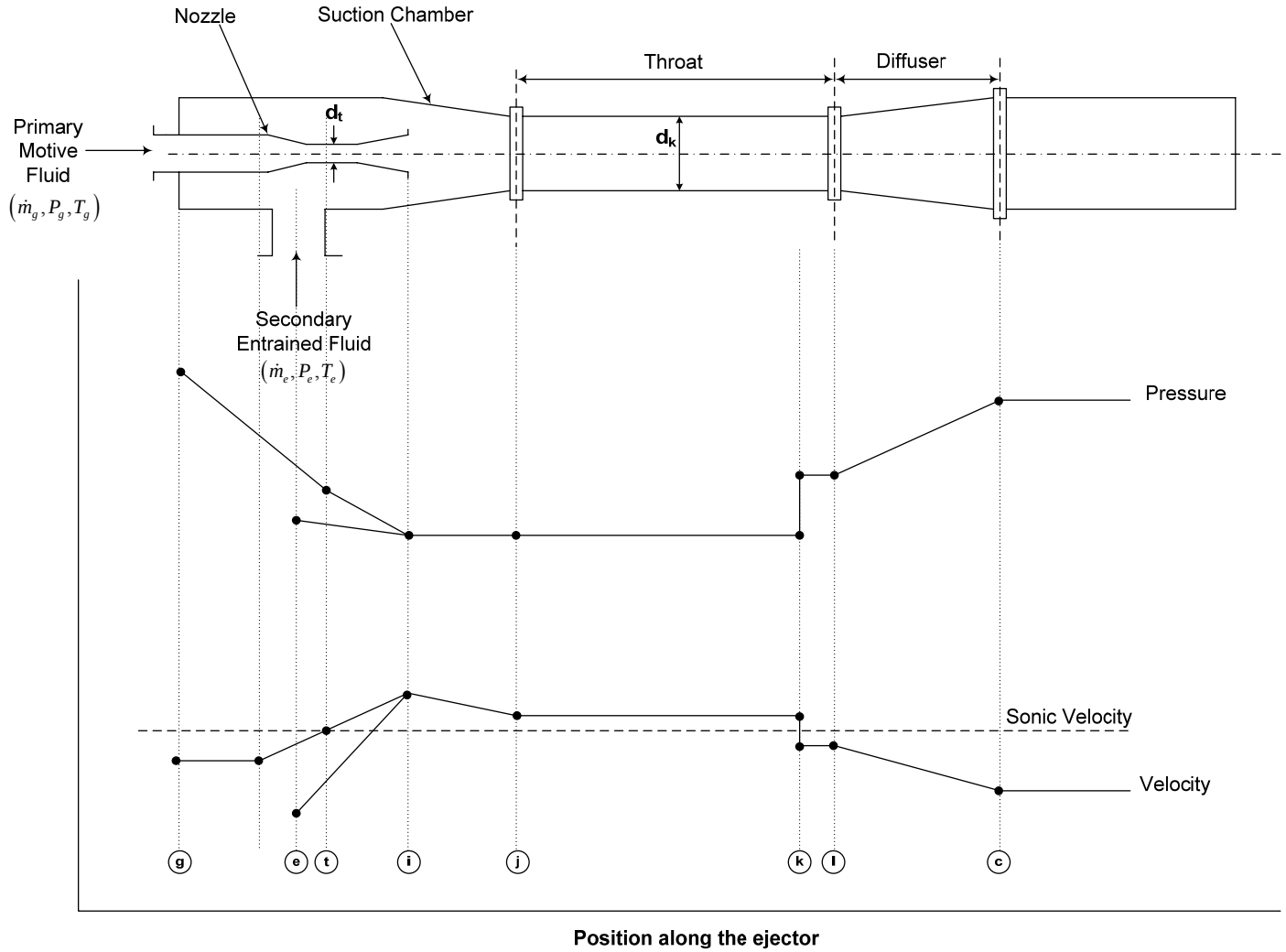

Figure 4.4 Variation of pressure and velocity at different positions along the ejector

$$M^*_k = \frac{M^*_{g_2} + wM^*_{e_2}\sqrt{\frac{T_e}{T_g}}}{\sqrt{\left((1+w)\left(1+w\frac{T_e}{T_g}\right)\right)}} \tag{4.10}$$

Following this, the Mach number at location *'k'* can be obtained by,

$$M_k = \sqrt{\frac{2M^{*\,2}_k}{\gamma+1-\left(M^{*\,2}_k(\gamma-1)\right)}} \tag{4.11}$$

For the value of M_k greater than unity, the fluid undergoes a transverse shock that changes the supersonic flow to subsonic. This shock is accompanied by a recovery in static pressure energy. The Mach number of the mixed fluids after the shock phenomenon is obtained by the expression:

$$M_l = \sqrt{\frac{M_k^{\,2} + \left(\frac{2}{\gamma-1}\right)}{\left(\frac{2\gamma}{\gamma-1}\right)M_k^{\,2} - 1}} \tag{4.12}$$

The increase in pressure across the shock wave at location *'k'* is obtained by combining the mass and momentum equations and is expressed as,

$$P_l = \left(\frac{1+\gamma M_k^{\,2}}{1+\gamma M_l^{\,2}}\right)P_k \tag{4.13}$$

The pressure lift in the diffuser section using the diffuser efficiency is given by,

$$P_c = \left(\left(\left(\eta_{b,3}\frac{\gamma-1}{2}M_l^{\,2}+1\right)\right)^{\frac{\gamma}{\gamma-1}}\right)P_l \tag{4.14}$$

Finally the ratio of the nozzle throat area to the diffuser constant area is given by the equation:

$$\frac{A_t}{A_k}=\left[\left(\frac{P_c}{P_g}\right)\left(\frac{1}{\sqrt{(1+w)\left(1+w\cdot\frac{T_e}{T_g}\right)\left(1-\frac{2}{\gamma+1}\right)}}\right)\left(\frac{P_l}{P_c}\right)^{1/\gamma}\sqrt{\left(1-\left(\frac{P_l}{P_c}\right)^{\frac{\gamma-1}{\gamma}}\right)}\right]\left(\frac{\gamma+1}{2}\right)^{\frac{1}{\gamma-1}} \quad (4.15)$$

And the ratio of the nozzle throat to the nozzle outlet area is given by,

$$\frac{A_i}{A_t}=\sqrt{\frac{1}{M_{g_i}{}^2}\left(\frac{2}{\gamma+1}\left(1+\frac{(\gamma-1)}{2}M_{g_i}{}^2\right)\right)^{\left(\frac{\gamma+1}{\gamma-1}\right)}} \quad (4.16)$$

4.3 Validation

After modeling the ejector cooling system according to the method described above, the next step is to verify the obtained results with the available experimental results. For this purpose, the experimental results reported by Huang [47] were used. In this work, the experimental data for several operating temperatures as well as different ejector geometries was collected. The refrigerant R141b was used as the working fluid and the values of the entrainment ratio as well as the area ratios were reported for different combinations of operating temperatures.

The comparison for the entrainment ratios obtained from the present study with the experimental results for various operating temperatures are shown in table 4.1, whereas as those for the area ratios are shown in Table 4.2. These results are further visualized in Fig. 4.5 and 4.6 respectively

Table 4.1 Comparison between the theoretical and experimental values of entrainment ratio at constant evaporator temperature of 8°C and pressure of 0.040 MPa

T_g (°C)	T_c (°C)	entrainment ratio (w)		
		Theoretical (present study)	Experimental	Error (%)
95	31.30	0.4363	0.4377	-0.32
95	33.00	0.3927	0.3937	-0.25
95	33.60	0.3784	0.3457	9.46
95	34.20	0.3646	0.3505	4.02
95	36.30	0.3199	0.2814	13.68
95	37.10	0.3042	0.2902	4.82
95	38.80	0.273	0.2273	20.11
95	38.60	0.2765	0.2552	8.35
95	41.00	0.2364	0.2043	15.71
95	42.10	0.2195	0.1859	18.07
90	31.50	0.4039	0.4446	-9.15
90	33.80	0.3476	0.3488	-0.34
90	36.70	0.2869	0.304	-5.63
90	37.50	0.2718	0.2718	0.00
90	38.90	0.2469	0.2246	9.93
84	28.00	0.4704	0.5387	-12.68
84	30.50	0.3952	0.4241	-6.81
84	32.30	0.3487	0.3883	-10.20
84	33.60	0.3182	0.3117	2.09
84	35.50	0.2778	0.288	-3.54
78	24.40	0.5637	0.6227	-9.47
78	26.90	0.4662	0.4889	-4.64
78	29.10	0.3955	0.4393	-9.97
78	29.50	0.3839	0.3922	-2.12
78	32.50	0.3061	0.3257	-6.02
			Average error =	1.00

Table 4.2 Comparison between the theoretical and experimental values of area ratio (A_k/A_t) at constant evaporator temperature of 8°C and pressure of 0.040 MPa

T_g (°C)	T_c (°C)	Area ratio (A_k/A_t)		
		Theoretical (present study)	Experimental	Error (%)
95	31.30	10.4200	10.6400	-2.07
95	33.00	9.6210	9.8300	-2.13
95	33.60	9.3610	9.4100	-0.52
95	34.20	9.1100	9.1700	-0.65
95	36.30	8.3010	8.2800	0.25
95	37.10	8.0190	8.2500	-2.80
95	38.80	7.4600	7.2600	2.75
95	38.60	7.5230	7.7300	-2.68
95	41.00	6.8100	6.7700	0.59
95	42.10	6.5130	6.4400	1.13
90	31.50	9.0120	9.4100	-4.23
90	33.80	8.0970	8.2800	-2.21
90	36.70	7.1170	7.7300	-7.93
90	37.50	6.8750	6.9900	-1.65
90	38.90	6.4770	6.4400	0.57
84	28.00	9.0440	9.4100	-3.89
84	30.50	7.9780	8.2800	-3.65
84	32.30	7.3190	7.7300	-5.32
84	33.60	6.8890	6.9900	-1.44
84	35.50	6.3210	6.4400	-1.85
78	24.40	9.2110	9.4100	-2.11
78	26.90	8.0200	8.2800	-3.14
78	29.10	7.1540	7.7300	-7.45
78	29.50	7.0110	6.9900	0.30
78	32.50	6.0590	6.4400	-5.92
			Average error =	-2.24

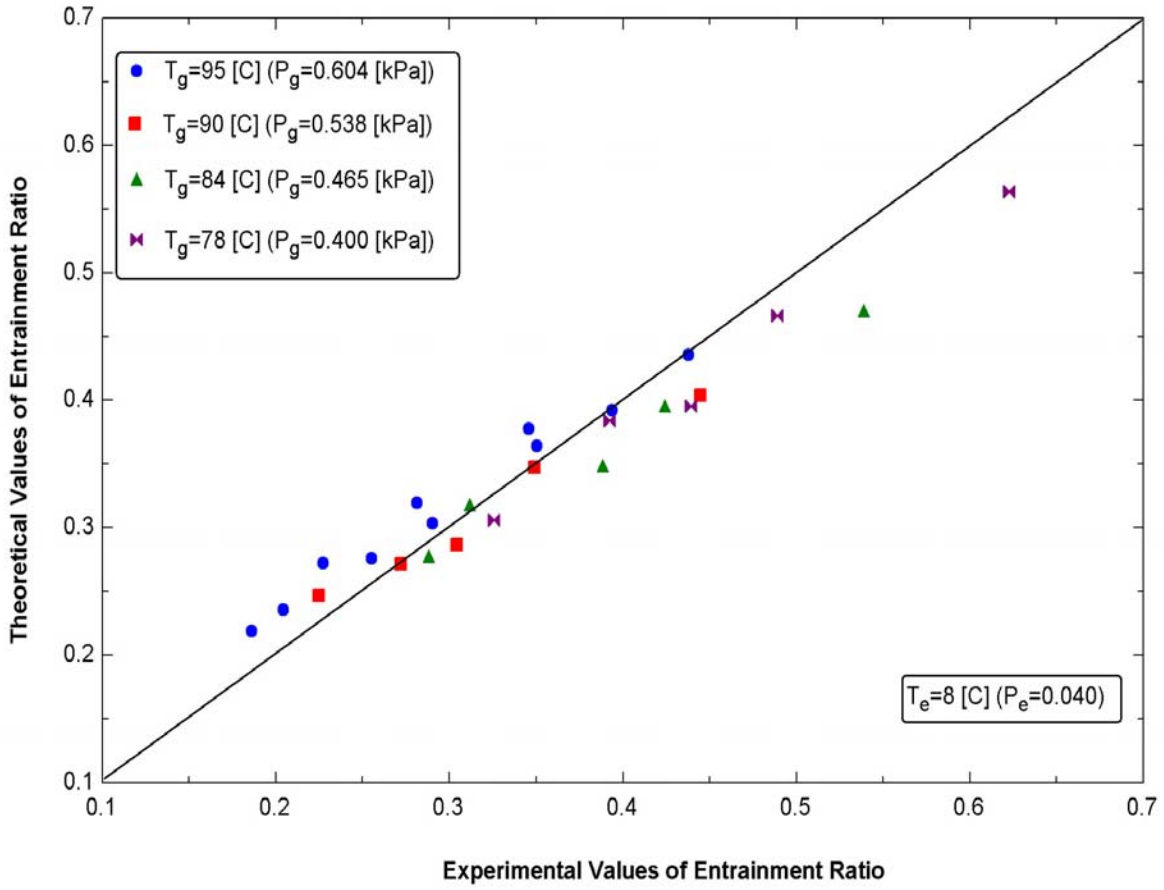

Figure 4.5 Comparison between the theoretical and experimental values of entrainment ratio at constant evaporator temperature of 8^{o}C and pressure of 0.040 MPa

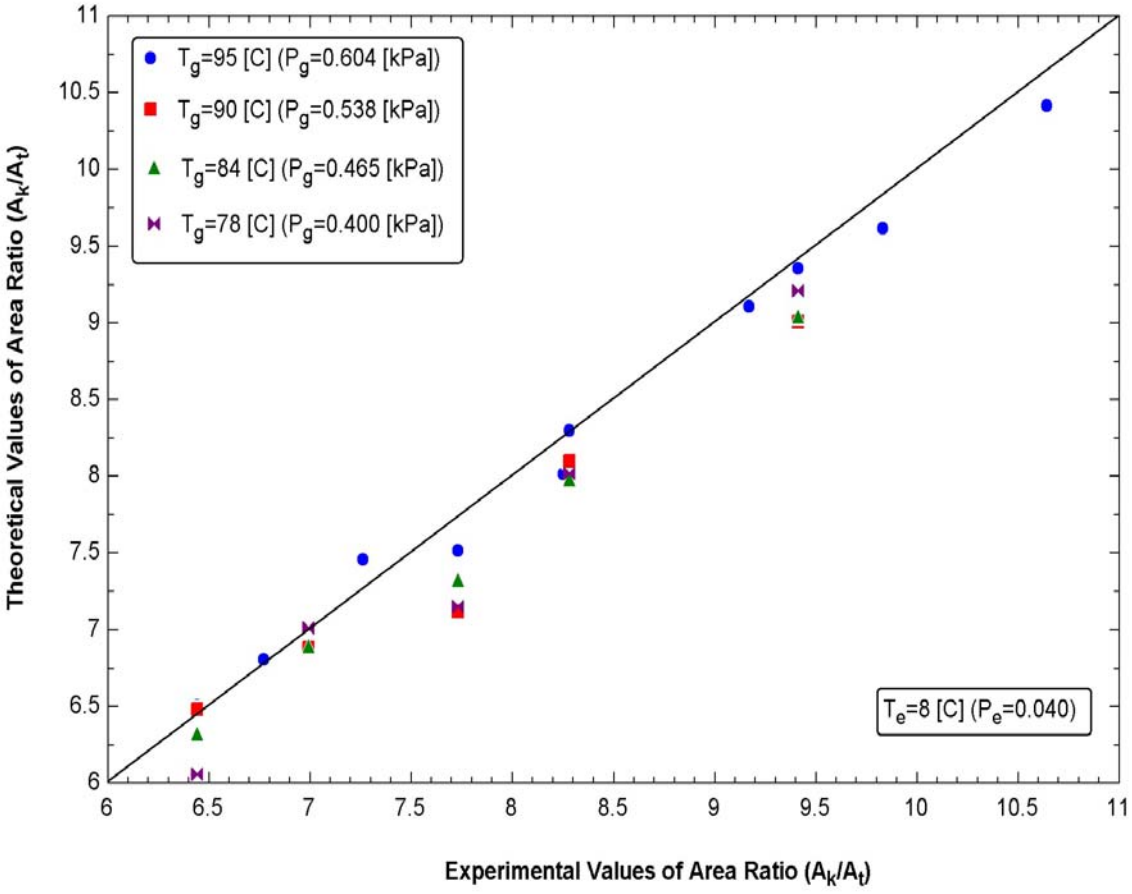

Figure 4.6 Comparison between the theoretical and experimental values of area ratio (A_k/A_t) at constant evaporator temperature of 8^{o}C and pressure of 0.040 MPa

A careful examination of the results shown in Tables 4.1 and 4.2 as well as the Figures 4.5 and 4.6 indicates that although the value of individual percentage error is high for certain conditions, the average error for both the entrainment ratio as well as the area ratio is within the acceptable range (≤ 5%). The variation of the entrainment ratio along with the area ratio, for different combinations of the operating temperatures is also observed. The important point that is to be noted is that there exist certain combinations of the operating temperatures at which the error between the theoretical and the experimental values is extremely small. Therefore an attempt should be made to evaluate the performance of the ejector at these values in order to confirm with the actual situation. Furthermore the ejector should be designed in such a way that these operating conditions are maintained.

CHAPTER 5

RESULTS AND DISCUSSION

5.1 Chilled Water System: Energy Consumption

In order to analyze the performance of the chilled water system and the effect of different pumping schemes, a load profile has to be used. This load profile determines the variation of load according to the ambient conditions. This is necessary because the chilled water system is designed to deliver full load at particular values of ambient dry bulb and wet bulb temperatures. But for majority of the time, these ambient conditions are not prevalent [3] thereby forcing the system to operate at part load conditions.

5.1.1 Load Profiles

The load profiles for three different cities: Dhahran, Riyadh and Jeddah are used in this study. These load profiles are developed based on the concept that the design dry bulb temperature for a particular location is the point at which the chilled water system operates at full load capacity (100% load). Beyond this design temperature, the supplied load is set equal to the calculated system capacity whereas the building load is assumed to increase linearly (Fig.5.1).The supplied load decreases to 20% following a linear relationship corresponding to a temperature of 60^{o}F.

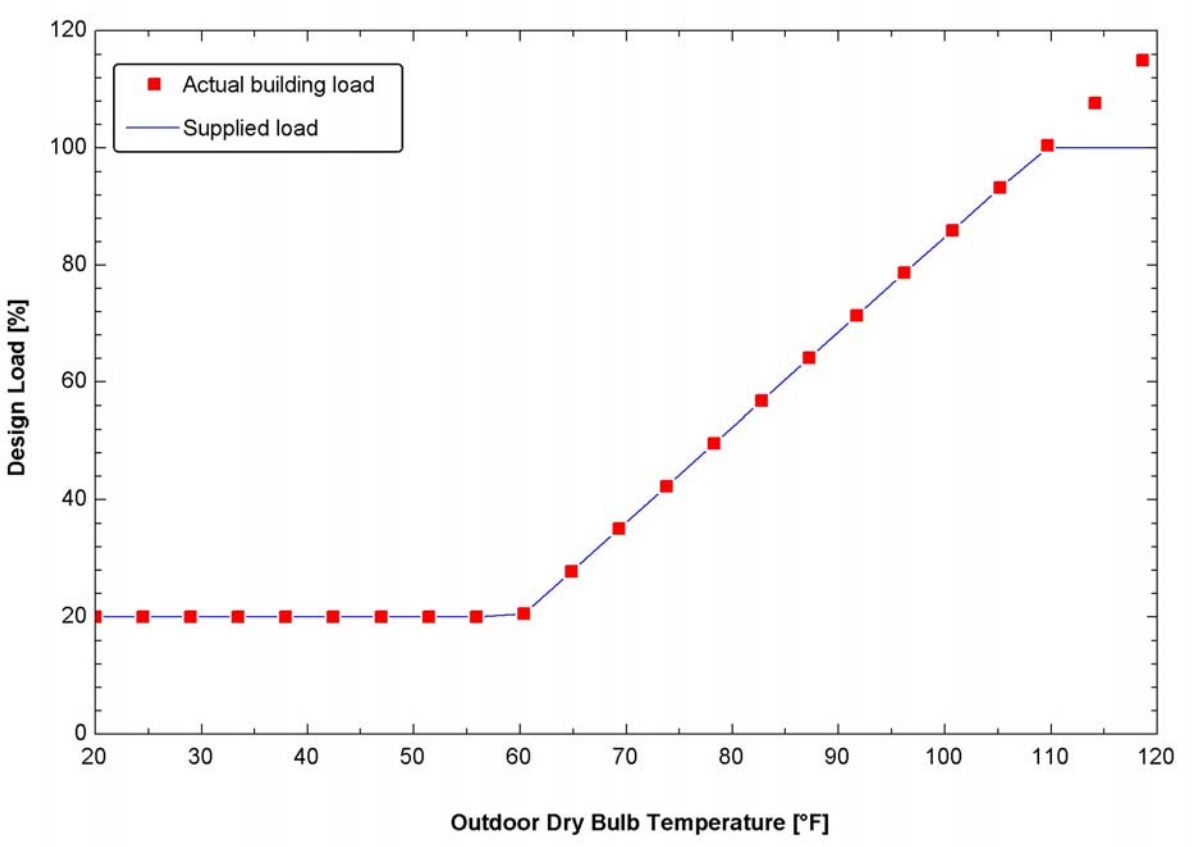

Figure 5.1 Difference between actual and supplied load

The load requirement then remains constant at a value of 20% for all temperatures below 45^{o}F. Another important aspect of the load profile is that below 45^{o}F free cooling is assumed. This implies that there is no cooling load when the ambient temperature drops below 45^{o}F. Practically, there is a certain amount of cooling load, but the energy required for free cooling is not considered in this analysis.

The load profiles developed for Dhahran, Riyadh and Jeddah, based on their corresponding design conditions, are shown in figures 5.1, 5.2 and 5.3 respectively.

5.1.2 Weather Data (Bin Data)

For the purpose of analyzing the overall energy consumption of the chilled water systems incorporated with different pumping schemes, the bin method is used. This method utilizes the bin data which can be defined as the number of hours that a certain ambient temperature was prevalent in each individual set of several equally sized intervals of ambient temperature. The instantaneous energy calculations are performed at several outdoor dry bulb temperature conditions and then multiplied by the number of hours of occurrence of each condition. The bin data for the three cities Dhahran , Riyadh and Jeddah as reported in [49] are depicted in tables 5.1, 5.2 and 5.3 respectively.

5.1.3 Analysis of Energy Consumption

Having obtained the weather data and utilizing the developed load profiles, the performance of the chilled water system is simulated for the three different pumping schemes. The simulations are also carried out for different locations.

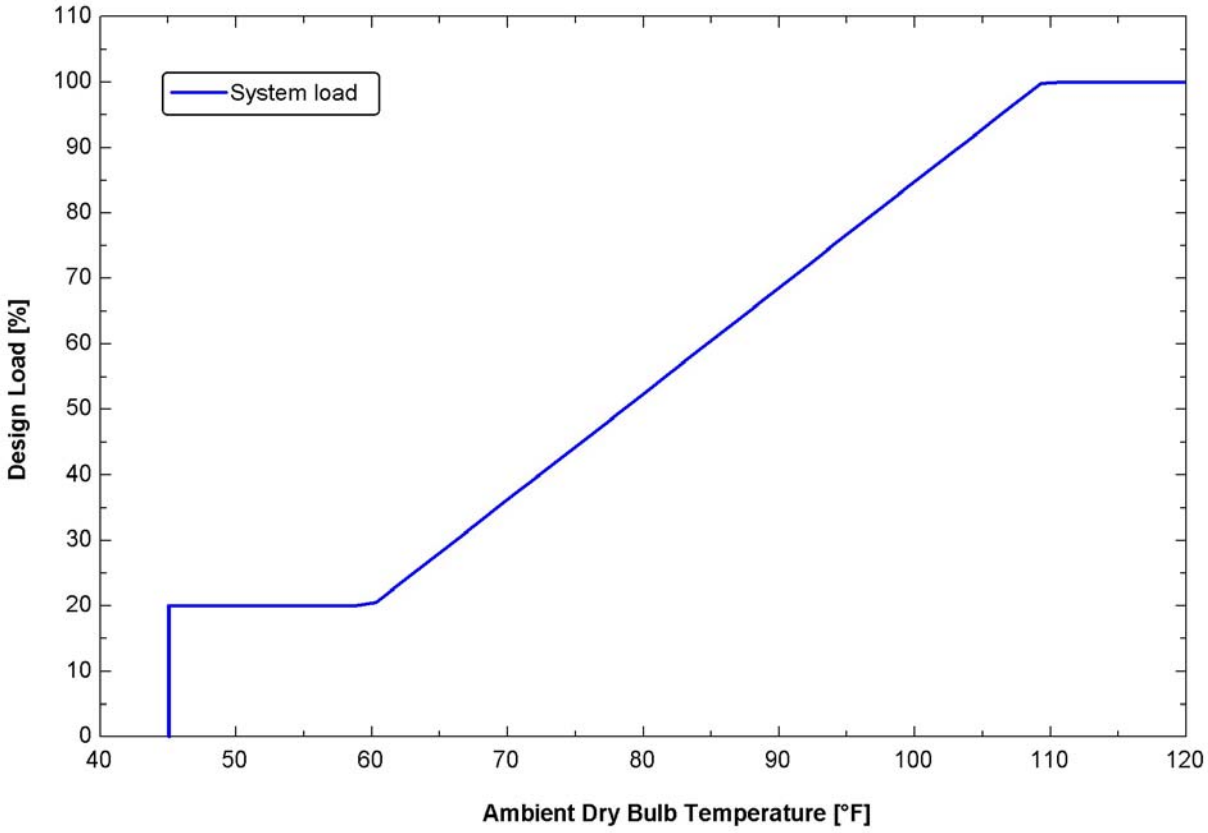

Figure 5.2 Load profile for the city of Dhahran

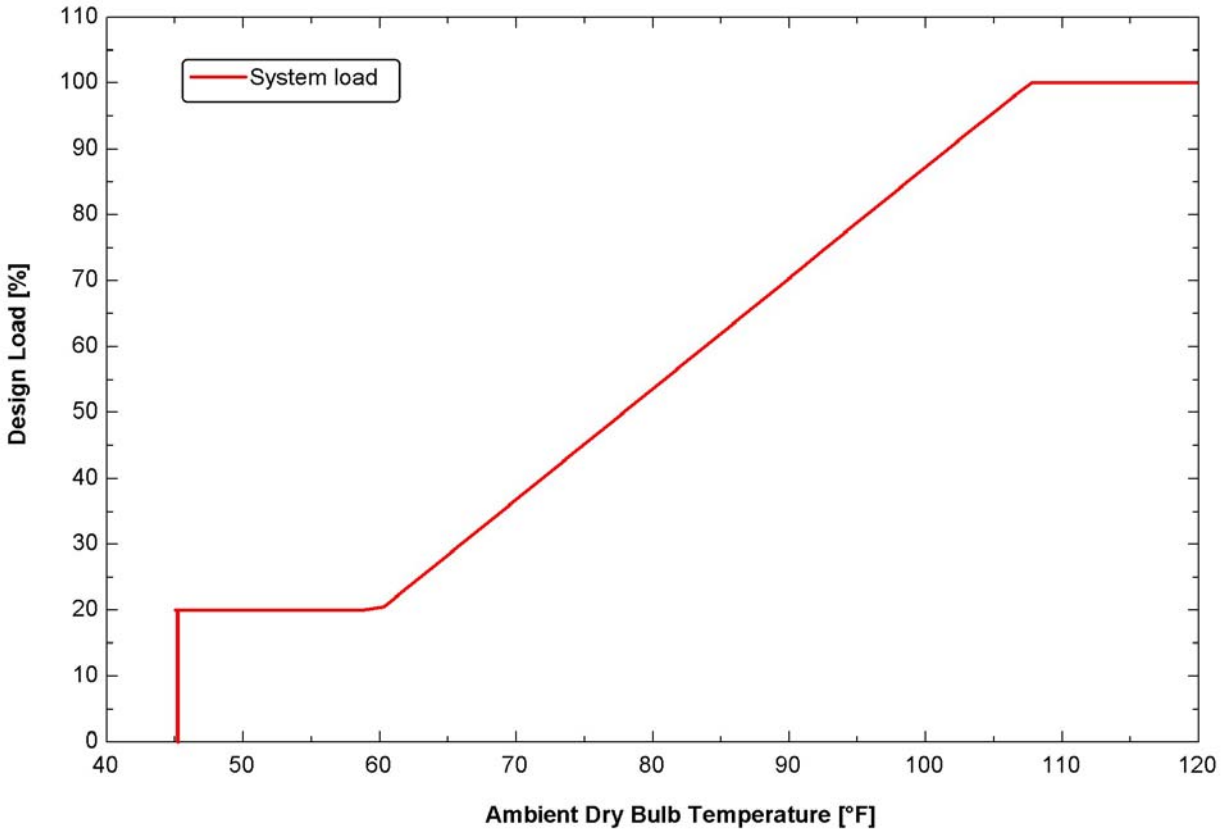

Figure 5.3 Load profile for the city of Riyadh

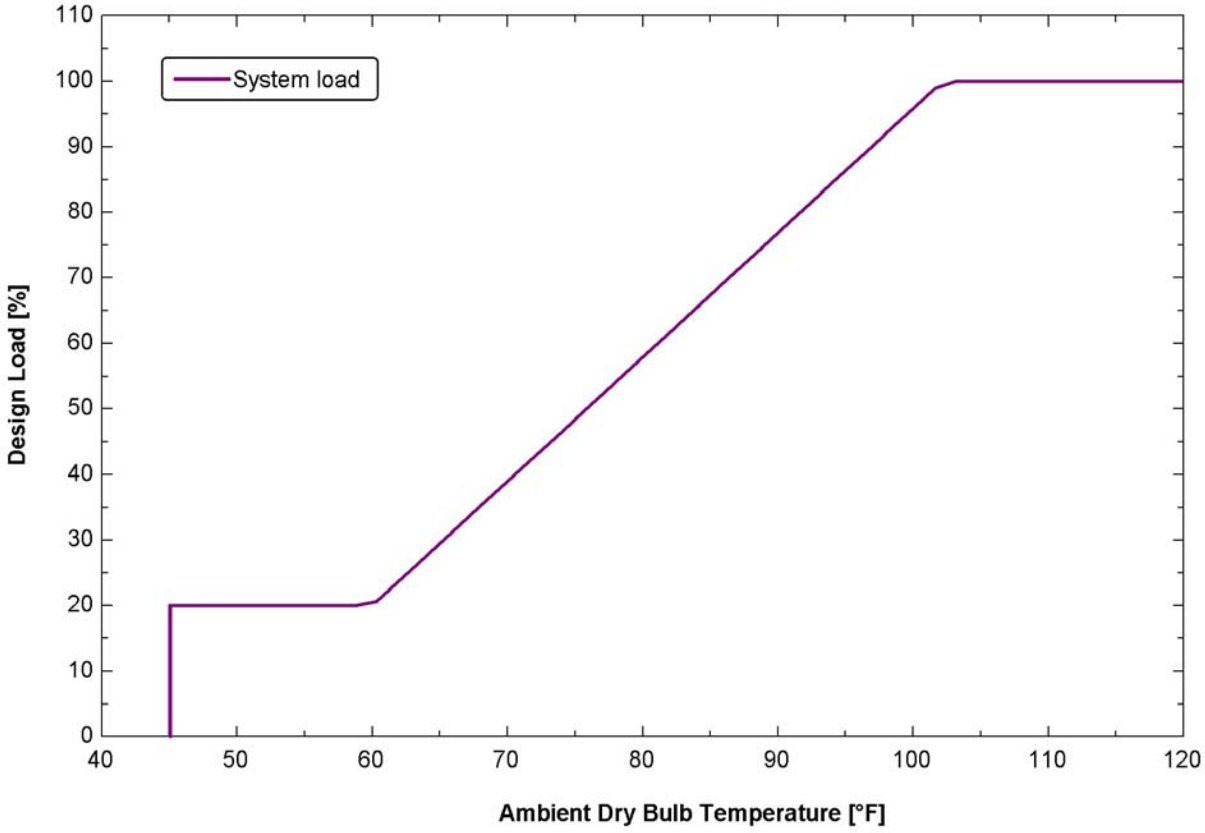

Figure 5.4 Load profile for the city of Jeddah

Table 5.1 Bin data and design temperatures for Dhahran

Design Dry Bulb Temperature = 109.4 ^{o}F
Design Wet Bulb Temperature = 84.2 ^{o}F

Dry bulb (^{o}F)	**Wet bulb (^{o}F)**	**No. of hours**
42.3	35.2	80
47.3	39.5	281
52.3	45.7	504
57.2	50.2	640
62.4	51.3	956
67.5	54.0	845
72.1	56.6	909
77.2	58.3	774
82.2	67.3	1067
87.3	69.0	876
92.3	72.0	744
97.3	74.0	596
102.4	77.0	319
107.4	81.0	146
112.5	86.5	10

Table 5.2 Bin data and design temperatures for Riyadh

Design Dry Bulb Temperature = 107.6 ^{o}F
Design Wet Bulb Temperature = 77.0 ^{o}F

Dry bulb (^{o}F)	**Wet bulb (^{o}F)**	**No. of hours**
37.2	28.6	56
42.3	33.3	178
47.3	42.8	363
52.3	44.6	568
57.2	45.1	646
62.4	46.8	739
67.5	51.8	668
72.1	55.8	809
77.2	60.8	871
82.2	62.6	943
87.3	64.2	778
92.3	64.4	665
97.3	66.2	617
102.4	68.9	561
107.4	69.3	267
112.5	69.6	16

Table 5.3 Bin data and design temperatures for Jeddah

Design Dry Bulb Temperature = 102.2 ^{o}F
Design Wet Bulb Temperature = 84.2 ^{o}F

Dry bulb (^{o}F)	**Wet bulb (^{o}F)**	**No. of hours**
52.3	50.0	5
57.2	53.6	52
62.4	55.0	233
67.5	59.5	719
72.1	60.8	1413
77.2	67.5	1605
82.2	68.4	1956
87.3	73.7	1489
92.3	75.0	971
97.3	77.0	264
102.4	82.4	43
107.4	86.0	6
112.5	89.6	3
117.5	90.0	1

5.1.3. (a) Analysis for Dhahran

The variation of the energy consumption for the existing system in building 59 (single loop constant primary) is shown in fig 5.5. It can clearly be seen that as the ambient temperature increases, the power consumption of the system also increases. But the total energy consumed depends on the number of hours the particular ambient temperature is existing. Therefore, although the power consumed is the highest at an ambient temperature of about 110^{o}F; the energy consumption is the lowest at this temperature as this temperature exists only for a very short duration throughout the year

The effect of changing the existing pumping scheme in building 59 from constant primary to constant primary-variable secondary as well as to single loop variable primary is represented graphically in Fig. 5.6. Several important observations can be made from this figure. It is observed that the maximum energy consumption drops from about 325,000 kWh for the case of single loop constant primary system to 300,000 kWh for the constant primary, variable secondary system and further to a value of around 280,000 kWh for the single loop, variable primary flow system. Furthermore, at the full load conditions corresponding to the design dry bulb temperature, the energy consumption of all the three pumping scheme is almost equal. The difference is more distinguishable at part load conditions (corresponding to temperatures less than the design temperature) at which the chilled water system operates for the majority of its lifetime.

Finally by adopting the constant primary, variable secondary pumping scheme is place of the existing one, the energy consumption can be reduced by 8%, whereas by employing

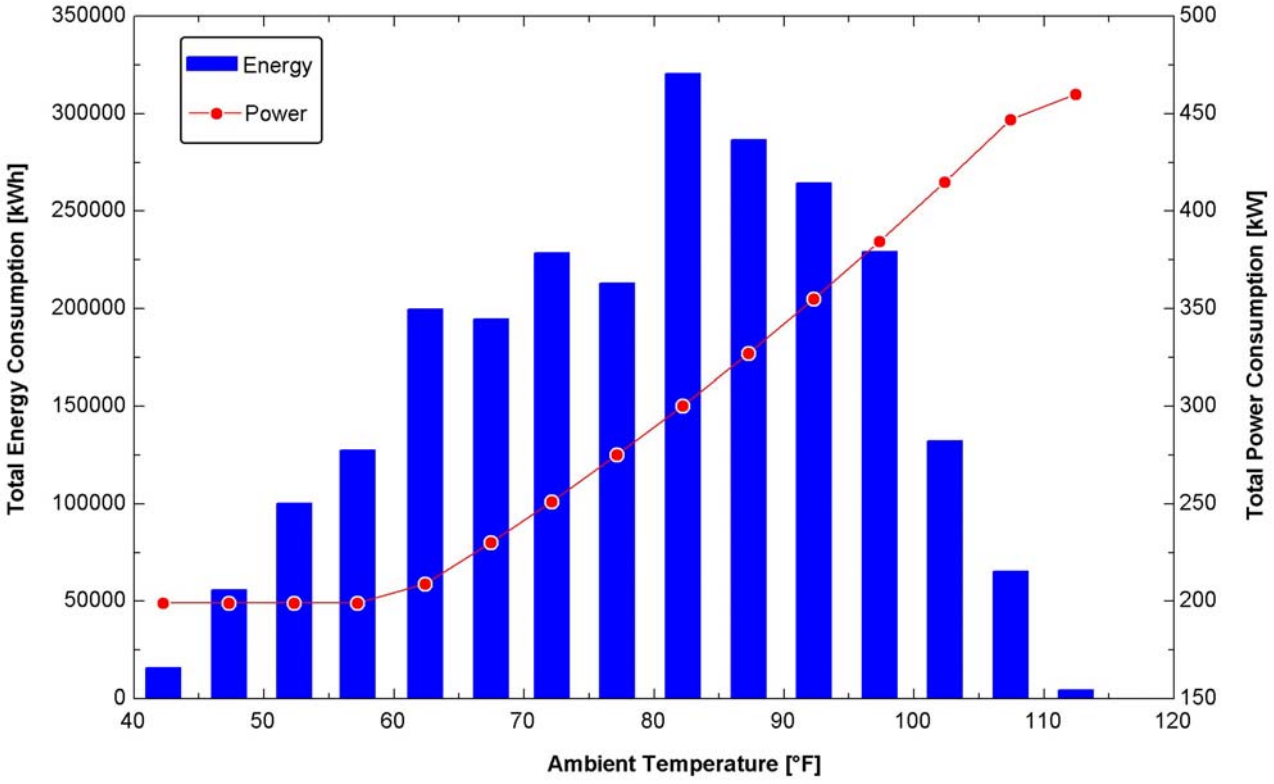

Figure 5.5 Variation of total energy and power consumption for single loop constant primary flow pumping scheme

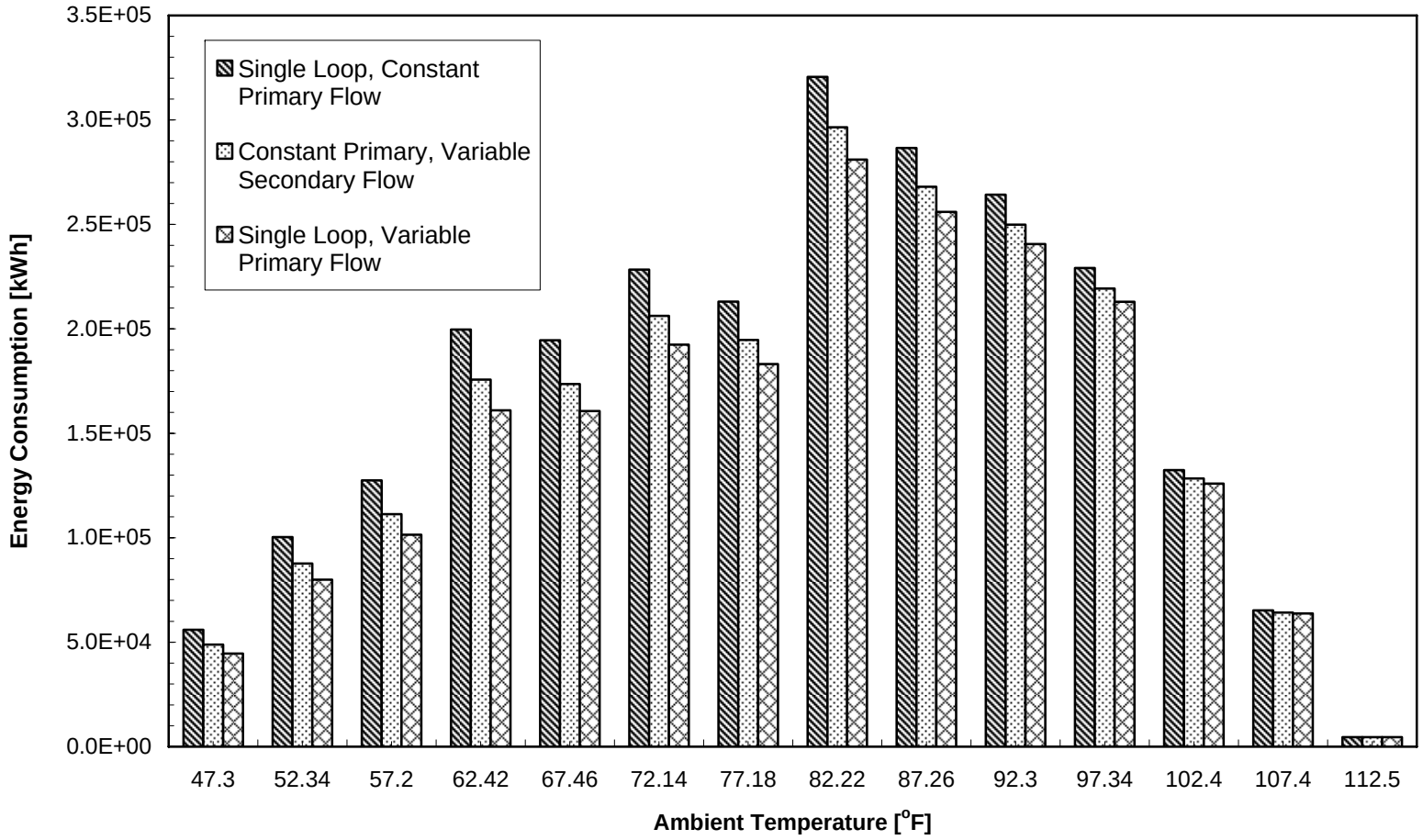

Figure 5.6 Energy consumption of the three different pumping schemes for the climatic conditions of Dhahran

the single loop variable primary scheme, savings in energy consumption of about 13% can be achieved. The majority of these savings result from the reduction in pumping power as is quite apparent from Fig. 5.7.

5.1.3. (b) Analysis for Riyadh and Jeddah

A similar investigation of energy consumption is carried out for the cities of Riyadh and Jeddah by utilizing their respective load profiles and bin data. The results obtained are shown in Fig. 5.8 and 5.9 for Riyadh and Dhahran respectively. The energy consumption reaches to maximum of about 300,000 kWh for Riyadh, whereas that for Jeddah goes as high as 600,000 kWh. The average energy consumption for Jeddah is also much higher than Riyadh.

The most important information that can be obtained by examining the variation of energy consumption by the chilled water system for all the three locations (Fig. 5.6, 5.8 and 5.9) is that in all cases, the energy consumed by the primary-secondary pumping scheme is less than that consumed by the single loop constant primary scheme. The reduction in energy consumption is further increased by adopting the single loop variable flow scheme.

For the city of Riyadh a reduction in energy consumption by 7.4% is obtained by applying the primary-secondary pumping scheme and this reduction is increased to 12% by using the single loop, variable primary scheme. For the case of the Jeddah energy reductions of 7% and 11 % are obtained by applying the primary-secondary pumping scheme and the single loop, variable primary scheme respectively.

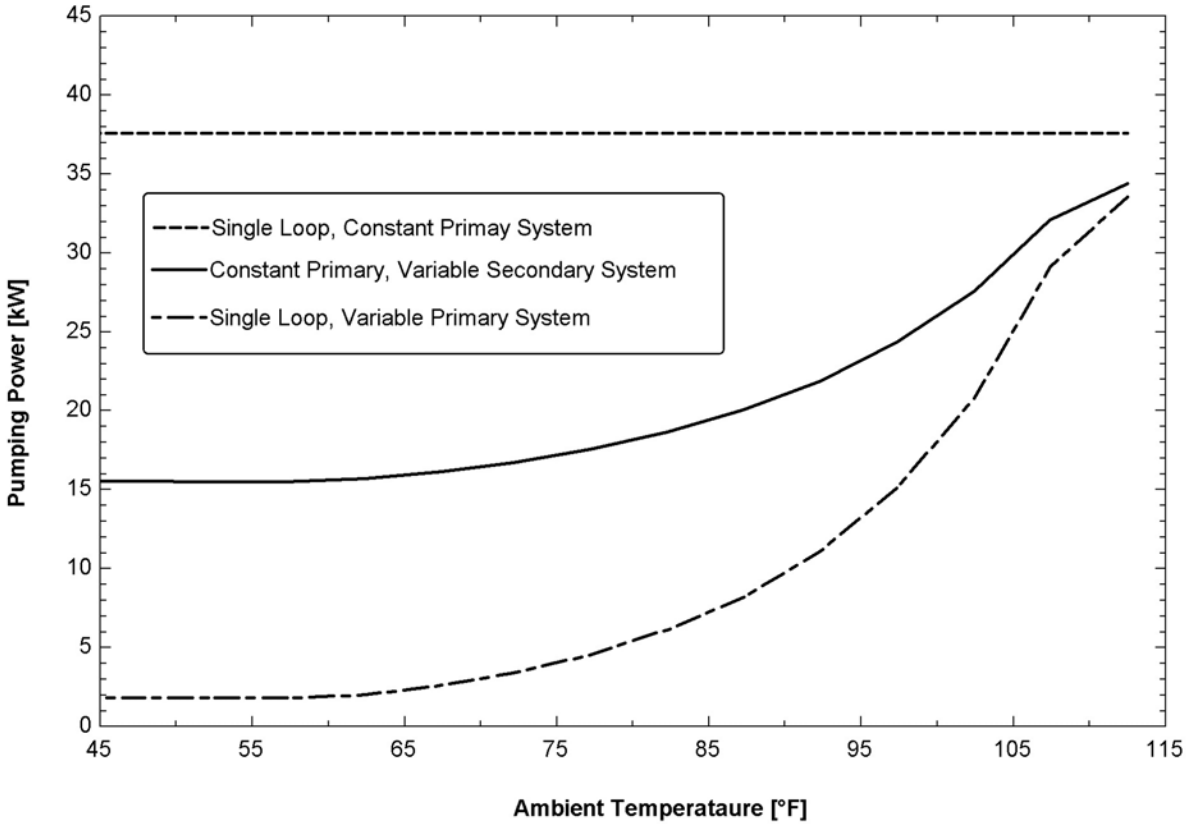

Figure 5.7 Variation of pumping power for different pumping schemes

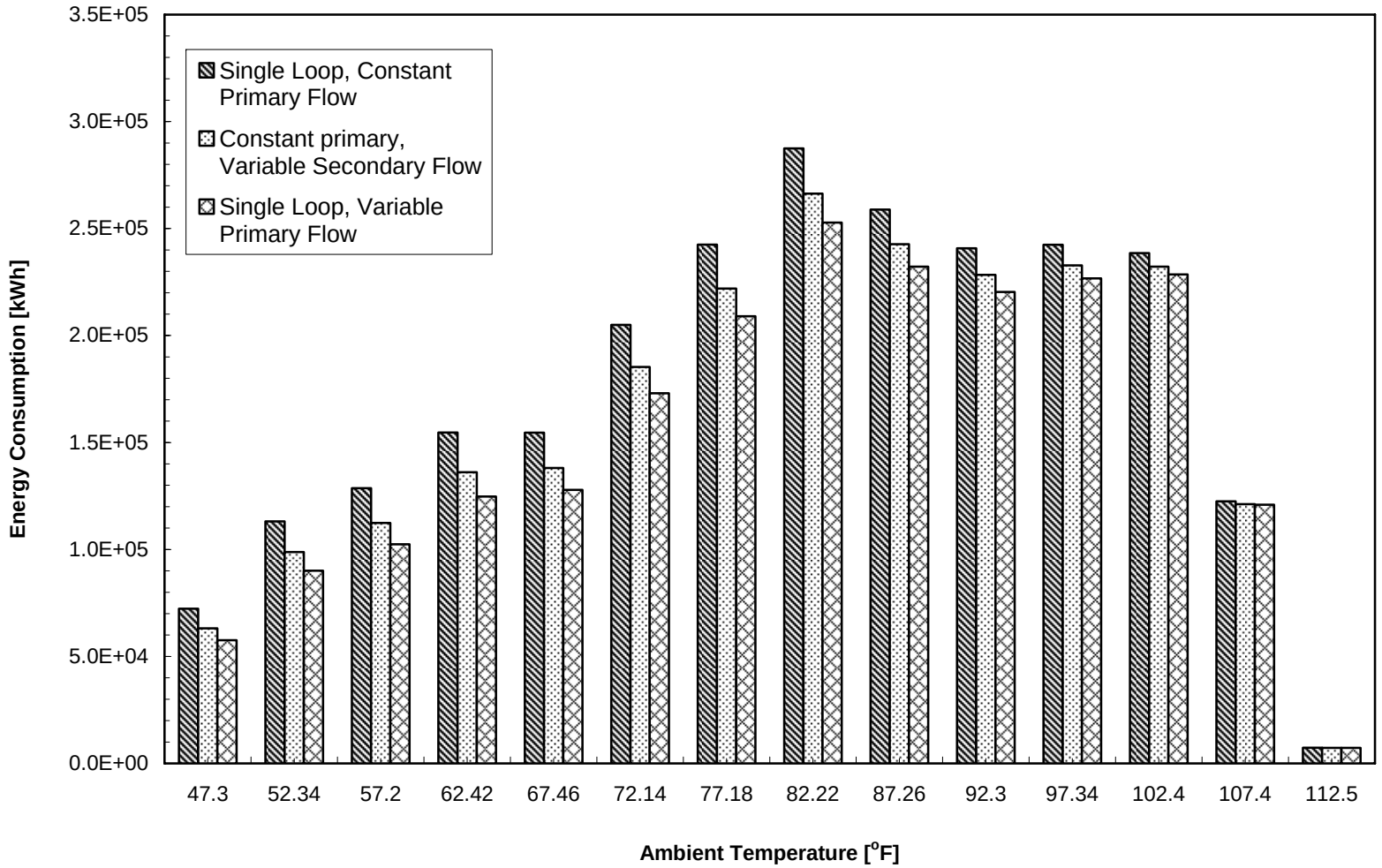

Figure 5.8 Energy consumption of the three pumping schemes for the climatic conditions of Riyadh

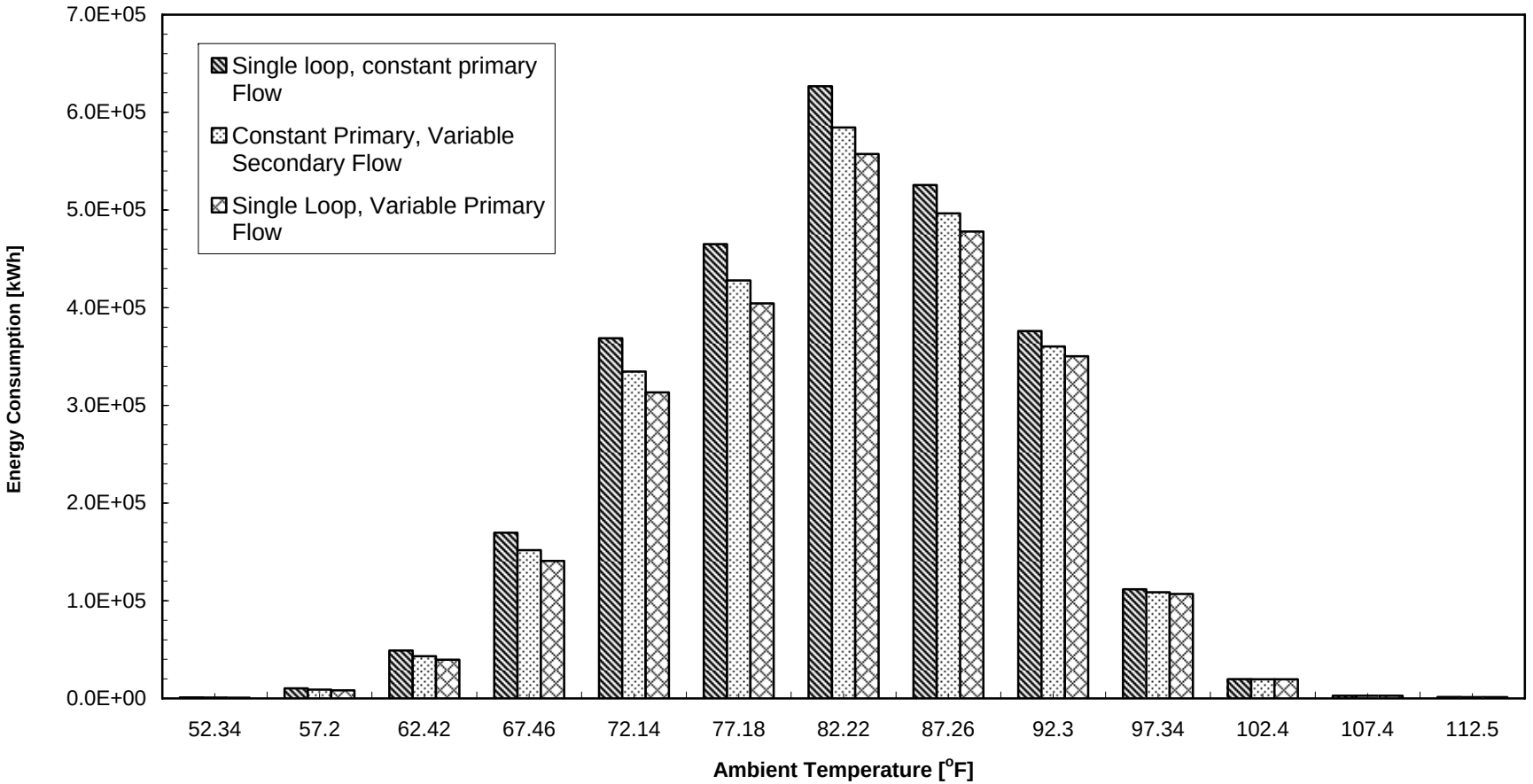

Figure 5.9 Energy consumption of the three pumping schemes for the climatic conditions of Jeddah

5.2 Chilled Water System: Analysis of Exergy

The exergy balance for the various components of the chilled water system is performed according to the method described in section 3.7 for all the three pumping schemes. The analysis is performed for the conditions of Dhahran, Riyadh and Jeddah. The values of exergy destruction at full load and 50% load on the chilled water system are calculated and the results are reported in tables 5.4, 5.5 and 5.6. It can be seen that for the different locations, the major source of exergy destruction in all the three pumping schemes is the compressor followed by the air handler. Another important observation is that, at full load the rate of exergy destruction for the single loop variable primary flow is slightly higher than the constant primary-variable secondary flow pumping scheme but still less than the single loop constant primary flow. However, at 50% load, the single loop variable primary flow pumping scheme has the lowest exergy destruction rate for all the locations. A clearer picture of the distribution of the irreversibilities is available in Figures 5.10, 5.11 and 5.12. The fact that the different pumping schemes do not have a significant effect on the exergy destruction is also highlighted in these figures.

Another important factor that must be kept in mind, while analyzing the exergy destruction for the primary secondary pumping scheme is the inclusion of the irreversibility caused by the mixing of fluids in the bypass loop. At full load conditions, there is no flow in the bypass loop and hence mixing does not take place. Therefore the exergy destruction in this situation is almost zero (table 5.5). However, at part load conditions a certain amount of supply chilled water is bypassed which then mixes with the return chilled water. Thus, the exergy destruction due to this mixing cannot be neglected.

Table 5.4 Exergy analysis of the pumping schemes for the conditions of Dhahran

Chilled Water System Components	Exergy Destruction Rate $\left(\dot{X}\right)$ [kW]					
	Single Loop, Constant Primary Pumping Scheme		Constant Primary, Variable Secondary Pumping Scheme		Single Loop, Variable Primary Pumping Scheme	
	Full Load (T_{amb}=109.4°F)	50% Load (T_{amb}=78.53°F)	Full Load (T_{amb}=109.4°F)	50% Load (T_{amb}=78.53°F)	Full Load (T_{amb}=109.4°F)	50% Load (T_{amb}=78.53°F)
Compressor	172.7	111.2	171.5	109.7	172.5	110.9
Air Handler	40.350	8.432	40.500	6.816	40.520	6.797
Evaporator	6.160	1.932	6.152	1.891	6.152	2.149
Condenser	4.766	0.963	4.754	0.925	4.761	0.904
Cooling Tower	0.057	0.008	0.057	0.008	0.057	0.008
Chilled Water Primary Pump	2.368	1.695	0.523	0.381	1.739	0.124
Chilled Water Secondary Pump	---	---	1.307	0.102	---	---
Condenser Pump	0.295	0.212	0.295	0.212	0.295	0.212
Air Handler Fan	0.049	0.009	0.049	0.009	0.048	0.009
Chilled Water Primary Loop	3.550	2.577	0.581	0.421	3.851	0.362
Chilled Water Secondary Loop			3.008	0.458		
Condenser Water piping	0.639	0.474	0.639	0.474	0.639	0.474
Mixing Between Bypass and Return Water	---	---	0.003	1.156	---	---
Total	**230.9**	**127.5**	**228.6**	**122.8**	**230.5**	**121.9**

Table 5.5 Exergy analysis of the three pumping schemes for the conditions of Riyadh

Chilled Water System Components	Exergy Destruction Rate $\left(\dot{X}\right)$ [kW]					
	Single Loop, Constant Primary Pumping Scheme		Constant Primary, Variable Secondary Pumping Scheme		Single Loop, Variable Primary Pumping Scheme	
	Full Load (T_{amb}=107.6°F)	50% Load (T_{amb}=77.85°F)	Full Load (T_{amb}=107.6°F)	50% Load (T_{amb}=77.85°F)	Full Load (T_{amb}=107.6°F)	50% Load (T_{amb}=77.85°F)
Compressor	172.7	111.2	171.4	109.7	172.3	6.576
Air Handler	38.630	8.197	38.550	6.595	38.540	110.9
Evaporator	6.059	1.915	6.041	1.874	6.038	2.130
Condenser	4.688	0.9541	4.665	0.917	4.662	0.896
Cooling Tower	0.056	0.008	0.056	0.008	0.056	0.008
Chilled Water Primary Pump	2.329	1.680	0.514	0.378	1.496	0.119
Chilled Water Secondary Pump	---	---	1.158	0.101	---	---
Condenser Pump	0.290	0.210	0.290	0.210	0.290	0.210
Air Handler Fan	0.062	0.009	0.062	0.009	0.062	0.009
Chilled Water Primary Loop	3.492	2.555	0.571	0.417	3.364	0.359
Chilled Water Secondary Loop	---	---	2.744	0.454	---	---
Condenser Water piping	0.628	0.470	0.628	0.470	0.628	0.470
Mixing Between Bypass and Return Water	---	---	0.144	1.146	---	
Total	**228.9**	**127.2**	**226.2**	**122.5**	**227.5**	**121.7**

Table 5.6 Exergy analysis of the three pumping schemes for the conditions of Jeddah

Chilled Water System Components	Exergy Destruction Rate $\left(\dot{X}\right)$ [kW]					
	Single Loop, Constant Primary Pumping Scheme		Constant Primary, Variable Secondary Pumping Scheme		Single Loop, Variable Primary Pumping Scheme	
	Full Load (T_{amb}=102.2°F)	50% Load (T_{amb}=75.83°F)	Full Load (T_{amb}=102.2°F)	50% Load (T_{amb}=75.83°F)	Full Load (T_{amb}=102.2°F)	50% Load (T_{amb}=75.83°F)
Compressor	172.7	111.2	171.4	109.7	172.3	110.9
Air Handler	33.650	7.517	33.570	5.960	33.56	5.942
Evaporator	5.755	1.865	5.738	1.826	5.735	2.073
Condenser	4.453	0.930	4.431	0.893	4.429	0.873
Cooling Tower	0.053	0.008	0.053	0.008	0.053	0.008
Chilled Water Primary Pump	2.122	1.637	0.489	0.368	1.420	0.117
Chilled Water Secondary Pump	---	---	1.099	0098	---	---
Condenser Pump	0.275	0.204	0.275	0.204	0.275	0.204
Air Handler Fan	0.632	0.009	0.063	0.009	0.063	0.009
Chilled Water Primary Loop	3.316	2.489	0.542	0.406	3.193	0.350
Chilled Water Secondary Loop	---	---	2.606	0.443	---	---
Condenser Water piping	0.597	0.457	0.597	0.458	0.597	0.458
Mixing Between Bypass and Return Water	---	---	0.137	1.114	---	---
Total	**223.1**	**126.3**	**220.4**	**121.8**	**221.6**	**120.9**

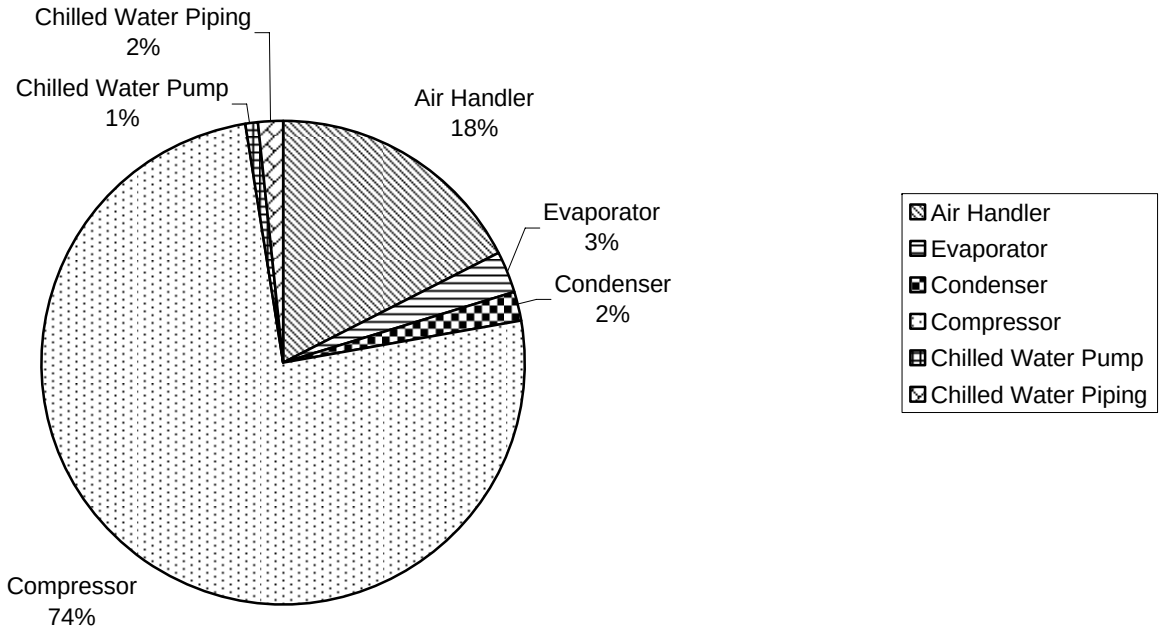

Figure 5.10 Breakdown of exergy destruction for the single loop, constant primary system at full load

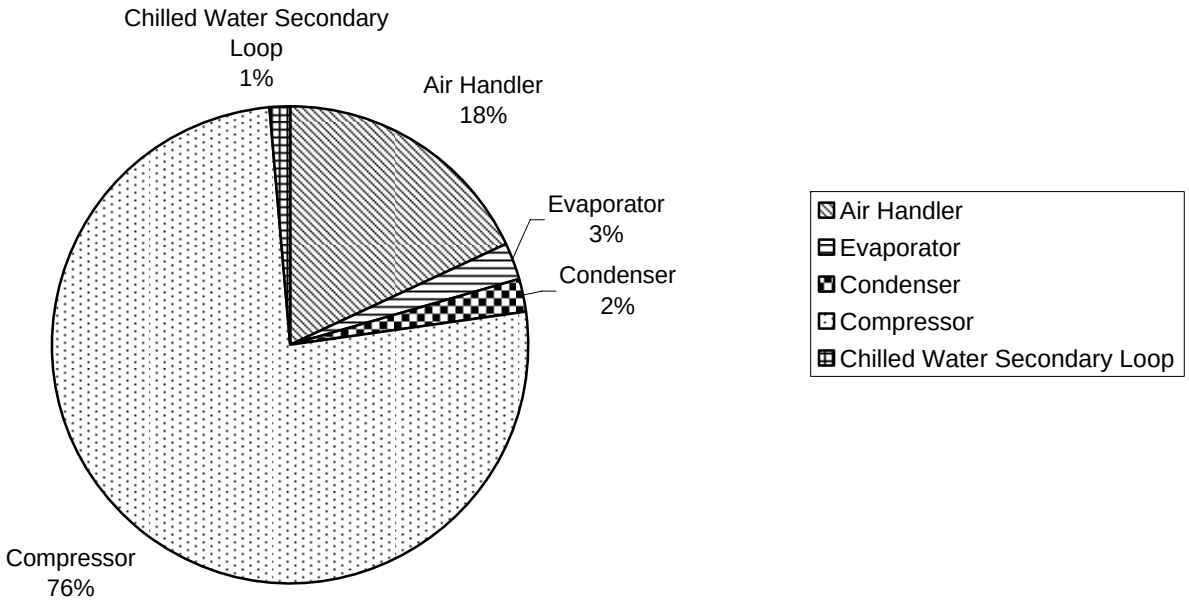

Figure 5.11 Breakdown of exergy destruction for the constant primary, variable secondary system at full load

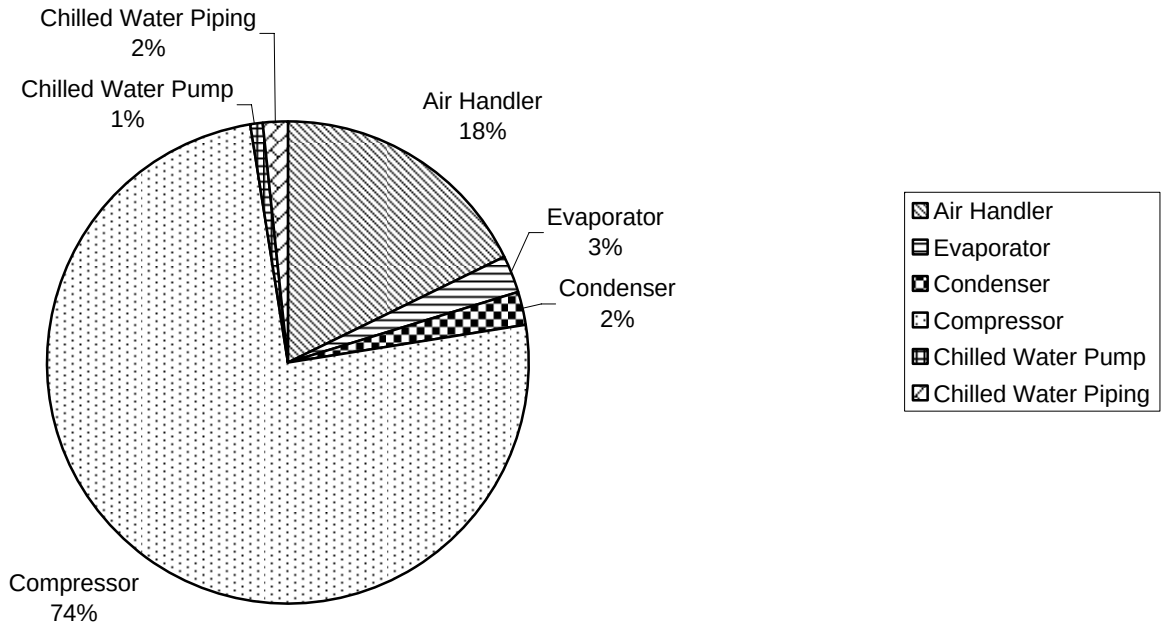

Figure 5.12 Breakdown of exergy destruction for the single loop, variable primary system at full load

5.3 Chilled Water System: Condensate Extraction from Air Handler cooling coil

The two components of the chilled water system that are most affected by the ambient conditions include the air handlers and the cooling towers. When the ambient conditions are hot and humid, a significant amount of water is collected from the air handlers. The amount of water collected depends mainly on two factors: the out-door relative humidity and the percentage of fresh air that is mixed with the return air to maintain the ventilation requirements. The variation of the water extracted from the air handler cooling coil for the existing chilled water system in building 59 for the design temperature of Dhahran, as well as two other temperatures, is shown in Figures 5.13, 5.14 and 5.15 respectively. In order to generate these curves, a particular value of the dry bulb temperature is maintained and the relative humidity as well as the percentage of fresh air introduced into the system is varied. In the present chilled water system being used in building 59, a ratio of 15% fresh air to 85% return air is maintained. At this ratio and at an ambient dry bulb temperature of 109.4 ^{o}F, it is observed that there is no significant condensate formation up to about 40% relative humidity. However, an increase in relative humidity beyond 40% is accompanied by a sharp increase in condensate formation (Fig 5.13). Therefore at a relative humidity of 100%, the rate of condensate extraction reaches to a value of about 20 kg/min.

The dependence of the rate of water extraction on the ambient dry bulb temperatures can be seen in Figures 5.13, 5.14 and 5.15. Examination of these figures reveal that as the ambient dry bulb temperature decreases, the amount of water that can be extracted from the cooling coils also reduces. It can be seen from Fig. 5.14 that at an ambient temperature of 95 ^{o}F and 15% ratio of fresh air, significant amounts of condensate can

only be collected when the ambient relative humidity is more than 60%. Moreover, when the ambient dry bulb temperature reduces to 83.4 ^{o}F, the minimum ambient relative humidity should be more than 90% in order to yield a considerable amount of condensate at a ratio of 15% fresh air.

Certain applications such as restaurants, hospitals etc. require that a larger percentage of fresh be mixed with the return air. Under such circumstances, the percentage of fresh air may go as high as 100%. From Fig. 5.13 it is observed that for the present chilled water system when the ambient temperature is equal to the design temperature (109.4 ^{o}F) and 50% fresh air is mixed with return air in the air handlers, the maximum rate of condensate extraction obtained is almost 30 kg/min. The maximum possible rate of water extraction from the present chilled water system at the design temperature corresponds to the condition that 100% fresh air is allowed in the air handler and that the ambient relative humidity is also 100%. This value comes out to be in the order of 33 kg/min. As the ambient temperature decreases to 95 ^{o}F, this maximum possible value drops to about 25 kg/min (Fig. 5.14) and further reduces to 17 kg/min at an ambient dry bulb temperature of 82.4 ^{o}F (Fig. 5.15).

In the next step, by utilizing the bin data for Dhahran, Riyadh and Jeddah, the total amount of water that can be extracted from the cooling coils of the air handler annually is calculated. These calculations are performed for various percentages of fresh air. The results from the analysis of the city of Riyadh are not considered in this analysis as the ambient conditions of Riyadh do not yield any significant results. This is mainly due to the relatively dry ambient conditions existing in Riyadh throughout the year.

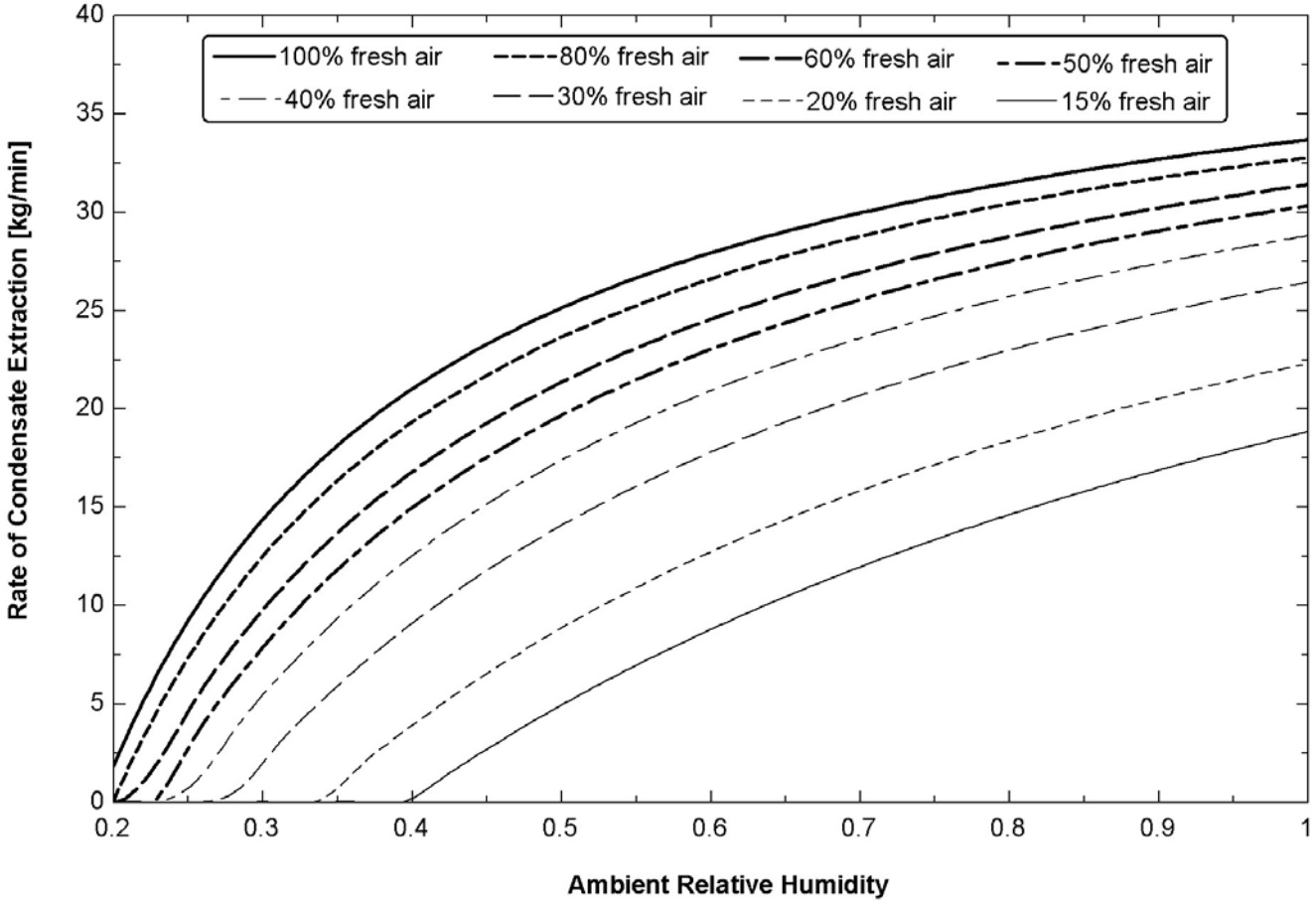

Figure 5.13 Variation of rate of condensate extraction with relative humidity for T_{amb}=109.4^{o}F (43^{o}C)

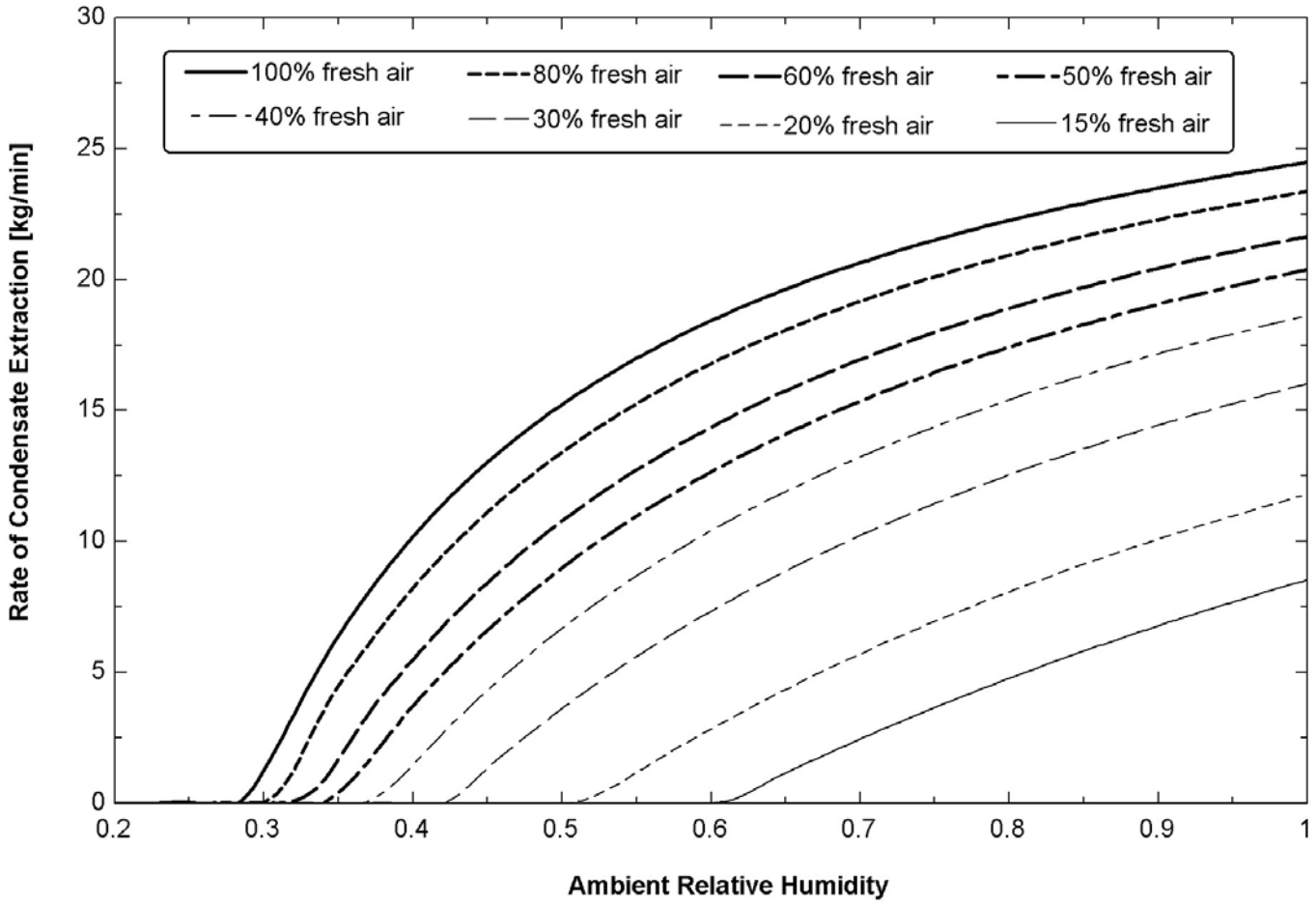

Figure 5.14 Variation of rate of condensate extraction with relative humidity for T_{amb}=95^{o}F (35^{o}C)

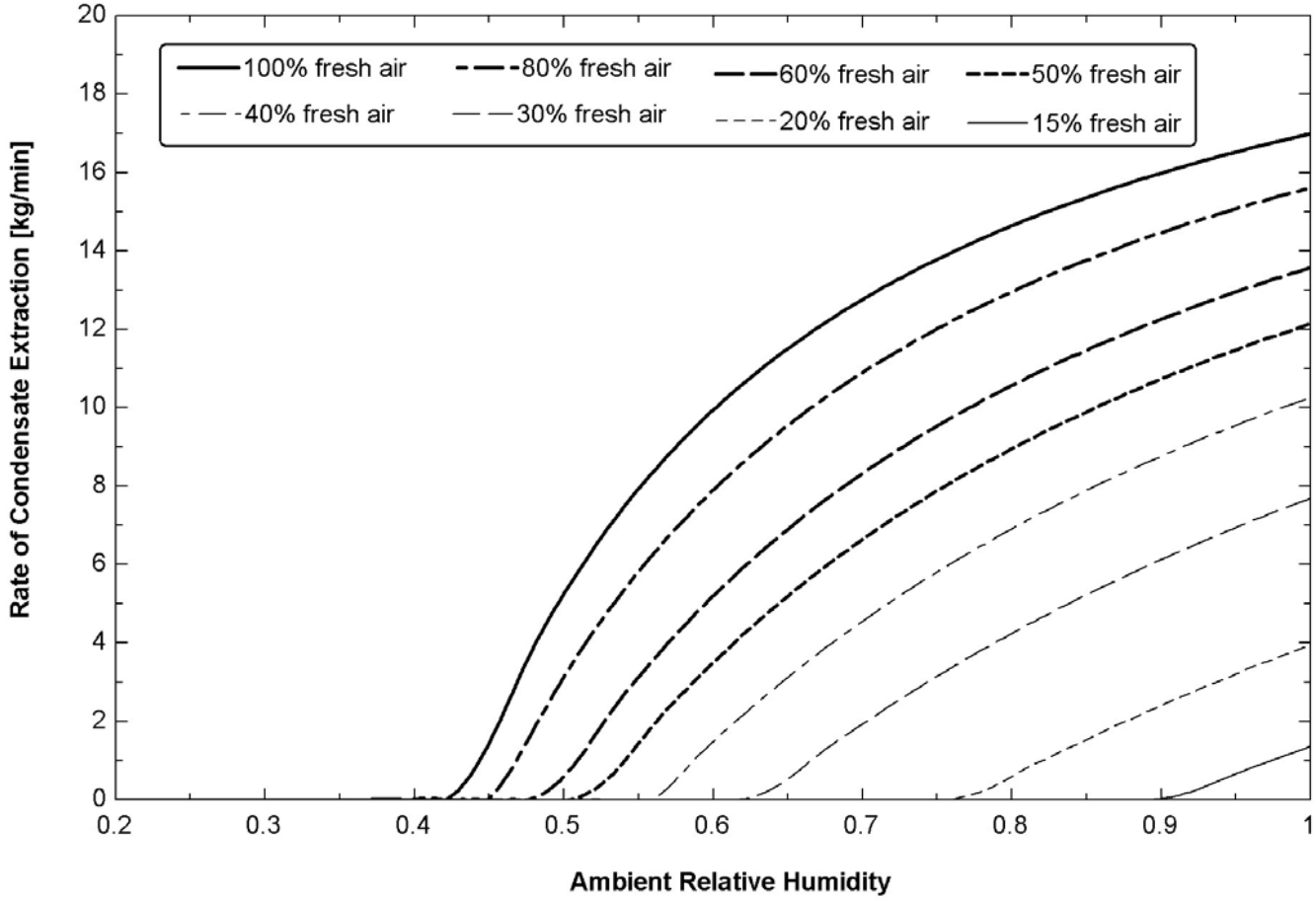

Figure 5.15 Variation of rate of condensate extraction with relative humidity for T_{amb}=82.4^{o}F (28^{o}C)

From Fig. 5.16 it is evident that at 15% fresh air the amount of water collected is quite negligible. However, a sharp increase in the amount of water collected is observed when the percentage of fresh air is increased. At about 30% fresh air the total amount of water collected annually for both Dhahran and Jeddah is almost around 30,000 kg, as shown in Fig. 5.16. But due to the predominately humid conditions existing in Jeddah, the maximum amount of water that can be extracted from the air handlers of chilled water system being considered is three times the amount that can be collected for the conditions of Dhahran. This result is represented graphically in Fig. 5.17.

5.4 Ejector Cooling System: Performance Analysis.

The value of COP of the ejector cooling system is related to the entrainment ratio as well as the difference between the enthalpies at the inlet and outlet of the generator and the evaporator as given in eqn.4.4. The entrainment ratio is in turn dependent on the operating temperatures, which include the evaporator, condenser and generator temperatures, as well as on the working fluid of the system. In order to analyze the effect of the operating temperatures on the entrainment ratio as well as on the COP of the ejector cooling system, a series of parametric studies using R134a as the working fluid are conducted. The refrigerant R134a is chosen because it has an ODP of zero. The variation of the entrainment ratio and the COP with the evaporator and the condenser temperatures is shown in Figures 5.18 and 5.19, respectively. The generator temperature is maintained at a constant temperature of 90 ^{o}C. It is quite obvious from the figures that as the evaporator temperature is increased, the value of the entrainment ratio and the COP also increases. The reverse is true for the case of condenser temperature i.e. an increase in condenser temperature causes a decrease in the entrainment ratio and the COP.

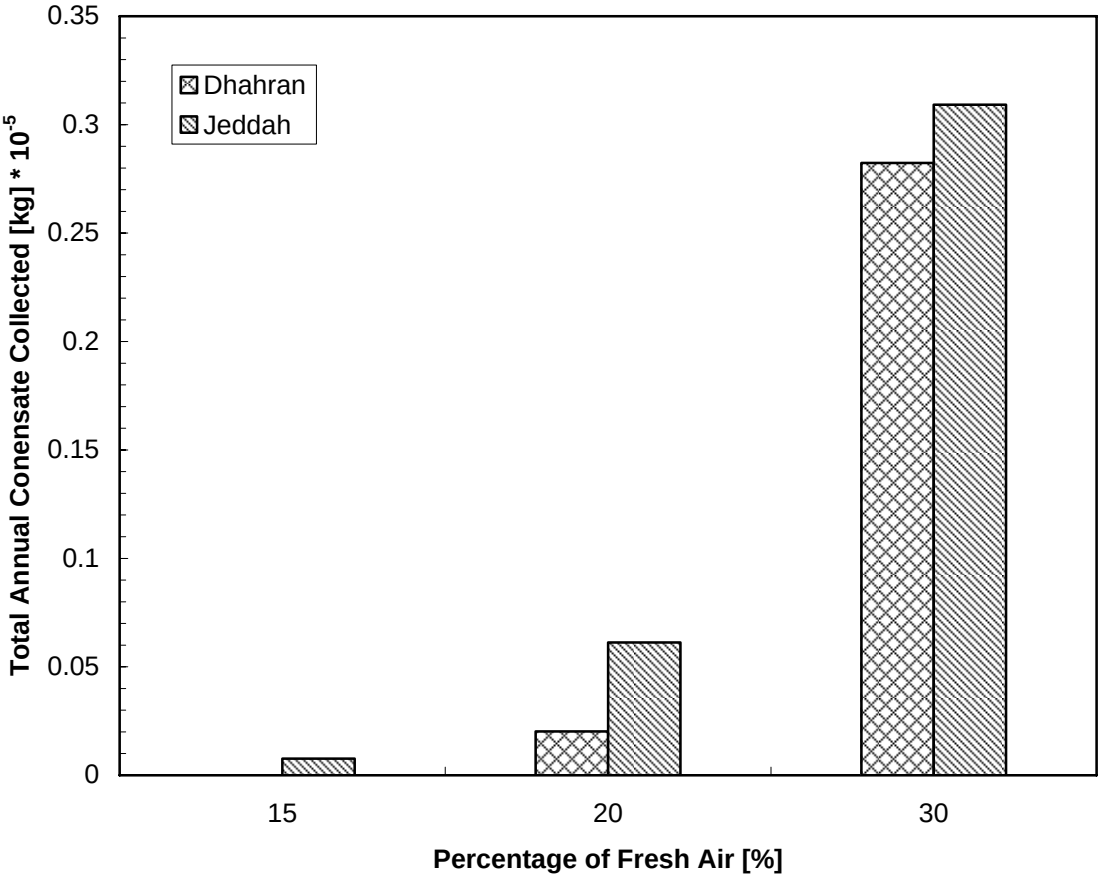

Figure 5.16 Variation of the total water collected from cooling coils for lower percentages of fresh air

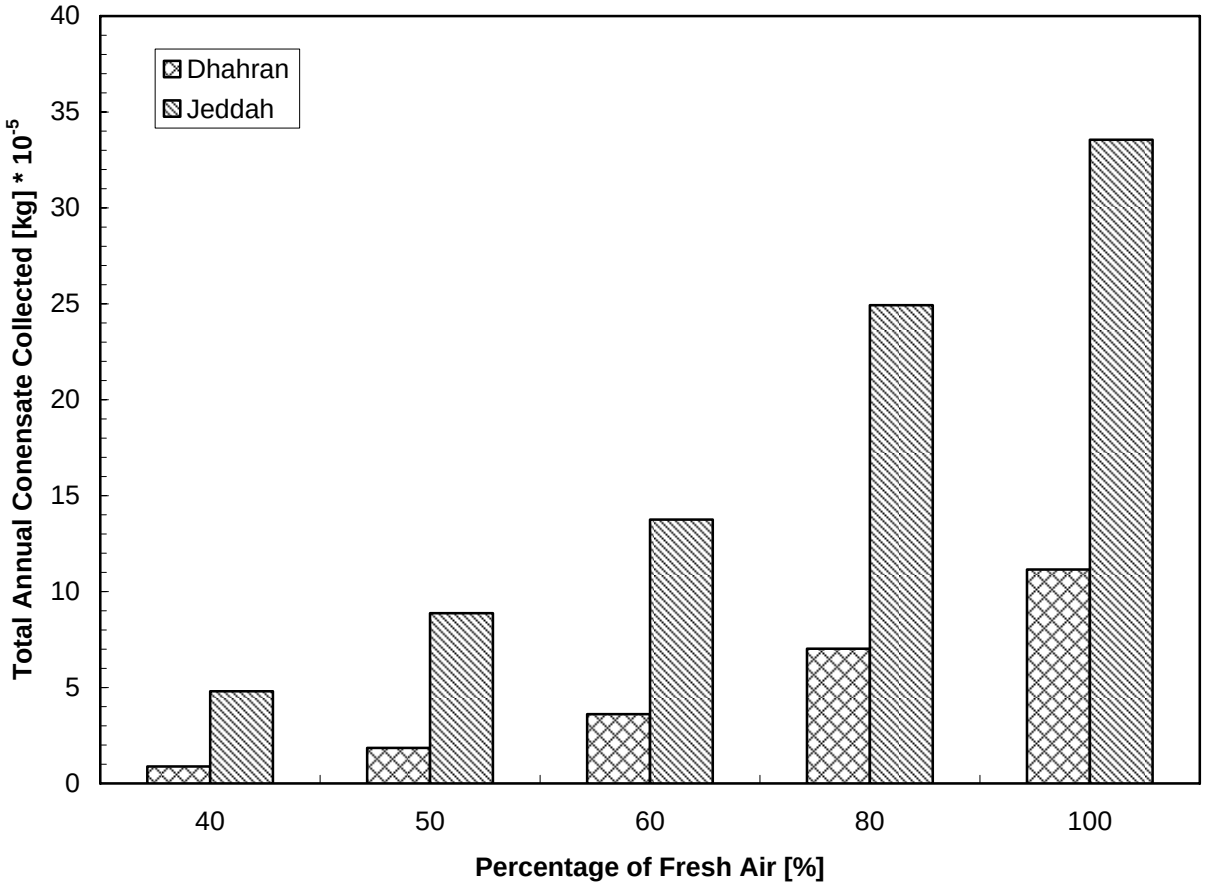

Figure 5.17 Variation of the total water collected from cooling coils for higher percentages of fresh air

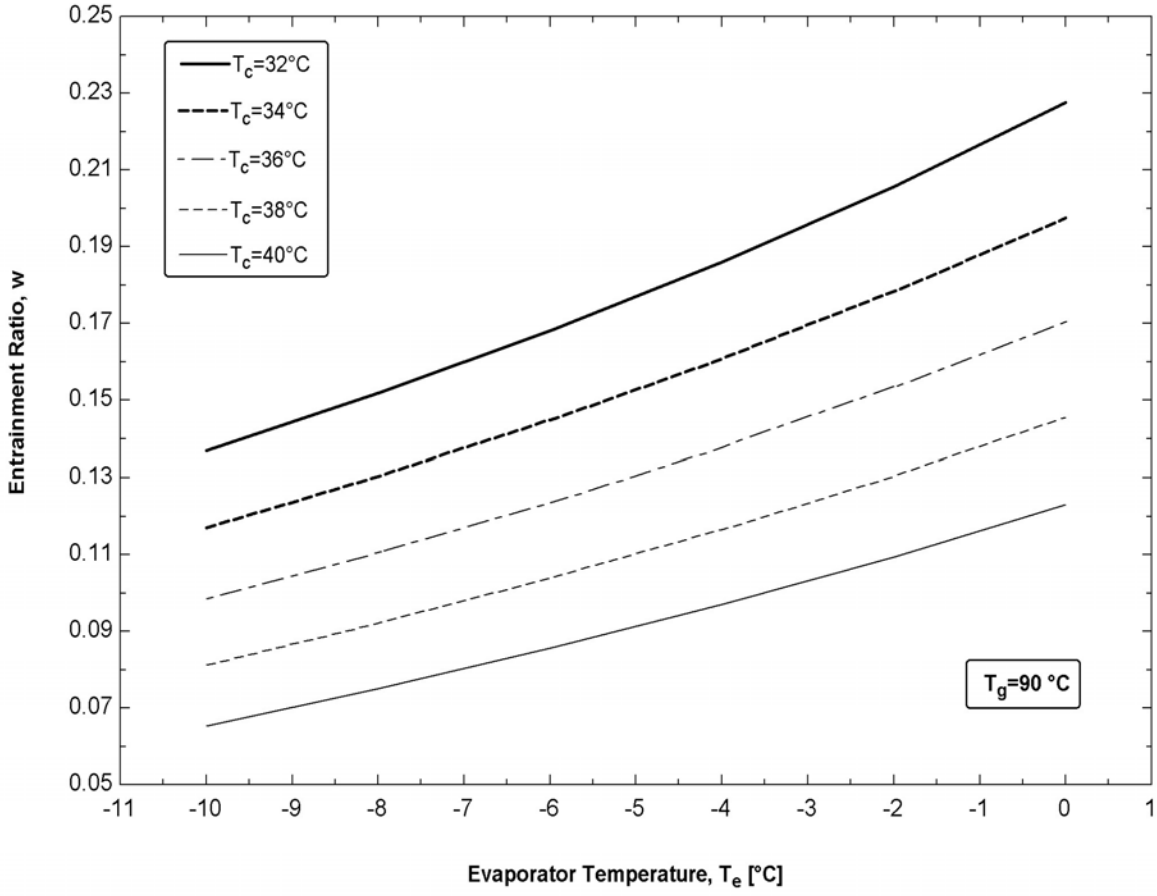

Figure 5.18 Variation of the entrainment ratio with evaporator and condenser temperatures at T_g=90^{o}C

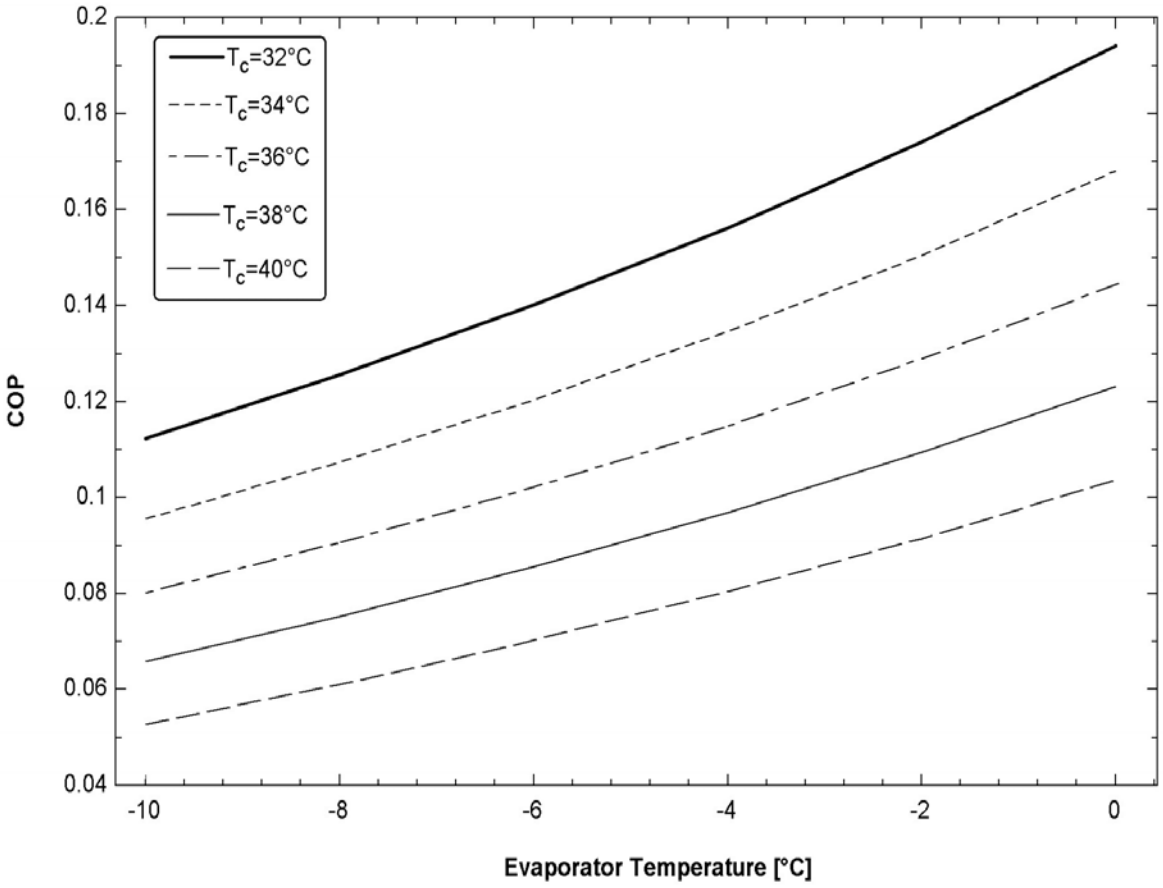

Figure 5.19 Variation of the COP with evaporator and condenser temperatures at T_g=90^{o}C

Figures 5.20 and 5.21 illustrate the fact that an increase in generator temperature is accompanied by a corresponding increase in the entrainment ratio as well as the COP. The trend of variation of the entrainment ratio and the COP with the condenser and generator temperatures is represented graphically in Fig.5.22 and Fig.5.23 respectively.

Finally, the effect of the refrigerant on the entrainment ratio as well as the COP is investigated. In order to perform this study, the temperature of the generator, condenser and the evaporator are fixed at a constant value and the working fluid of the ejector cooling system is changed by utilizing a selection of ten most commonly used refrigerants. The results obtained for the entrainment ratio as well as the COP are presented in Figures 5.24 and 5.25 respectively. Careful observation of Fig. 5.24 reveals that, for the given set of operating temperatures, the highest entrainment ratio is obtained by using the refrigerant R141b, while the lowest is obtained by employing the refrigerant R22. However, as far as the COP of the ejector cooling system is concerned, the highest value is obtained when the refrigerant R717 is used as the working fluid, whereas the lowest value is obtained by using the refrigerant R114 as shown in Fig. 5.25.

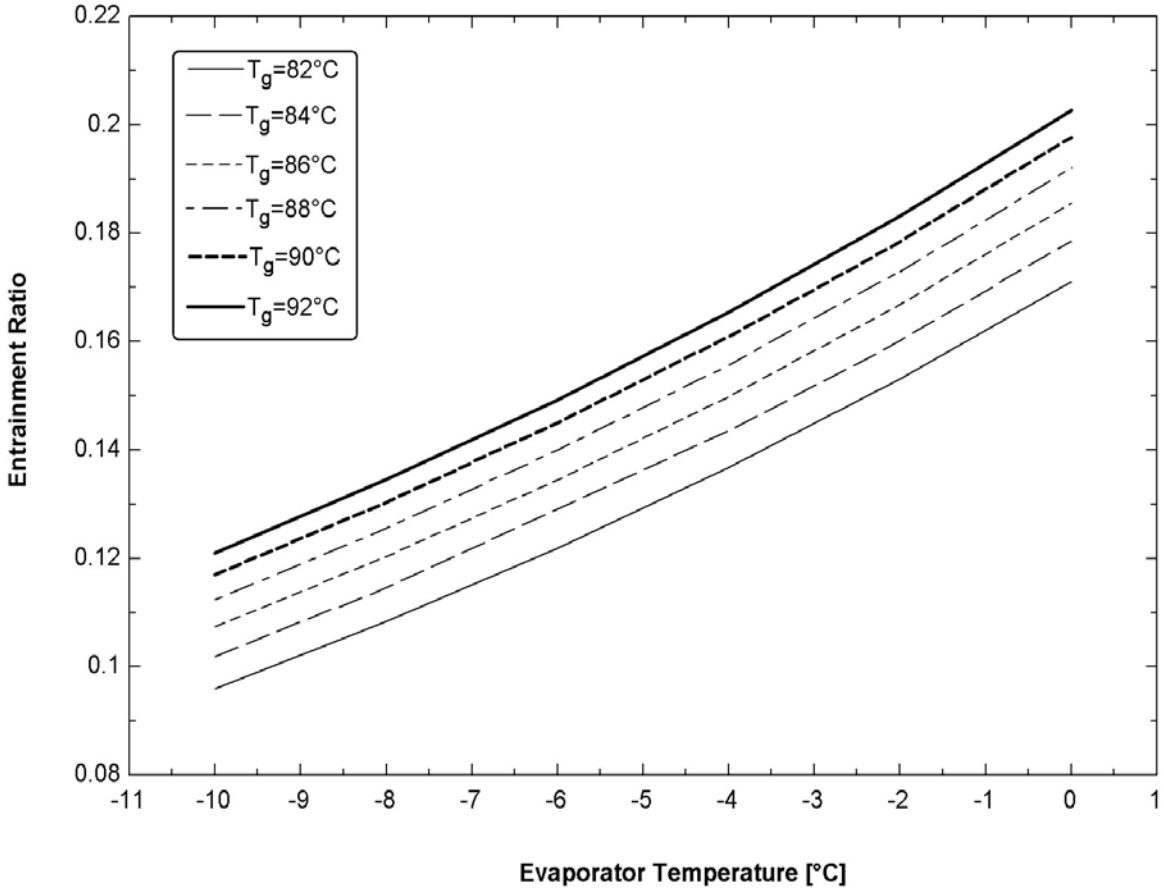

Figure 5.20 Variation of the entrainment ratio with evaporator and generator temperatures at T_c=34^{o}C

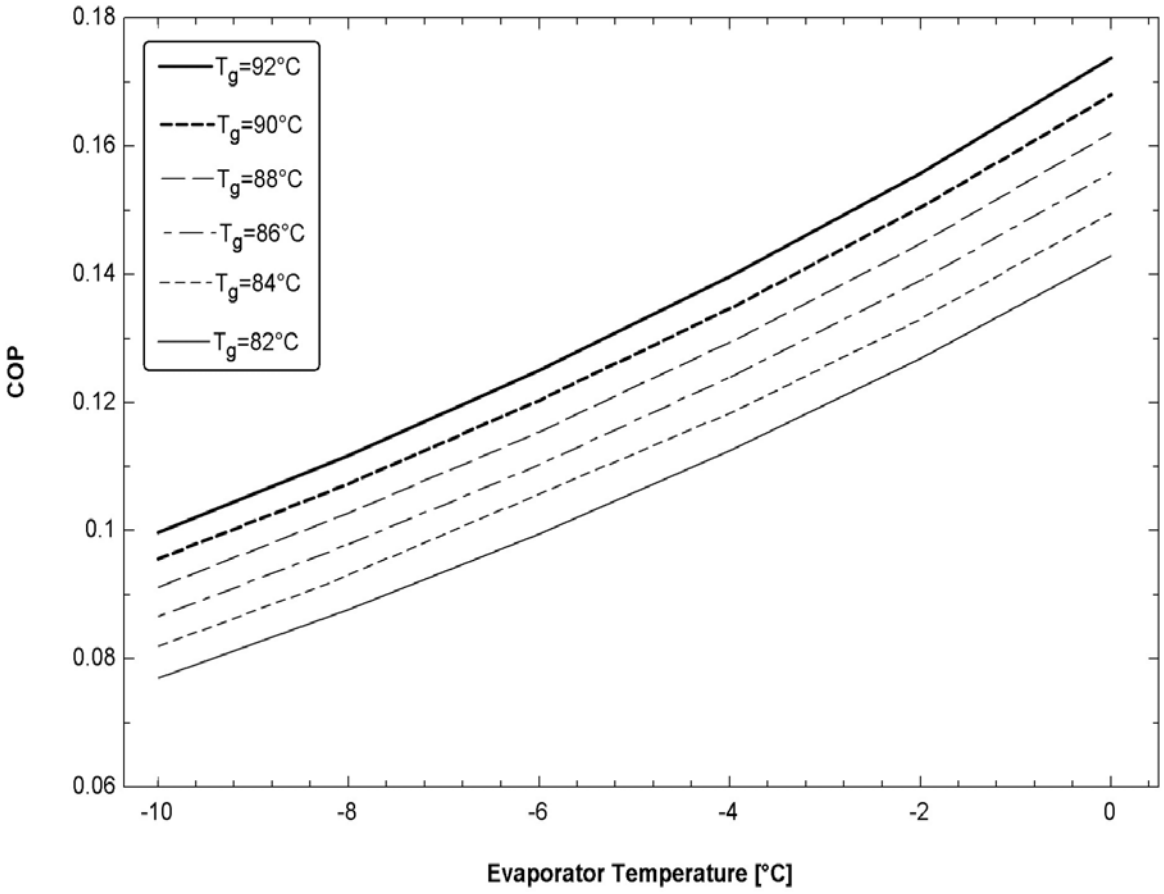

Figure 5.21 Variation of the COP with evaporator and generator temperatures at T_c=34^{o}C

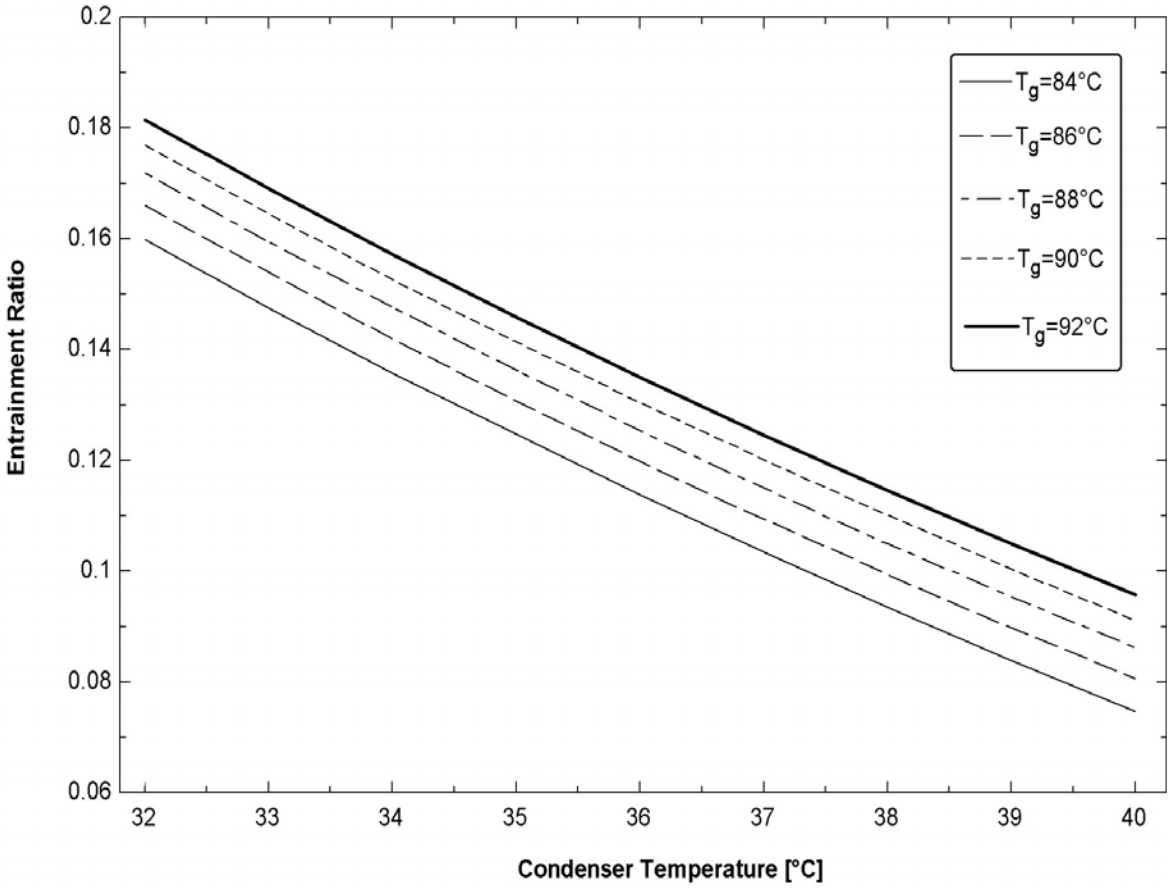

Figure 5.22 Variation of the entrainment ratio with condenser and generator temperatures at T_e=-5 ^oC

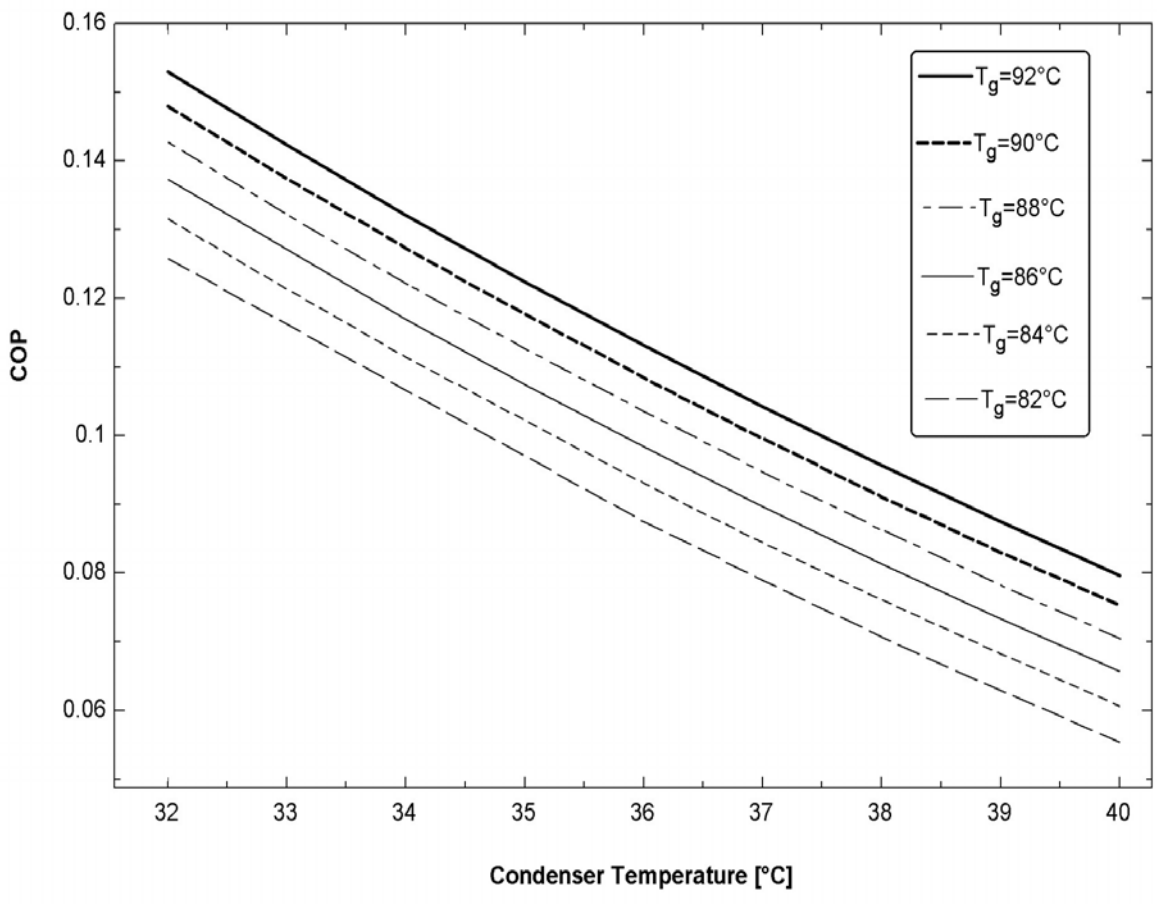

Figure 5.23 Variation of the COP with condenser and generator temperatures at T_e=-5 ^oC

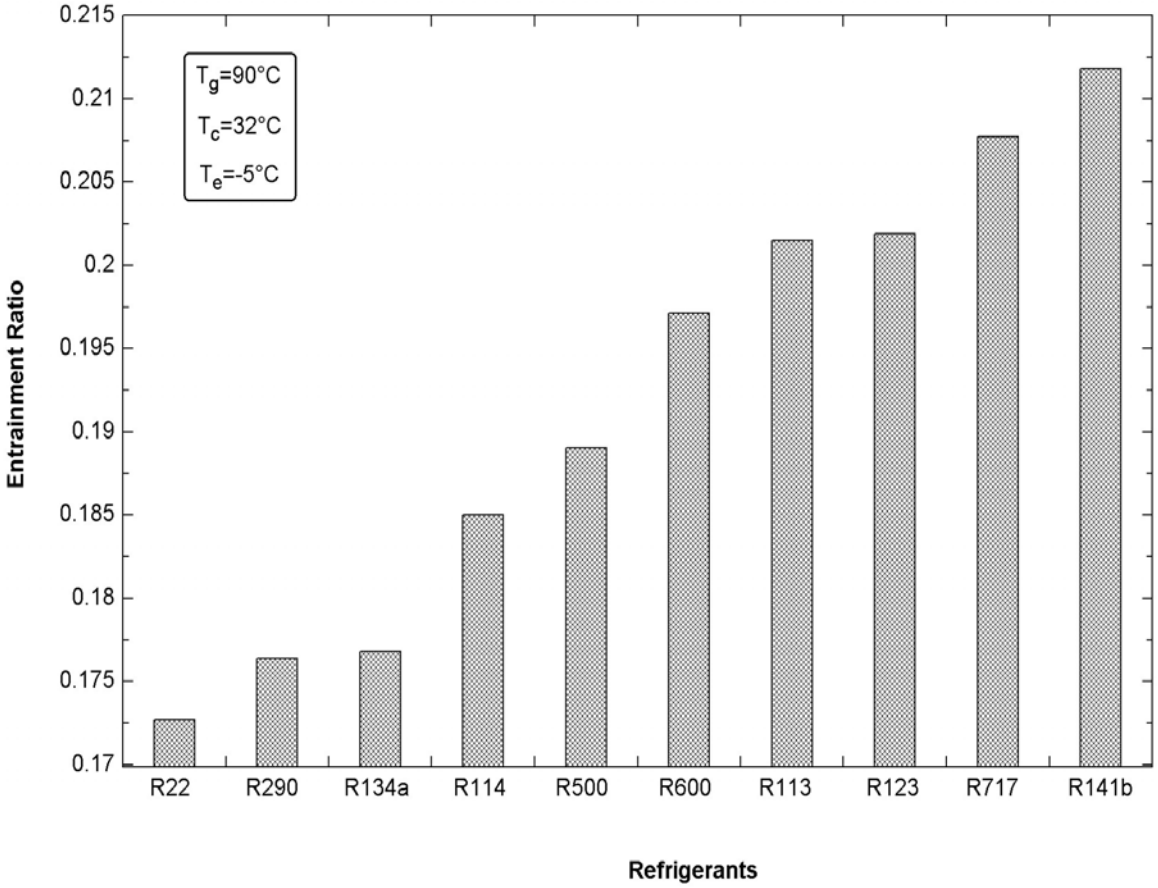

Figure 5.24 Variation of the entrainment ratio with different refrigerants

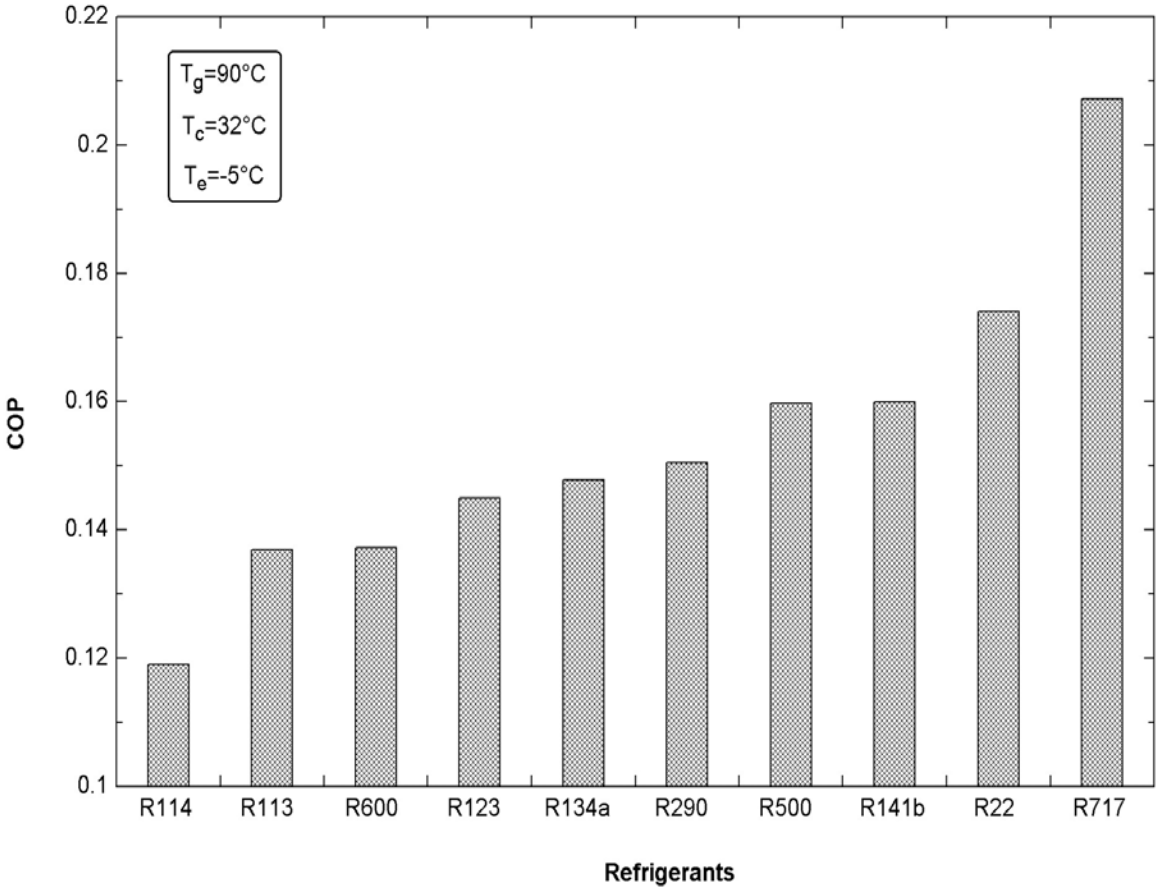

Figure 5.25 Variation of the COP with different refrigerants

5.5 Ejector Cooling System: Exergy Analysis.

In order to explain the variation of COP of the ejector cooling system with respect to various system temperatures an irreversibility analysis of the ejector cycle is carried out. In this regard, a cooling capacity of *5 kW* for the ejector system is considered. The room temperature is taken as $22\ ^oC$ whereas the dead state or reference temperature of $30\ ^oC$ is assumed in the entire analysis. The remaining assumptions are the same as discussed earlier in section 4.1. An exergy balance for the individual components of the ejector cooling system is carried out and then these values are added to determine the total irreversible losses of the system. Considering figures 4.1 are 4.2, the irreversible losses (or exergy destruction) for the generator, ejector, condenser, evaporator, and expansion device, respectively, can be expressed as,

$$I_{generator} = \left[\dot{m}_g \left(s_1 - s_6 \right) - \left(\frac{\dot{Q}_g}{T_g} \right) \right] T_0 \tag{5.1}$$

$$I_{ejector} = \left[\left\{ \left(\dot{m}_g + \dot{m}_e \right) s_3 \right\} - \left(\dot{m}_g s_1 \right) - \left(\dot{m}_e s_2 \right) \right] T_0 \tag{5.2}$$

$$I_{condenser} = \left[\left\{ \left(\dot{m}_g + \dot{m}_e \right) \left(s_4 - s_3 \right) \right\} + \left(\frac{\dot{Q}_c}{\left(T_0 \right)} \right) \right] T_0 \tag{5.3}$$

$$I_{evaporator} = \left[\left\{ \dot{m}_e \left(s_2 - s_5 \right) \right\} - \left(\frac{\dot{Q}_e}{T_{room} + 273} \right) \right] T_0 \tag{5.4}$$

$$I_{expansion} = \left\{ \dot{m}_e \left(s_5 - s_4 \right) \right\} T_0 \tag{5.5}$$

Finally, the total irreversible losses for the ejector cooling cycle can be summed up as,

$$I_{total} = I_{ejector} + I_{generator} + I_{condenser} + I_{evaporator} + I_{expansion} \quad (5.6)$$

Figures 5.26, 5.27 and 5.28 show the variation of the total as well as the individual component irreversibilities of the various components of the ejector cooling system with the generator, condenser and evaporator temperatures, respectively. It can be clearly seen from Figures 5.26 and 5.28 that as the generator and the evaporator temperatures are increased, the irreversibility of the system decreases. This results in an increase in the COP of the system as visualized in Figures 5.19 and 5.21.The reduction in total irreversibility with an increase in evaporator temperature results mainly from the reduction of pumping power, the heat required by the generator and the heat rejected from the condenser.

On the contrary, referring to Figure 5.27, it is observed that increasing the condenser temperature raises the exergy destruction of the system and hence results in the reduced COP of the ejector cooling system. This reduction in COP with an increase in condenser temperature is clearly depicted in Figure 5.19.

Further examination of Figures 5.26, 5.27 and 5.28 reveals that the major source of exergy destruction in the ejector cooling system is the ejector itself. The main cause for this exergy destruction in the ejector is the expansion-contraction losses that occur due to the flow inside the ejector through the convergent-divergent nozzle, and the non-ideal adiabatic expansion in the nozzle. Followed by the ejector, the major exergy destruction in the ejector cooling system occurs in the generator condenser and evaporator as these components transfer heat over a finite temperature difference.

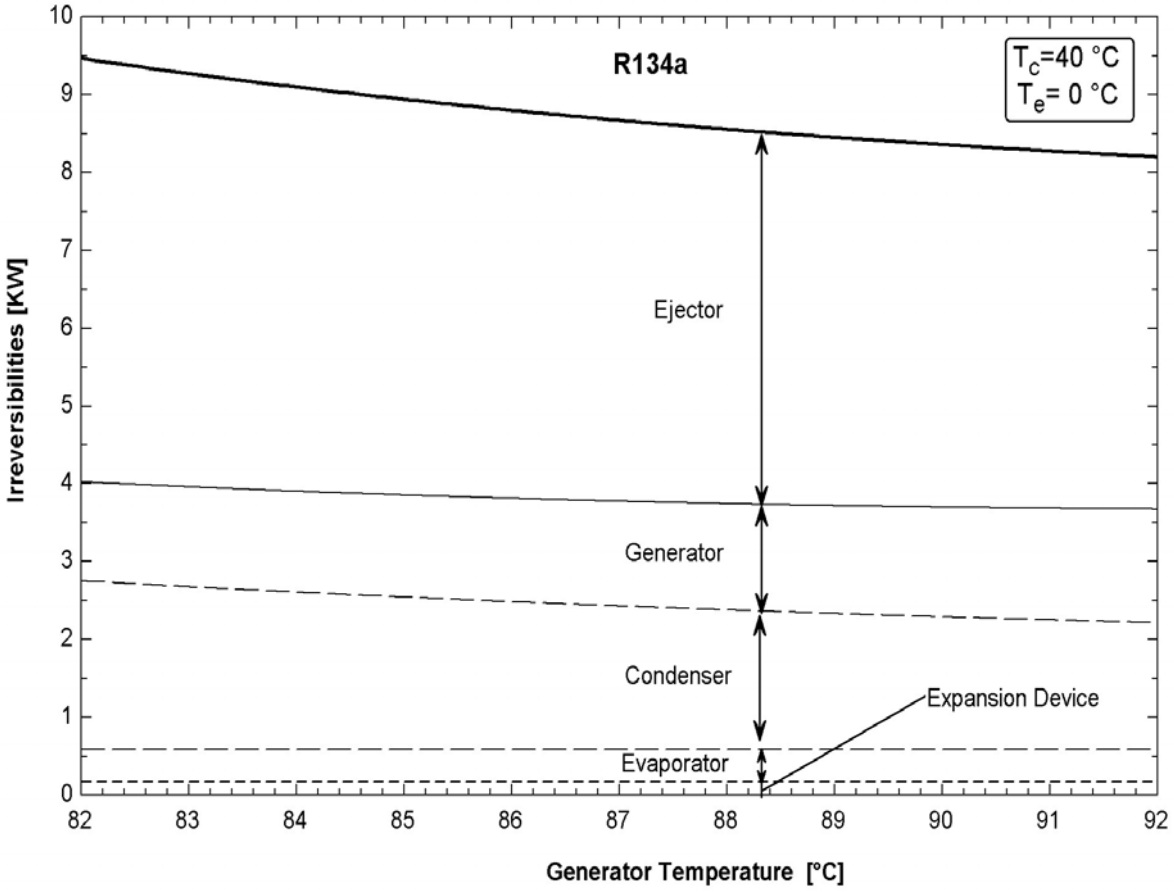

Figure 5.26 Irreversibilities in various components vs. generator temperature

The throttling process in the expansion device causes an exergy loss which is the smallest in the ejector cooling system because of the small pressure drop through the expansion device.

Figures 5.29 and 5.30 show the effect of generator temperature on the total irreversibilities as well as the COP of the ejector cooling system, respectively; with respect to the use of various refrigerants. It is seen that for all the refrigerants considered, as increase in evaporator temperature reduces the total irreversibility of the system. It is important to notice that for some refrigerants such as *R22,* the magnitude of the reduction in irreversibility does not directly agree with the corresponding increase in COP. This is mainly due to the physical as well as the chemical properties of this refrigerant. Nevertheless, the trend followed by all the refrigerants in terms of total irreversibility as well as COP with an increase in generator temperature remains the same.

Figures 5.31 and 5.32 illustrate the effect of increasing condenser temperature on the total irreversibilities and COP of the system with respect to six commonly used refrigerants. The effect of various refrigerants on the total irreversibilities as well as the COP of the ejector cooling system with increasing evaporator temperature are depicted in Figures 5.33 and 5.34. Thus, from the above analysis, it can be safely generalized that an increase in the generator and the evaporator temperatures improves the COP of the ejector cooling system irrespective of the refrigerant that is used as the working fluid. The opposite is true for the case of the condenser temperature as its increase reduces the COP and increases the irreversibilities of the system regardless of the refrigerant being used in the system.

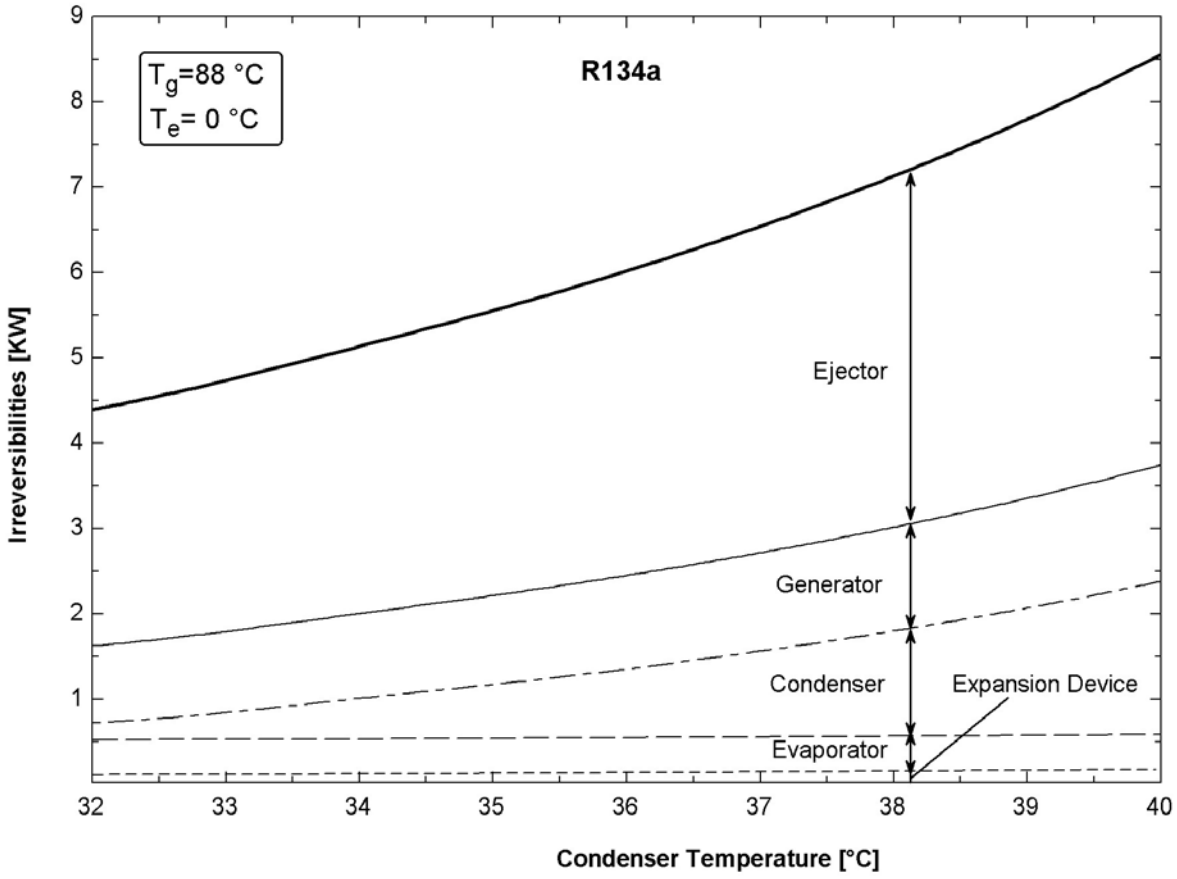

Figure 5.27 Irreversibilities in various components vs. condenser temperature

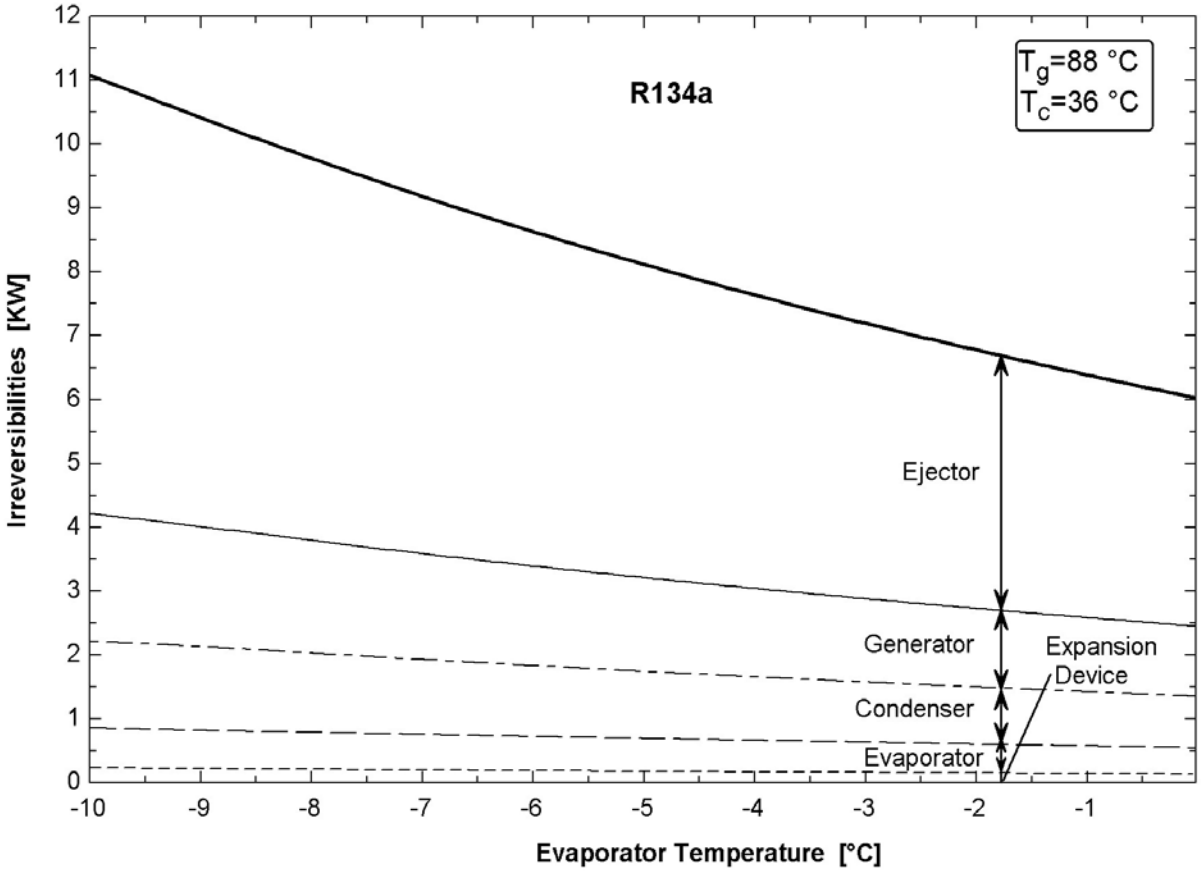

Figure 5.28 Irreversibilities in various components vs. evaporator temperature

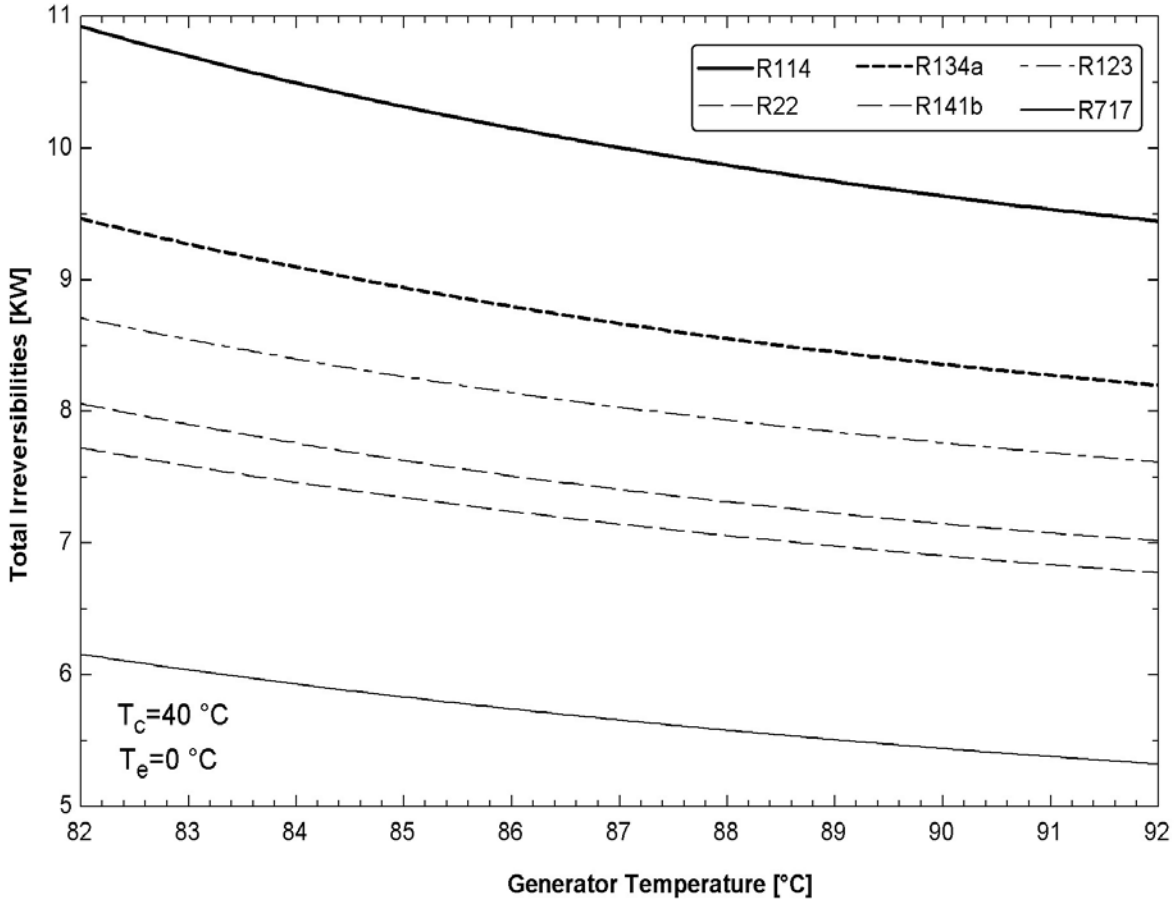

Figure 5.29 Effect of generator temperature on irreversibilities for various refrigerants

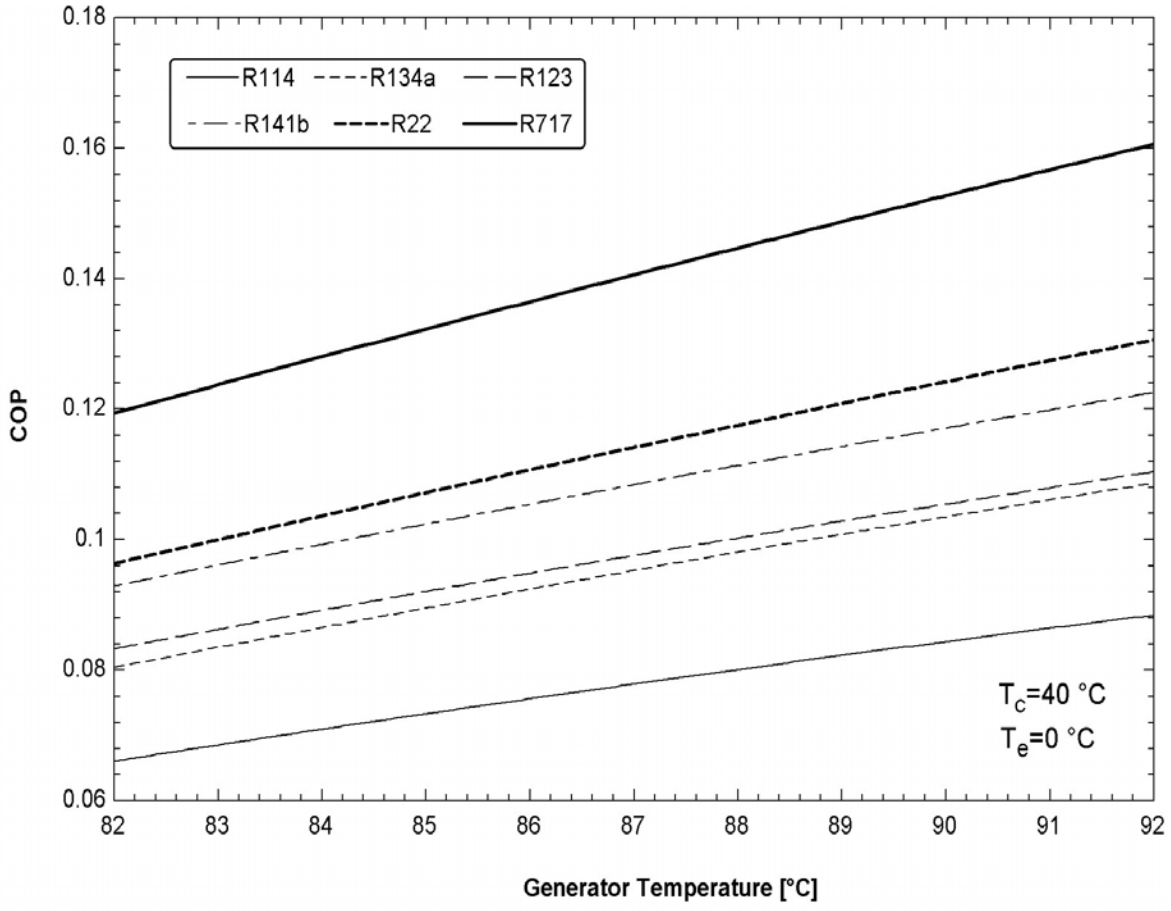

Figure 5.30 Effect of generator temperature on COP for various refrigerants

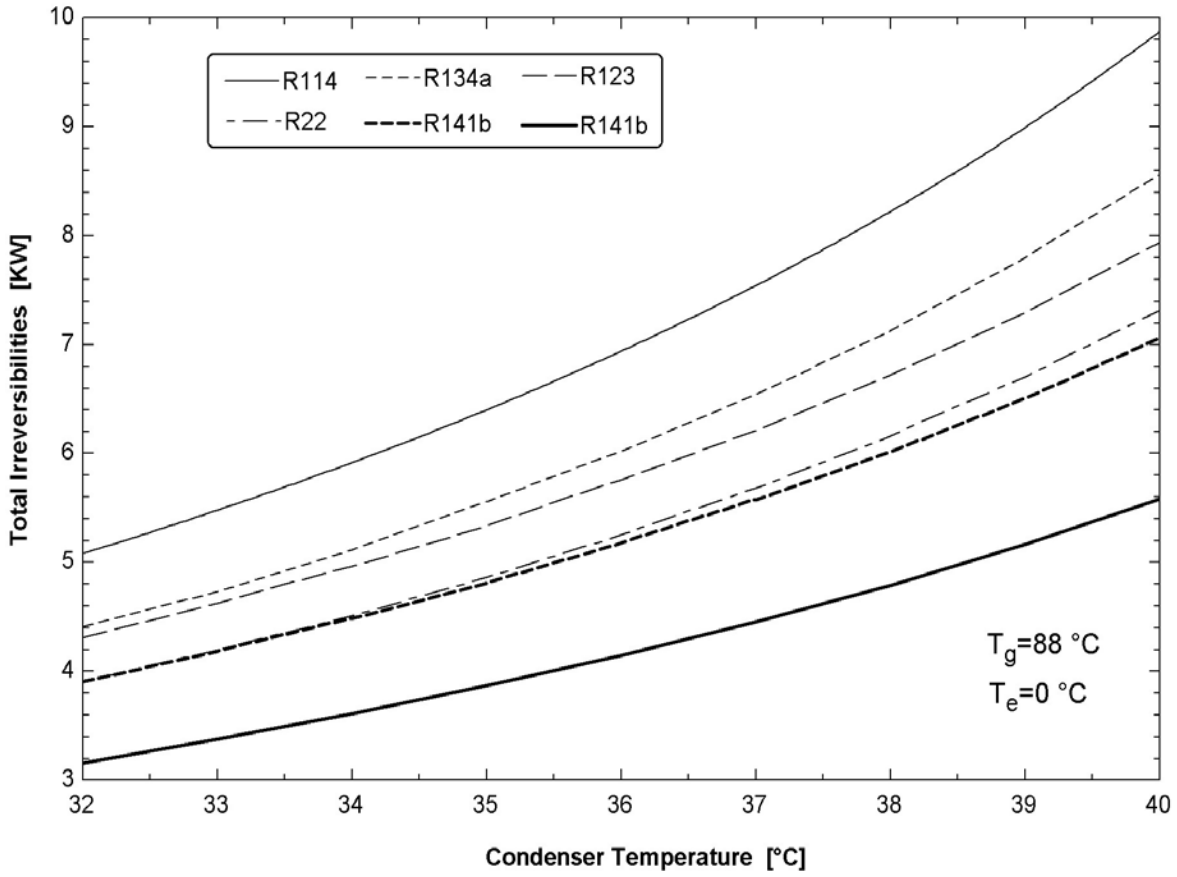

Figure 5.31 Effect of condenser temperature on irreversibilities for various refrigerants

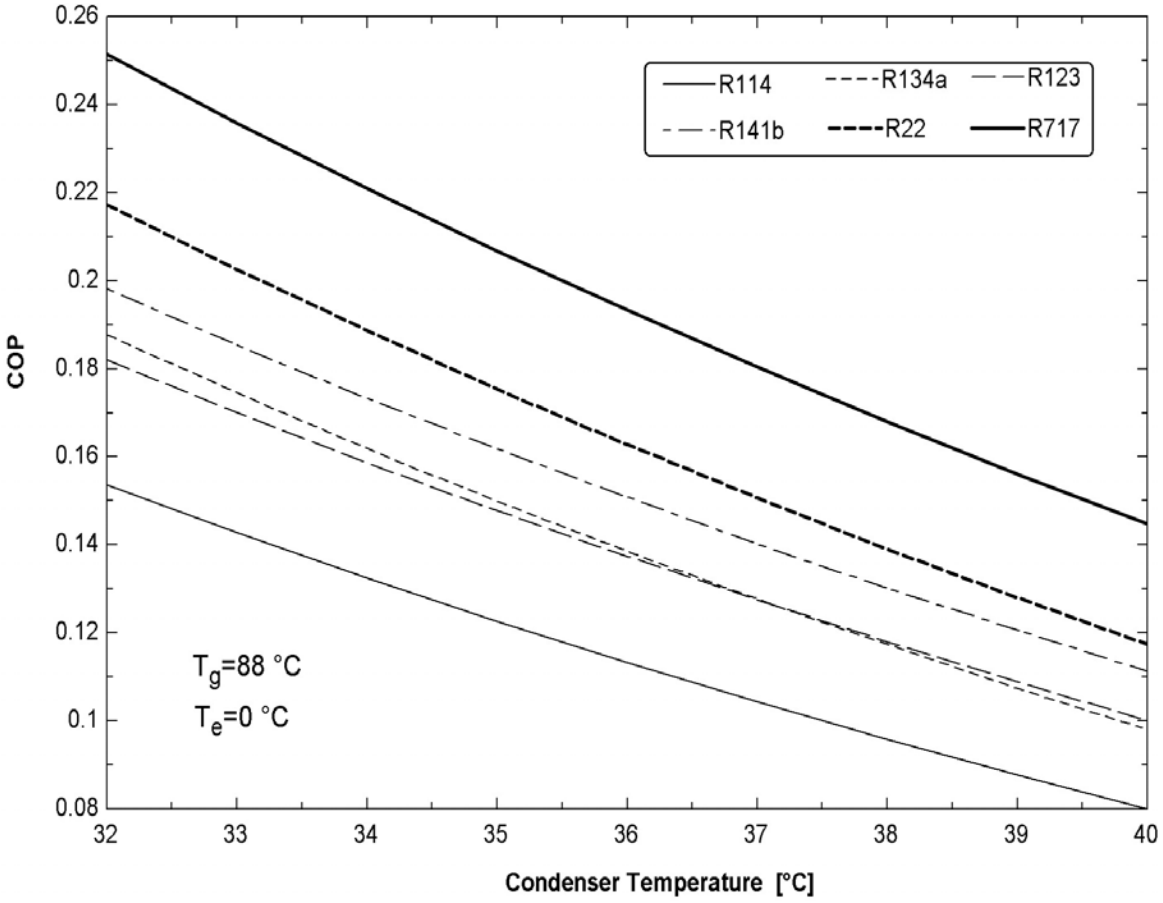

Figure 5.32 Effect of condenser temperature on COP for various refrigerants

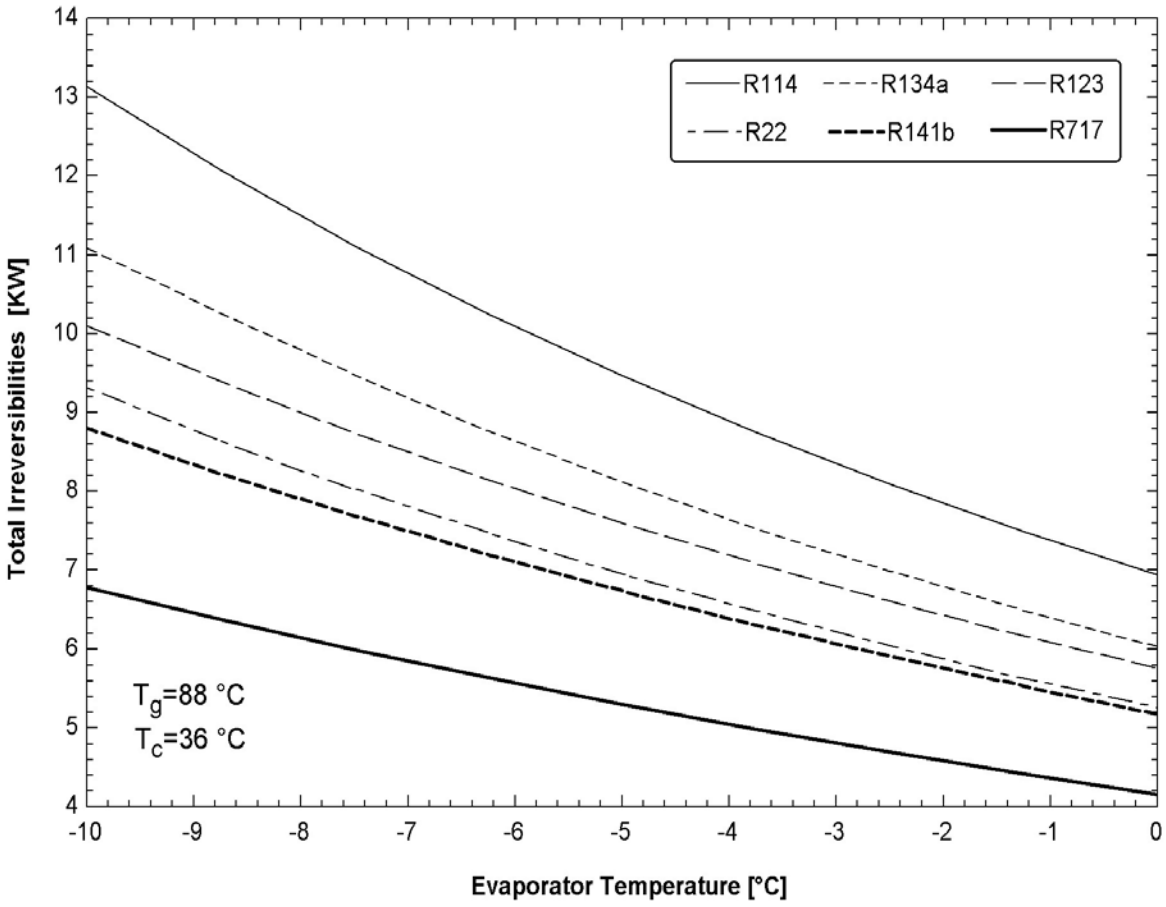

Figure 5.33 Effect of evaporator temperature on irreversibilities for various refrigerants

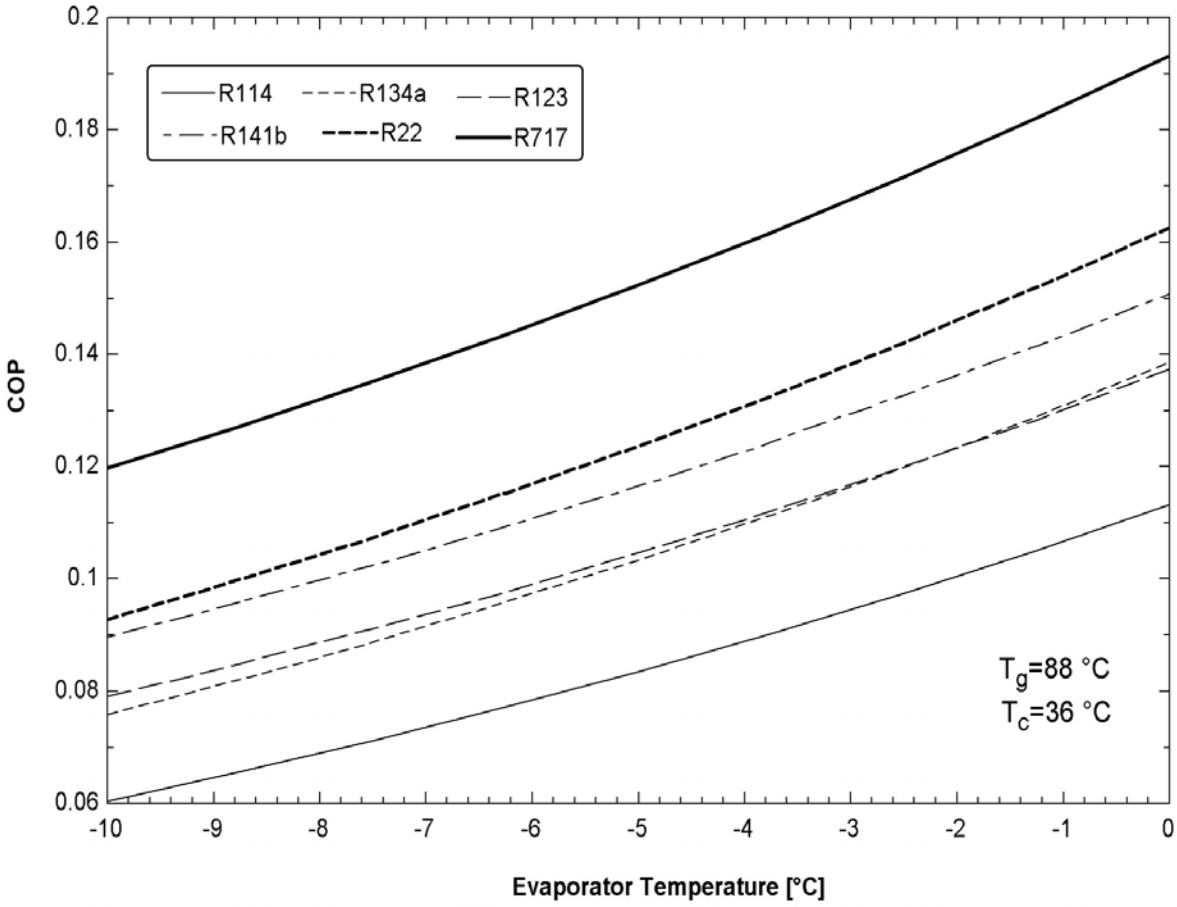

Figure 5.34 32 Effect of evaporator temperature on COP for various refrigerants

5.6 Incorporation of the Ejector Cooling System with the Chilled water System

5.6.1 System Description

The final phase of the present study deals with analyzing the effects of combining the ejector cooling system with the existing central chilled water system. The method adopted for this combination utilizes an intercooler [50,24] to combine the ejector cooling with the chilled water systems. It may be noted that in the present study, the cooling effect obtained by the ejector system is not directly used to cool the refrigerant in the condenser of the existing vapor compression chilled water system. Instead, the cooling tower of the chilled water system is replaced by an ejector cooling system. This ejector system cools the water which is in turn utilized to cool the refrigerant in the chiller condenser. In other words, the function of the cooling tower in a conventional chilled water system is eliminated by an ejector cooling system as shown in Fig.5.35.

The reason for choosing this type of combination is mainly due to the fact that the condenser is an integral part of the chiller assembly and does not exists as a separate component. The condenser is a shell and tube heat exchanger designed specifically to transfer the heat from the refrigerant to the cooling water, and both are maintained at constant flow rates for smooth operation of the chiller unit. However, the working fluid in the ejector cooling system is mostly a refrigerant and due to the difference in density, its flow rate may not necessarily be the same as that of the cooling water. Furthermore if the refrigerant is introduced directly into the chiller condenser, the performance of the chiller may become unpredictable. This is due to the reason that the condenser is not designed to

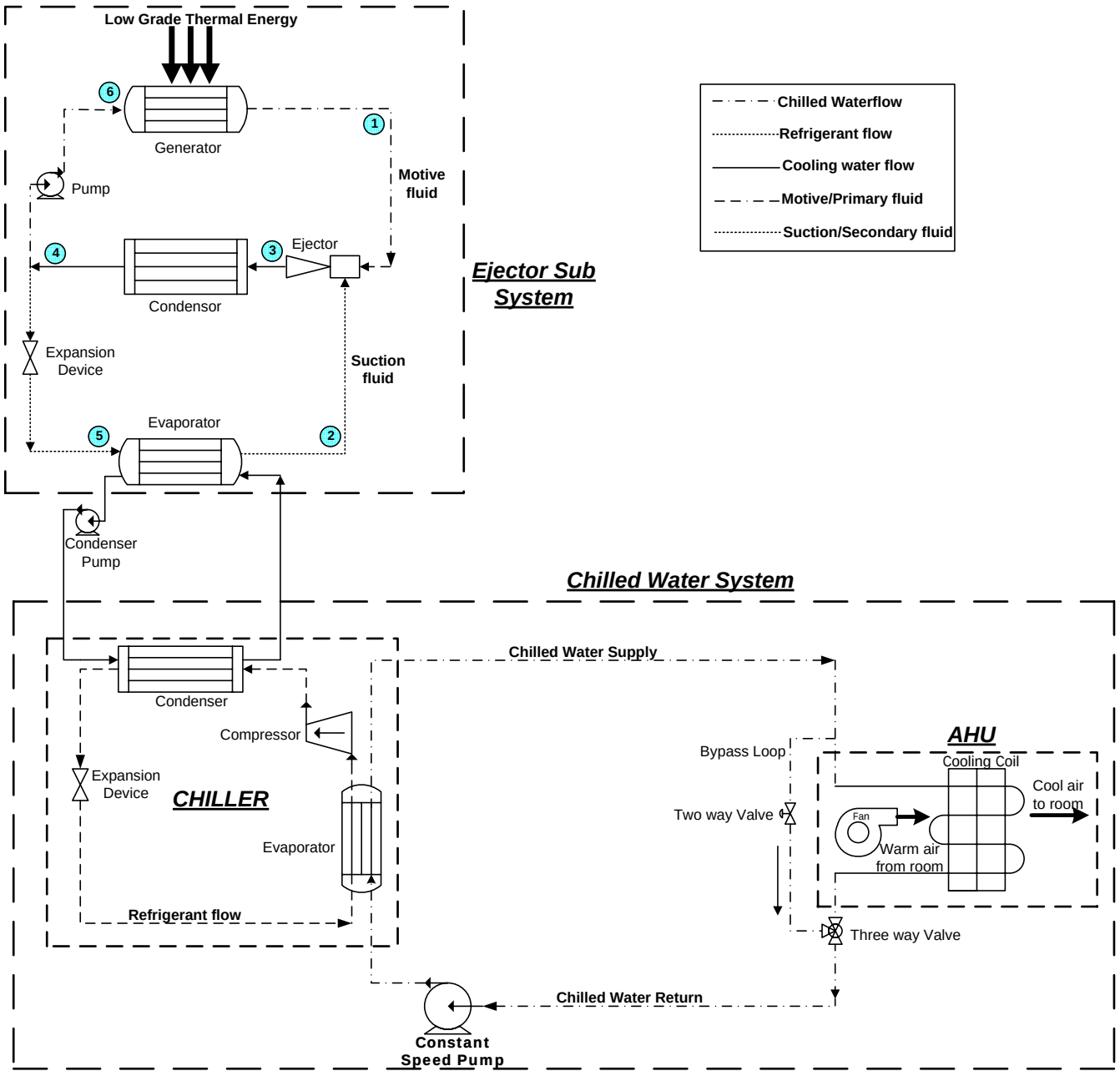

Figure 5.35 Combination of the central chilled water system with the ejector cooling system

transfer heat between two fluids that are in the vapor phase. Therefore considering the aforementioned reasons, only water which takes the heat from the refrigerant in the chiller condenser is cooled by the ejector cooling system in the present scheme.

5.6.2 System Performance Analysis

In the existing chilled water system servicing building 59, the condenser pump maintains a constant water flow rate at 1600 GPM. When the ambient relative humidity increases, the cooling capacity of the cooling tower is greatly diminished. As a consequence of this, the water coming from the chiller condenser is not cooled to the desired extent. This causes the temperature of the refrigerant in the condenser to rise above the design conditions. In order to accommodate this temperature rise, the lift of the compressor has to be increased which is only possible by increasing the compressor power. But the compressor power cannot be increased beyond its full load value. Thus, under such circumstances, additional chillers and cooling towers have to be brought online to maintain the desired comfort conditions and to ensure smooth and stable functioning of the chilled water system.

The abovementioned phenomenon is clearly visualized in Fig. 5.36. At an ambient temperature of 109.4^{o}F, and outdoor relative humidity of 50%, which is the design condition of Dhahran, the power consumed by the compressor for both the systems is identical. This location is denoted by the point '*L*' in Fig. 5.36. This power is the maximum full load power of the compressor. However, when the relative humidity increases beyond 50%, the power requirement of the compressor is increased beyond its full load capacity, which can only be fulfilled by starting other back up chillers.

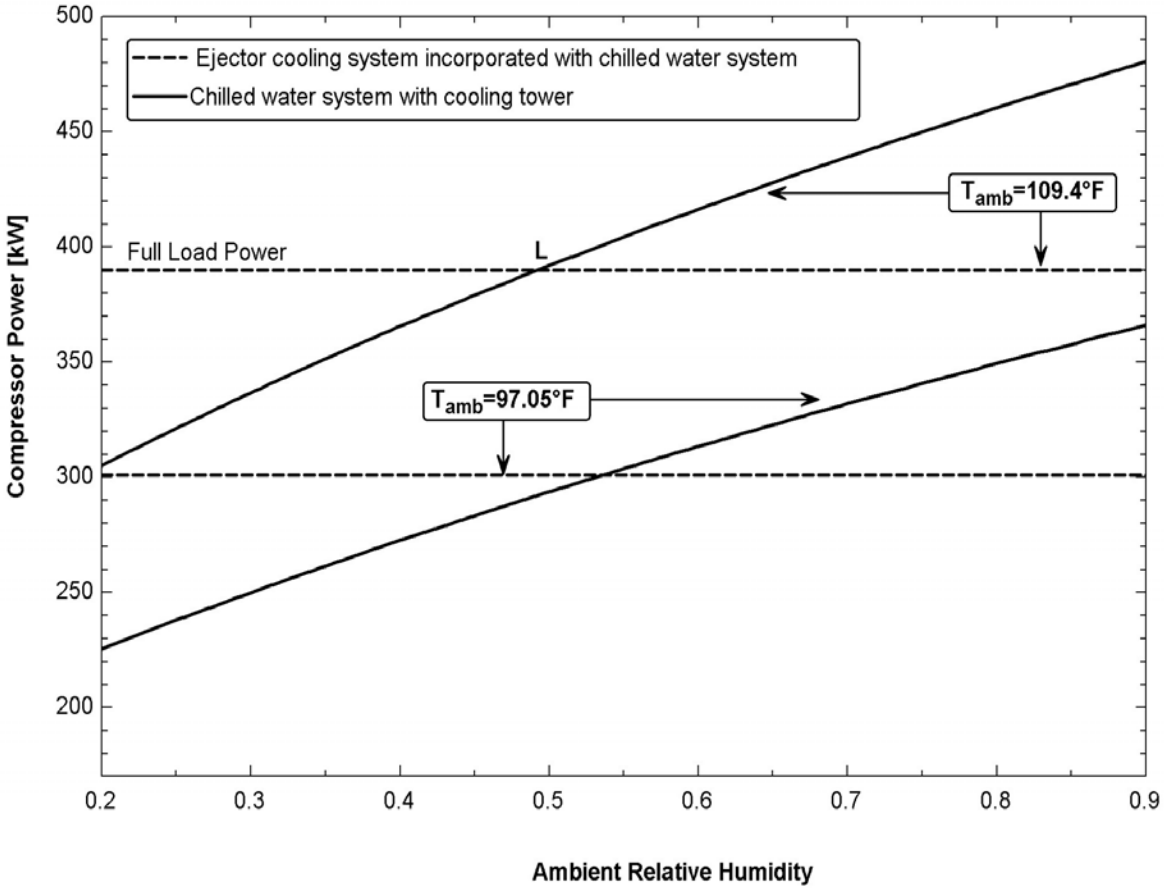

Figure 5.36 Comparison of compressor power for the chilled water system with cooling tower and with ejector cooling system

Similarly the variation of the compressor power with the relative humidity, when the chilled water system is operated with the cooling tower, at an ambient temperature below the design temperature is also shown in Fig. 5.36. It can clearly be seen that when the ambient temperature is 97.05^{o}F and the out door relative humidity is about 55%, the power consumption of compressor with the cooling tower as well as the ejector cooling system is identical. However, when the ambient relative humidity increases to values beyond 55%, the power consumption of the compressor increases sharply but remains below the full load power.

The ejector cooling system is however driven by any low grade thermal energy and hence its performance is not affected by the variation of ambient relative humidity. The thermal energy could be solar energy or the energy from flue gases emitted from various industrial processes. Thus the ejector cooling system can be designed to maintain a constant water supply temperature to the condenser irrespective of the out-door relative humidity. The effect of a situation when the water inlet to the condenser is maintained at a constant value of 93.04^{o}F, on the compressor can also be seen in Fig. 5.36. The power consumption of the compressor is independent of the ambient relative humidity. The disadvantage of this system, as is quite obvious from Fig. 5.36, is that in situations when the relative humidity is less than 50%, the cooling capacity of the cooling tower is enhanced which results in a drop in compressor power consumption. On the contrary, the power consumption of the compressor for a system using ejector cycle to cool the condenser water remains unaffected by the change in relative humidity. It may be noteworthy that, for the location of Dhahran, the ambient relative humidity is rarely less than 50% at the design as well as other generally high prevailing temperatures.

The main governing equations of the ejector cooling sub system can be summarized as;

$$w = \frac{\dot{m}_{ref,evap,ejec}}{\dot{m}_{ref,gen,ejec}} \tag{5.7}$$

$$\dot{m}_{ref,cond,ejec} = \dot{m}_{ref,gen,ejec} + \dot{m}_{ref,evap,ejec} \tag{5.8}$$

Referring to Fig. 5.35, the heat transfer in the evaporator of the ejector which acts as an intercooler to cool the condenser water is given as,

$$\dot{Q}_{evap,ejec} = \dot{m}_{ref,evap,ejec}\left(h_2 - h_5\right) \tag{5.9}$$

This heat transfer is equivalent that which would have originally occurred in the cooling tower and can also be expressed as:

$$\dot{Q}_{tow} = \dot{m}_{w,tow} C_{p,w,tow}\left(T_{w,tow,in} - T_{w,tow,out}\right) \tag{5.10}$$

Where

$$\dot{m}_{w,tow} = \dot{m}_{w,pump,cond,chw} \tag{5.11}$$

Finally, referring to the Fig.5.35, the heat transfer in the generator and condenser of the ejector system can be represented by the following equations:

$$\dot{Q}_{gen,ejec} = \dot{m}_{ref,gen}\left(h_1 - h_6\right) \tag{5.12}$$

$$\dot{Q}_{cond,ejec} = \dot{m}_{ref,cond,ejec}\left(h_3 - h_4\right) \tag{5.13}$$

For a constant value of the chilled water system condenser inlet temperature equal to 93.04 ^{o}F, the variation of external low grade thermal energy required to run the generator

of the ejector cooling system with changing chilled water condenser outlet temperatures is shown in Fig. 5.37. This fluctuation in the chilled water condenser outlet temperature is a result of varying relative humidity. The effect of different entrainment ratios is also incorporated in this figure.

It can be seen that as the value of the chilled water condenser outlet temperature increases, a larger amount of energy is required by the generator to power the chilled water system. As an example, for an entrainment ratio of 0.5, the power required by the generator at a chilled water condenser outlet temperature of 102.4^{o}F is about 6 MW.

Furthermore, it is also observed that a greater amount of energy is required to run the system at low values of the entrainment ratio. This is because the COP of the ejector system reduces with a decrease in the entrainment ratio and the system performs inefficiently. The power required by the generator shoots up drastically when the entrainment ratio drops below 0.3, and reaches values as high as 11 MW.

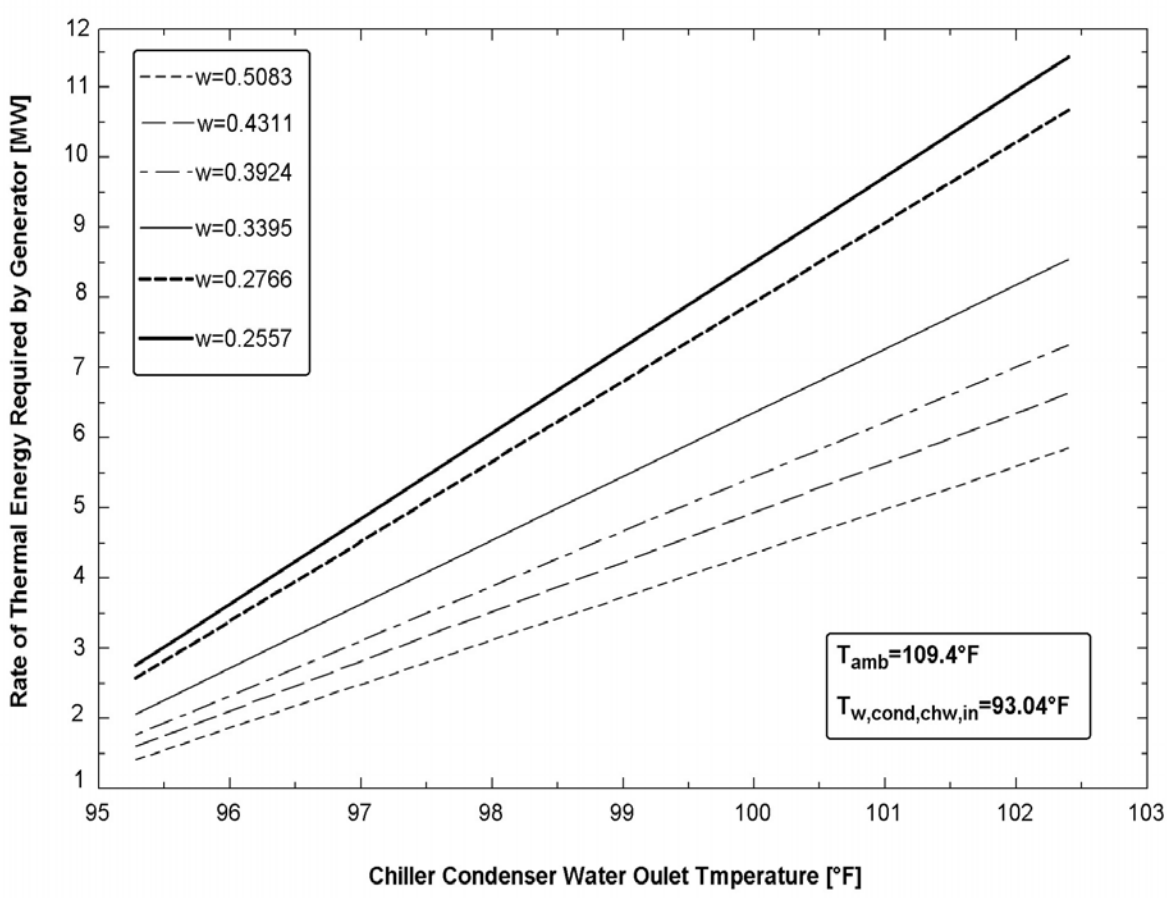

Figure 5.37 Variation of generator power with chilled water condenser outlet temperature and entrainment ratio

CHAPTER 6

CONCLUSIONS & RECOMMENDATIONS

6.1 Conclusions

The central chilled water system servicing the academic building 59 in the KFUPM campus located in Dhahran has been modeled numerically and its performance has been analyzed in detail. The effect of changing the existing pumping scheme, with the constant primary-variable secondary pumping scheme, as well as the variable primary pumping scheme has been investigated and the results are reported in terms of percentage of annual energy savings. This investigation is further extended to include the results for the cities of Riyadh and Jeddah.

An exergy analysis of all the three pumping schemes applied to the central chilled water being considered is performed in order to identify the major sources of irreversibilities. Following this, an investigation into the amount of water that can be collected from the air handler cooling coils throughout the year for the climatic of different locations is carried out. In the final phase of the study, the effect of incorporating an ejector cooling system into the existing central chilled water system, by replacing the cooling tower, is analyzed and the pros and cons of this combination are presented.

The main findings of the present study can be summarized as follows:

- By replacing the existing single loop constant primary pumping scheme with the constant primary-variable secondary scheme, savings in annual energy of about 8% can be achieved. These savings can further be increased to 12% by employing the single loop, variable pumping scheme.

- The savings in annual energy if the chilled water system being considered is operated in Riyadh and Jeddah using the constant primary-variable secondary scheme is around 7%. However, if the single loop variable pumping scheme is adopted, the energy savings for Riyadh will increase to 12%, whereas for Jeddah to a value of 11%.

- The exergy analysis shows that major sources of exergy destruction or irreversibilities in the chilled water system are the compressor and the air handlers. Almost 75% of the total exergy destruction occurs is the compressor, whereas the air handlers account for nearly 18% of the total exergy destruction.

- Another important finding of the exergy analysis is that the different pumping schemes do not have a significant impact on the exergy destruction in a chilled water system.

- For the ambient conditions of Dhahran and considering only the existing chilled water system, when 15% fresh air is inducted into the air handler, the annual amount of condensate that can be extracted from the cooling coil of the air handler is almost negligible. However, when this percentage of fresh air is increased to 40%, which is the minimum requirement for several air conditioning

applications, the amount of water that can be extracted from the air handlers is almost 89,000 kg. The maximum possible rate of water extraction, corresponding to 100% ambient relative humidity and 100% fresh air, at the design temperature (109.4^{o}F) is 33.68 kg/min.

- Owing to the relatively hot and dry conditions prevailing in the city of Riyadh, the analysis of water extraction is not carried out for Riyadh. On the contrary, for the conditions persisting in Riyadh, the supply air in the air handlers has to be humidified in order to maintain the desired comfort conditions. However, the scenario for the city of Jeddah is quite the opposite as even at a value of 15% fresh air almost 750 kg of water can be collected from the air handler annually. At 40 % fresh air this value reaches to a whopping 480,000 kg/year. Furthermore, the maximum possible rate of water extraction for Jeddah is three times that of Dhahran.

- The performance of an ejector cooling system is greatly influenced by the operating temperatures. In addition to this, the COP of the ejector cooling system is directly related to the entrainment ratio and hence a high value of the entrainment ratio automatically translates into a system having a high COP. The entrainment ratio of the ejector cooling system, being operated by a particular refrigerant, can be increased by:

    1. Increasing the generator temperature

    2. Reducing the condenser temperature, and

    3. Increasing the evaporator temperature.

- It is found that for a particular set of operating temperatures in the ejector cooling system, the maximum entrainment ratio is obtained by using the refrigerant R141b. whereas the maximum COP is achieved when refrigerant R717 is used as the working fluid.

- The main advantage of replacing the cooling tower of the chilled water system with an ejector cooling system is that a constant water inlet temperature for the chiller condenser is assured, regardless of the ambient relative humidity.

- Although the ejector cooling system has a COP of less than one, and a large amount of power is required by the generator to operate the cycle, this system can prove to be very economical when low grade energy input such as solar energy is utilized. For the ambient conditions of Dhahran where the average solar insolation is considerably high, this method of incorporation of the ejector cooling system with the existing chilled water system is a feasible and profitable alternative.

6.2 Recommendations

The following recommendations are listed for future work:

1. A cost analysis should be performed while investigating the effect of changing the present pumping scheme with the primary secondary pumping scheme as well as the variable primary pumping scheme. This analysis should include various costs, such as the initial cost of procuring additional pumps as well as materials, the cost of labor required, the cost of designing and implementing the control systems etc.

2. The effect of replacing the constant speed condenser pump in the chilled water system with a variable speed pump, thereby varying the flow rate of the cooling water in the chiller condenser should also be looked into.

3. An experimental investigation of an ejector cooling system incorporated with the chilled water system should be carried out. Moreover, if solar energy is used to power the generator of the ejector cooling system, the total amount of solar energy and if necessary, the additional auxiliary energy required to operate the system can be calculated for the climatic conditions of Dhahran as well as other cities.

4. The effect of the different refrigerants on the entrainment ratio as well as the COP of the ejector for different operating temperatures should be investigated further.

5. A scheme in which the cooling effect of the refrigerant in the ejector cooling system is directly used to cool the refrigerant in the chiller condenser should also be analyzed, both theoretically as well as experimentally

6. Lastly, the possibility of using the water extracted from the cooling coils of the air handler to cool the condenser refrigerant in the ejector cooling system should also be explored.

REFERENCES

[1] "SAUDI ARABIA - Saudi Arabia's Energy Base," *APS Review Downstream Trends*, Sept. 2007.

[2] F. A. Al-Sulaiman and S. M. Zubair, "A survey of energy consumption and failure patterns of residential air-conditioning units in eastern Saudi Arabia," *Energy*, Vol. 21, No. 10, pp. 967-975, 1996.

[3] *ASHRAE Handbook-Fundamentals. American Society of Heating Refrigeration and Air conditioning Engineers,* 2003.

[4] Y. A. Cengel and M. A. Boles, *Thermodynamics: An Engineering Approach*, 6 ed McGraw Hill, New York, 2007.

[5] I. Dincer and Y. A. Cengel, "Energy, entropy and exergy concepts and their roles in thermal engineering," *Entropy*, Vol. 3, No. 3, pp. 116-149, 2001.

[6] G. K. Alexis and E. K. Karayiannis, "A solar ejector cooling system using refrigerant R134a in the Athens area," *Renewable Energy*, Vol. 30, No. 9, pp. 1457-1469, 2005.

[7] T.Michelsen, "Air Conditioner Condensate: The Silent Destroyer," *Roofing/Siding/Insulation (RSI)*, 2003.

[8] W. Kirsner, "The demise of the primary-secondary pumping paradigm for chilled water plant design," *Heating Piping Air Conditioning*, Vol. 68, No. 11, pp. 73-79, 1996.

[9] M. Schwedler and B. Bradley, "Variable-Primary-Flow systems... An idea for chilled-water plants the time of which has come.," *HPAC Engineering*, Vol. 72, No. 4, pp. 41-44, 2000.

[10] M. Liu, "Variable water flow pumping for central chilled water systems," *Journal of Solar Energy Engineering*, Vol. 124, pp. 300-304, 2002.

[11] S. T. Taylor, "Primary-only vs. primary-secondary variable flow systems," *ASHRAE*, Vol. 44, No. 2, pp. 25-29, 2002.

[12] W. P. Bahnfleth and E. B. Peyer, "Energy use and economic comparison of chilled-water pumping system alternatives," *ASHRAE transactions*, Vol. 112, No. 2, pp. 198-208, 2006.

[13] M. Baker, D. Roe, and M. Schwedler, "Prescription for Chiller Plants," *ASHRAE*, Vol. 48, No. 6, pp. 4-10, 2006.

[14] R. Yumrutas, M. Kunduz, and M. Kanoglu, "Exergy analysis of vapor compression refrigeration systems," *Exergy*, Vol. 2, No. 4, pp. 266-272, 2002.

[15] J. Harrell, "Improving efficiency in the SIUC campus chilled water system using exergy analysis." MS Thesis, Southern Illinois University at Carbondale, 2007.

[16] B. N. Taufiq, H. H. Masjuki, T. M. I. Mahlia, M. A. Amalina, M. S. Faizul, and R. Saidur, "Exergy analysis of evaporative cooling for reducing energy use in a Malaysian building," *Desalination*, Vol. 209, No. 1-3, pp. 238-243, 2007.

[17] Y. Dai, J. Wang, and L. Gao, "Exergy analysis, parametric analysis and optimization for a novel combined power and ejector refrigeration cycle," *Applied Thermal Engineering*, Vol. 29, No. 10, pp. 1983-1990, 2009.

[18] A. Khaliq, R. Kumar, and I. Dincer, "Exergy Analysis of an Industrial Waste Heat Recovery Based Cogeneration Cycle for Combined Production of Power and Refrigeration," *Journal of Energy Resources Technology*, Vol. 131, pp. 022402-1-022402-9, 2009.

[19] J. Yu, G. Tian, and Z. Xu, "Exergy analysis of Joule-Thomson cryogenic refrigeration cycle with an ejector," *Energy*, Vol. 34, No. 11, pp. 1864-1869, 2009.

[20] J. M. Abdulateef, K. Sopian, M. A. Alghoul, and M. Y. Sulaiman, "Review on solar-driven ejector refrigeration technologies," *Renewable and Sustainable Energy Reviews*, Vol. 13, No. 6-7, pp. 1338-1349, 2009.

[21] J. Guo and H. G. Shen, "Modeling solar-driven ejector refrigeration system offering air conditioning for office buildings," *Energy and Buildings*, Vol. 41, No. 2, pp. 175-181, 2009.

[22] J. H. Wang, J. H. Wu, S. S. Hu, and B. J. Huang, "Performance of ejector cooling system with thermal pumping effect using R141b and R365mfc," *Applied Thermal Engineering*, Vol. 29, No. 10, pp. 1904-1912, 2009.

[23] C. Pollerberg, A. H. H. Ali, and C. Dotsch, "Solar driven steam jet ejector chiller," *Applied Thermal Engineering*, Vol. 29, No. 5-6, pp. 1245-1252, 2009.

[24] E. Rusly, L. Aye, W. W. S. Charters, and A. Ooi, "CFD analysis of ejector in a combined ejector cooling system," *International Journal of Refrigeration*, Vol. 28, No. 7, pp. 1092-1101, 2005.

[25] H. Vidal and S. Colle, "Simulation and economic optimization of a solar assisted combined ejector-vapor compression cycle for cooling applications.," *Applied Thermal Engineering*, Vol. 30, No. 5, pp. 478-486, 2010.

[26] A. Khalil, "Dehumidification of atmospheric air as a potential source of fresh water in the UAE," *Desalination*, Vol. 93, No. 1, pp. 587-596, 1993.

[27] B. A. Habeebullah, "Potential use of evaporator coils for water extraction in hot and humid areas," *Desalination*, Vol. 237, No. 1-3, pp. 330-345, 2009.

[28] S. A. Klein, "Engineering Equation Solver-8.1.7.5," *F-Chart Software, Wisconsin*, 2009.

[29] S. E. Klawunder, "Modeling and Analysis of Chilled Water Systems." MS Thesis, Georgia Institute of Technology, 2000.

[30] F. P. Incropera and D. P. Dewitt, *Fundamentals of Heat and Mass Transfer*, 6 ed. John Wiley and Sons, 2007.

[31] F. C. McQuiston, J. D. Parker, and J. D. Spitler, *Heating, Ventilating, and Air Conditioning: Analysis and Design*, 6 ed. John Wiley & Sons USA, 2005.

[32] A. Bejan, *Convection heat transfer*, 2 ed. John Wiley & Sons, 1995.

[33] D. G. Rich, "The effect of fin spacing on the heat transfer and friction performance of multi-row, smooth plate fin-and-tube heat exchangers," *ASHRAE Transactions*, Vol. 79, No. 2, pp. 137-145, 1973.

[34] Y. A. Cengel, *Heat transfer: A Practical Approach,* McGraw Hill Higher Education, 2003.

[35] S. E. Haaland, "Simple and explicit formulas for the friction factor in turbulent pipe flow," *Journal of Fluids Engineering*, Vol. 105, No. 1, pp. 89-90, 1983.

[36] F. M. White, *Fluid Mechanics 4 ed.* McGraw Hill, 1999.

[37] "Goulds Pumps Industrial Products, Division of ITT industries, Pump Selection System, available at http://www.gouldspumps.com/pss.html," 2010.

[38] J. B. Rishel, T. H. Durkin, and B. L. Kincaid, *HVAC Pump Handbook,* McGraw-Hill Professional, 2006.

[39] E. D. Weber, "Modeling and generalized optimization of commercial building chiller/cooling tower systems." Master's Thesis Georgia Institute of Technology, 1988.

[40] W. P. Silva and C. Silva, "LAB Fit curve fitting software (Nonlinear Regression and Treatment of Data Program) V 7.2. 39 (1999-2007)," 2007.

[41] G. F. Hewitt, G. L. Shires, and T. R. Bott, *Process Heat Transfer,* CRC press Boca Raton, FL, 1994.

[42] Y. A. Cengel and M. A. Boles, *Thermodynamics: An Engineering Approach* McGraw Hill, New York, 2007.

[43] *ASHRAE Handbook-Fundamentals. American Society of Heating Refrigeration and Air conditioning Engineers,* 2003.

[44] G. K. Alexis and E. D. Rogdakis, "A verification study of steam-ejector refrigeration model," *Applied Thermal Engineering*, Vol. 23, No. 1, pp. 29-36, 2003.

[45] K. Cizungu, A. Mani, and M. Groll, "Performance comparison of vapour jet refrigeration system with environment friendly working fluids," *Applied Thermal Engineering*, Vol. 21, No. 5, pp. 585-598, 2001.

[46] H. El-Dessouky, H. Ettouney, I. Alatiqi, and G. Al-Nuwaibit, "Evaluation of steam jet ejectors," *Chemical Engineering & Processing*, Vol. 41, No. 6, pp. 551-561, 2002.

[47] B. J. Huang, J. M. Chang, C. P. Wang, and V. A. Petrenko, "A 1-D analysis of ejector performance," *International Journal of Refrigeration*, Vol. 22, No. 5, pp. 354-364, 1999.

[48] D. W. Sun, "Variable geometry ejectors and their applications in ejector refrigeration systems," *Energy-The International Journal*, Vol. 21, No. 10, pp. 919-930, 1996.

[49] S. A. M. Said, M. A. Habib, and M. O. Iqbal, "Database for building energy prediction in Saudi Arabia," *Energy Conversion and Management*, Vol. 44, No. 1, pp. 191-201, 2003.

[50] Vidal Humberto and Colle Sergio, "Simulation and economic optimization of a solar assisted combined ejector-vapor compression cycle for cooling applications," *Applied Thermal Engineering*, Vol. 30, pp. 478-486, 2010.

VITA

NAME: Syed Ammar Ahmed Tirmizi Sujaulhaq Shafiulhaq

PLACE OF BIRTH: Manama, Bahrain.

ADDRESS: Building No.245, Flat No. 4,

Road 913, Block 909,

East Riffa,

Bahrain.

E-MAIL: ammartirmizi007@gmail.com

EDUCATIONAL QUALIFICATION:

M.S *(Mechanical Engineering)*

March 2010

King Fahd University of Petroleum and Minerals

Dhahran, Saudi Arabia.

B.Tech *(Mechanical Engineering)*

May 2006

Faculty of Engineering and Technology

Jamia Millia Islamia

New Delhi, India.